



UNIVERSITY *of the*
WESTERN CAPE

**Hydrothermal synthesis of hierarchical ZSM-5 with different Si/Al
ratio and their evaluation as catalysts in the catalytic cracking of
hexane**

By

Loyiso Clemence Nqakala

A dissertation submitted in fulfilment of the requirements for the degree of

Master of Science in the

Faculty of Natural Science

University of the Western Cape

Bellville/ South Africa

2021

Supervisor: Prof. Masikana Mdleleni

Co Supervisors: Dr. Ebrahim Mohiuddin

Dr Philani Perfect Mpungose

DECLARATION

I declare that “Steam-assisted hydrothermal synthesis of hierarchical ZSM-5 with different Si/Al ratio and their evaluation as catalysts in the catalytic cracking of hexane” is my own work submitted for the degree of Master of Science in chemistry at the University of the Western Cape, Bellville. This work has not been submitted for any degree or examination in any other university, and that all the sources I have used or quoted have been indicated and acknowledged by complete references.

Loyiso Clemence Nqakala (Mr.)

Date: January 2021



UNIVERSITY *of the*
WESTERN CAPE

Signature.....

ABSTRACT

Ethylene and propylene are greatly used for their importance as feedstocks for producing useful materials. Due to rise in prices and the demand of ethylene and propylene, the need to increase the selective production of these light olefins is necessary. To achieve this, zeolites, specifically ZSM-5 has been used to investigate catalytic cracking of several types of hydrocarbons for the production of these light olefins. This study focuses on developing hierarchical macro and/or mesoporous ZSM-5 zeolites with variable Si/Al ratios. The synthesized materials were then evaluated on their performance via catalytic cracking of hexane, dodecane and tyre derived oil [TDO] to produce light olefins, particularly ethylene and propylene.

These hierarchical zeolites were all prepared via a steam-assisted hydrothermal synthetic approach making use of hexadecyltrimethylammonium bromide [CTAB] as a mesoporous structure directing agent and tetrabutylammonium hydroxide [TBAOH] as a template for the formation of microporous zeolites. Stoichiometric quantities of sodium aluminate as an aluminum source and tetraethyl orthosilicate as a silica source were used for the formation of different Si/Al ratios in the range of 30-300. A process known as recrystallization was then performed for 48 hrs at high temperatures of 150 °C using a plastic Teflon flask placed inside a large stainless steel autoclave for the formation of crystals. The materials were then ion exchanged and calcined at 550 °C to form HZSM-5 catalysts. The resulting materials were characterized by XRF, FTIR, XRD, NH₃-TPD, TGA, HRSEM, nitrogen adsorption isotherms including BET surface area measurements and products obtained from the catalytic tests were analysed by GC.

XRF results showed that the calculated actual ZSM-5 Si/Al ratios were close to the expected batch ratios. According to the FTIR results, the intensity of the transmittance bands confirmed that the material reflects the crystallinity of ZSM-5 zeolites and is assigned to the five-membered rings of MFI zeolites. XRD analysis further confirmed that the prepared materials have a degree of crystallinity of the hierarchical ZSM-5 type with a partially ordered mesoporous structure. Three desorption peaks were demonstrated by the NH₃-TPD profiles. To our best knowledge, such observation of HZSM-5 with zeolites showing three desorption peaks has not been reported before. The total acidity calculated from the weak and strong acid sites of the prepared materials was found to decrease as the Si/Al increases in the following trend; SA=71 > 77 > 177 > 345.

Furthermore, the materials showed an increase in desorption temperature of the peak corresponding to strong acid sites as the Si/Al ratio decreased. This followed in the order SA=71>177>77>345. TGA analysis proved that the material was thermally stable, showing a little loss of moisture in the pores and on the surface. The HRSEM micrographs revealed sponge like morphologies with worm-like holes in the macropore range i.e. greater than 50 nm was also observed on the surface of the catalysts, proving that some macropores were successfully generated during the fabrication of these materials. BET and pore size analysis using the BJH method showed that the prepared materials had high surface areas due to the development of mesopores with narrow pore size distribution of 5-7 nm. All the adsorption-desorption curves of the synthesized hierarchical ZSM-5 zeolites exhibited typical isotherms with behaviour of both Type I and Type IV. Therefore, a hierarchical structure with 3 pore ranges, i.e. micro, meso and macropores was proven to be developed. Furthermore, varying the Si/Al ratio was shown to mainly affect the chemical properties of the materials such as acidity although aluminium content did also have some effect on the crystallinity of the materials.

GC was used to analyse the liquid and gas products obtained during the catalytic cracking of hexane, dodecane and tyre derived oils with the prepared zeolite catalysts and the commercial catalyst. All the reactions were performed under optimized reaction conditions that were investigated using commercial catalyst with SA=80. The optimum conditions were chosen based on their catalytic performance and selectivity towards the formation of ethylene and propylene include; T = 550 °C, Time on stream [TOS] = 6 hours, N₂: feed dilution ratio = 1:1, feed flow rate = 0.1 ml/min, P = atm, WHSV = 15.82 hr⁻¹ and a catalyst mass = 0.25 g. The best results were obtained at high temperature, high WHSV as well as dilution of the feed with inert nitrogen. Low catalytic conversions were obtained during the catalytic cracking of hexane using the prepared catalysts. The observed low conversions were attributed to large pores that were generated during the fabrication of these HZSM-5 catalysts, making the smaller hexane molecule to pass through the catalyst pores without much interaction with the active sites. The SA=71 had the highest selectivity towards ethylene and propylene olefins due to its higher total acidity as compared to the other prepared catalysts. It was shown that the catalytic activity was directly related to the chemical properties of the ZSM-5, in particular the acidity which was varied by changing the Si/Al ratio. Furthermore, it was

shown that the catalytic activity is mainly due to the acid strength of the strong Bronsted sites rather than the total acidity or acid site quantity. The SA=71 was then used for cracking dodecane and tyre derived oil. Its catalytic activity and selectivity was compared to that of a commercial catalyst with SA=80 with similar acidity and Si/Al ratio. The SA=71 demonstrated remarkable improvement such as higher conversions of 100 % and improved selectivities towards ethylene and propylene [$> 60\%$] when using both feeds compared to the commercial catalyst. This was due to its bigger pores, which resulted to better diffusions in the catalyst pores. This allowed the reactants and product molecules to easily diffuse in and out of the pores of the catalyst and also interact with the active acid sites of the catalyst, leading to enhanced activity, selectivity to olefins and catalyst stability. This suggests that the prepared catalysts would be more effective on cracking longer chains as well as bulky molecules. They would also be more suitable catalysts for cracking oils such as those used as feedstocks in the FCC process.



ACKNOWLEDGEMENTS

This dissertation has been possible thanks to God Almighty for giving me strength to go on and not look back during this journey. I would also like to express my sincere gratitude to the following people who have been by my side and assisted me all the way to the completion of this work:

Firstly, I would like to express my great thanks to my main supervisor Prof Masikana Mdleleni at University of the Western Cape, PetroSA Synthetic Fuels Innovation Centre [PSFIC] for his support.

I would also like to acknowledge my second supervisor Prof. David Key, PSFIC.

Furthermore, I would like to extend my sincere gratitude to my co-supervisors Dr Ebrahim Mohiuddin and Dr Philani Perfect Mpungose at University of the Western Cape, PSFIC team. They have inspired me by their deep scientific knowledge in catalysis. They have been so generous for guiding and helping me with the writing of this dissertation. They sacrificed their time to look and read work starting from the first to the last page and gave me many valuable suggestions and corrections during the write up of this research project.

I would also like to extend my great thanks to my team Dr Baskaran Tangaraj, Winnie Monama, Tayibbah Tahier and Neo Sehloko who were always there to help with anything I needed and provided great support.

I would also like to thank PetroSA and NRF Postgraduate Scholarship for fully supporting me financially throughout the research project.

Lastly, I would like to thank the Chemistry Department and the SensorLab Research Group for their support.

Without all these individuals mentioned above, my Research Project was never going to be a success.

PUBLICATIONS

1. L.C. Nqakala, M. M. Mdleleni, D. Key, E. Mohiuddin, P.P. Mpungose, “*Steam-assisted hydrothermal synthesis of hierarchical ZSM-5 with different Si/Al ratio and their evaluation as catalysts in the catalytic cracking of hexane*” **To be submitted**

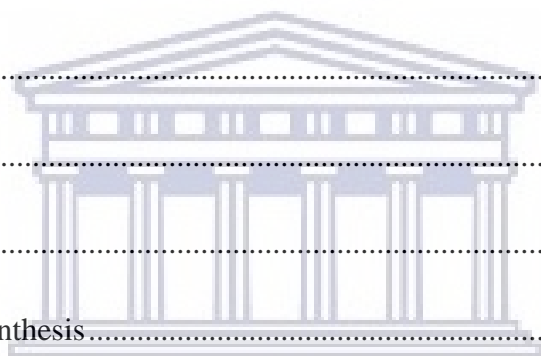


UNIVERSITY *of the*
WESTERN CAPE

CONTENTS

DECLARATION.....	i
ABSTRACT.....	ii
ACKNOWLEDGEMENTS.....	v
PUBLICATIONS.....	vi
CONTENTS.....	vii
LIST OF ABBREVIATIONS.....	xii
LIST OF FIGURES.....	xv
LIST OF TABLES.....	xix
THESIS OUTLINE.....	xx
CHAPTER 1: Introduction to Cracking Reactions.....	1
Chapter Overview.....	1
1.0 Cracking Reactions and Processes.....	1
1.1 Cracking Reactions.....	1
1.2 Cracking Processes.....	2
1.2.1 Steam Cracking Process.....	3
1.2.2 Fluid Catalytic Cracking Process.....	5
1.2.3 Hydro-Cracking Process.....	8
1.3 Catalytic Cracking Mechanism over Zeolites.....	10
1.3.1 Monomolecular (Protolytic Cracking) Mechanism.....	11
1.3.2 Bimolecular (Oligomerization Cracking) Mechanism.....	12
1.4 Feedstocks for Cracking Reactions.....	13

1.4.1 Cracking of Naphtha Olefins	15
1.4.2 Cracking of Paraffins	16
1.5 Effects of Hierarchical ZSM-5 on Catalytic Cracking	18
1.6 Tuning the Distribution of Al for the Production of Propylene	22
1.7 Conclusion	23
1.8 References	24
CHAPTER 2: Introduction to Zeolite Science and Practice	32
Chapter Overview	32
2.0 A brief historical background of zeolites	32
2.1 Zeolites	32
2.2 Zeolite ZSM-5	35
2.3 Synthesis of zeolites	36
2.4 Factors that affect zeolite synthesis	37
2.4.1 Si and Al reagents	38
2.4.2 SiO ₂ /Al ₂ O ₃ molar ratio [Si/Al]	38
2.4.3 Organic Structure Directing Agent	39
2.4.4 Effect of the Water Concentration	40
2.4.5 Crystallization temperature and time	41
2.5 Hierarchical zeolites	42
2.6 Methods used to synthesize hierarchical zeolites	44
2.6.1 The bottom-up approaches	46
2.6.1.1 Hard-templating	46
2.6.1.2 Soft-templating	48



UNIVERSITY of the
WESTERN CAPE

2.6.1.3 Non-templating	50
2.7 Influence of physical and chemical properties of hierarchical zeolites on catalysis	51
2.8 Problem Statement	53
2.9 Rationale and motivation for the research.....	54
2.10 Research aims and objectives	56
2.11 References	57
CHAPTER 3: Experimental Procedure for Catalyst Synthesis, Characterisation and Testing.....	66
Chapter Overview	66
3.0 Experimental Section	66
3.1 Chemicals used for synthesis	66
3.2 Synthesis of materials.....	67
3.2.1 Synthesis of ZSM-5 zeolite solution.....	67
3.2.2 Synthesis of hierarchical ZSM-5 zeolite with different Si/Al ratios.	67
3.2.3 Modification of ZSM-5 with Si/Al ratio of 30	68
3.2.4 ZSM-5 ion exchange from sodium form to hydrogen form	68
3.3 Characterization of Materials	68
3.3.1 X-ray fluorescence [XRF] spectroscopy.....	68
3.3.2 Fourier-Transform Infra-Red Spectrometry [FT-IR].....	68
3.3.3 X-ray Diffraction [XRD]	69
3.3.4 High Resolution Scanning Electron Microscopy [HRSEM]	69
3.3.5 NH ₃ -Temperature programmed desorption [NH ₃ -TPD].....	69
3.3.6 Thermogravimetric analysis [TGA].....	70
3.3.7 Brunauer Emmett and Teller [BET]	70

3.3.8 Gas Chromatography [GC].....	70
3.4 Catalyst testing	73
3.4.1 The reactor description and set-up.....	73
3.4.2 Experimental procedure.....	76
3.5 References	80
CHAPTER 4: Results and discussion of Catalyst Characterization	81
Chapter Overview	81
4.0 Catalyst Characterization	81
4.1 X-Ray Fluorescence [XRF].....	81
4.2 Fourier Transform Infrared Spectroscopy [FTIR].....	82
4.3 X-ray Diffraction [XRD].....	84
4.4 Ammonia-Temperature Programmed Desorption [NH ₃ -TPD]	88
4.5 Thermogravimetric Analysis [TGA].....	91
4.6 High Resolution Scanning Electron Microscopy [HRSEM].....	92
4.7 Nitrogen adsorption-desorption analysis.....	95
4.8 Conclusion.....	98
4.9 References	99
CHAPTER 5: Catalytic Activity Investigations	100
Chapter Overview	100
5.0 Optimisation studies	100
5.1 Effect of temperature on the catalytic cracking of hexane	100
5.2 The effect of catalyst loading on the catalytic cracking of hexane.	106
5.3 The effect of N ₂ : Hexane dilution ratios.....	110

5.4 Catalytic cracking of hexane over hierarchical ZSM-5 catalysts with different Si/Al ratios.....	115
5.5 Catalytic cracking of dodecane	121
5.6 Catalytic Cracking of Tyre Derived Oil [TDO]	126
5.7 Conclusion.....	128
5.8 References	129
CHAPTER 6: Conclusions and Recommendations	130
Chapter Overview	130
6.0 Summary and Conclusions	130
6.1 Recommendations and Future Work.....	136



UNIVERSITY *of the*
WESTERN CAPE

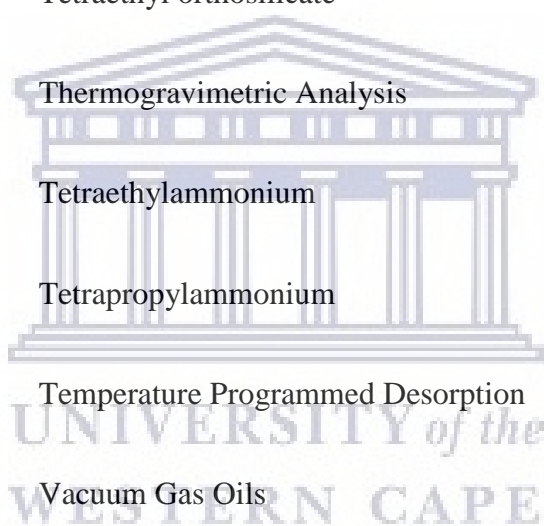
LIST OF ABBREVIATIONS

AIO	Aluminium monoxide
AlO ₄	Alumina
ATR	Attenuated Total Reflection
BEA	Beta
BET	Brunauer Emmett and Teller
BTX	Benzene Toluene Xylene
COD	Conversion of Olefins to Distillate
CBU	Composite Building Units
CTAB	Cetyltrimethylammonium bromide
CTACl	Cetyltrimethylammonium chloride
DGC	Dry Gel Conversion
EDS	Energy Dispersive Spectroscopy
EMC	Elf Mulhouse Chimie
ETOH	Ethanol
FAU	Faujasite
FCC	Fluid Catalytic Cracking
FED	Field Emission Gun
FT	Fischer-Tropsch
FTIR	Fourier Transform Infra-Red

GC	Gas Chromatography
HGO	Heavy Gas Oils
HRSEM	High Resolution Scanning Electron Microscopy
HRTEM	High Resolution Transmission Electron Microscopy
HZSM	Hierarchical Zeolite Socony
IUPAC	International Union of Pure and Applied Chemistry
LPG	Liquefied Petroleum Gas
LTA	Linde Type A
LTL	Linde Type L
MAS	Magnetic Angle Spinning
MCM	Mobil Composition of Matter
MEL	Mobil Eleven
MFI	Mobil Five
MTH	Methanol to Hydrocarbons
NaAlO ₂	Sodium Aluminate
NH ₃ -TPD	Temperature-Programmed Desorption
NMR	Nuclear Magnetic Resonance
OSDA	Organic Structure Directing Agent
PBU	Primary Building Unit
SBU	Secondary Building Unit



SDA	Structure Directing Agent
SEM	Scanning Electron Microscopy
SOD	Sodalite
T-atom	Tetrahedral atom
TBAOH	Tetrabutylammonium hydroxide
TDO	Tyre Derived Oil
TEM	Transmission Electron Microscopy
TEOS	Tetraethyl orthosilicate
TGA	Thermogravimetric Analysis
TMA	Tetraethylammonium
TPA	Tetrapropylammonium
TPD	Temperature Programmed Desorption
VGO	Vacuum Gas Oils
WHSV	Weight Hourly Space Velocity
XRD	X-ray diffraction
ZSM-5	Zeolite Socony Mobil – 5



LIST OF FIGURES

Figure 1: Catalytic cracking of long chain alkanes into shorter chains and aromatics (6).....	3
Figure 2: The demand growth of propylene (1).....	4
Figure 3: Reactor and regenerator operating conditions used in the fluid catalytic cracking [FCC] process (13).....	7
Figure 4: Haag-Dessau cracking mechanism for an alkane molecule [RH] that proceeds through a carbonium ion transition state (36).....	12
Figure 5: An alkane molecule cracking mechanism that consists of a hydride transfer step to a smaller carbenium ion [R1 ⁺] followed by β -scission (36).....	13
Figure 6: Quantities of various feedstocks used worldwide in steam cracking (50).....	15
Figure 7: Pictorial representation of a parent and a hierarchical zeolite (67).....	19
Figure 8: Unit building blocks formed by molecules of SiO ₄ and AlO ₄ (5).....	33
Figure 9: A part of a zeolite formed by a tetrahedral arrangement of the Si-O and Al-O bonds (5).....	33
Figure 10: Most widely used zeolite framework types and their ring sizes (8).....	34
Figure 11: A ZSM-5 zeolite molecular structure displaying well-defined channels and pores within the zeolite (5).....	36
Figure 12: Different factors that affect the zeolite synthesis (25).....	37
Figure 13: A parent zeolite with micropores and a hierarchical zeolite with both micro- and mesopores (45).....	43
Figure 14: A diagram representing different hierarchical zeolite development approaches (54).....	46
Figure 15: Schematic representation of template removal from soft-templating and hard-templating method (59).....	47
Figure 16: The fabrication of hierarchically porous tri-modal zeolites using a proposed micro-emulsion mechanism (69).....	49
Figure 17: Reactor description and setup.....	73
Figure 18: GC trace of the calibration gas used to identify gaseous hydrocarbon products.....	78

Figure 19: GC trace of the calibration used to identify liquid hydrocarbon products.	79
Figure 20: GC trace of the calibration of pure hexane.....	79
Figure 21: FTIR spectra of the prepared zeolite catalysts with variable Si/Al molar ratios.....	83
Figure 22: FTIR spectra of the SA=36 prepared at variable temperatures from 150-180 °C for 3-6 days.....	84
Figure 23: Wide and small angle [inset] XRD patterns of the synthesized hierarchical zeolite having variable Si/Al molar ratios in the range [36-345]	85
Figure 24: Wide and small angle [inset] XRD patterns of the SA=36" prepared for 3-6 days at temperatures of 150-180 °C.....	87
Figure 25: NH ₃ -TPD profiles of the synthesized HZSM-5 zeolites with different Si/Al ratios.	90
Figure 26: TGA profile showing the thermal behaviour of SA=77.....	91
Figure 27: SEM micrographs of the hierarchical ZSM-5 with variable Si/Al ratios in the range [71-345] synthesized at 150 °C for 48 hr.	94
Figure 28: N ₂ adsorption-desorption isotherms of the synthesized HZSM-5 materials.	96
Figure 29: Corresponding BJH pore size distribution of the synthesized HZSM-5 materials.	97
Figure 30: Catalytic conversions of hexane obtained when varying the temperature conditions. The reactions were carried out at different temperatures of 450, 500 and 550 °C. The following reaction conditions were used: Time on stream [TOS] = 6 hrs, N ₂ : Hexane dilution ratio = 1:1, feed flow rate = 0.1 ml/min, P = 1 atm, WHSV = 8 hr ⁻¹ , commercial ZSM-5 with SA = 80, catalyst mass = 0.5 g and also without a catalyst.	101
Figure 31: Selectivity towards paraffins and the BTEX products at different temperatures of 450, 500 and 550 °C formed during the 1st, 3rd and the 6th hour.....	103
Figure 32: Selectivity to olefins [C ₂ = to C ₄ =] at different temperatures of 450, 500 and 550 °C during the 1st, 3rd and 6th hour.	104
Figure 33: Selectivity towards propylene at different temperatures of 450-550 °C.	106
Figure 34: Catalytic conversions of hexane obtained when varying the catalyst loadings. The following reaction conditions were used: Time on stream [TOS] = 6 hrs, T=550 °C, commercial ZSM-5 with SA = 80, N ₂ : Hexane dilution ratio = 1:1, feed flow rate = 0.1 ml/min, P = 1 atm, WHSV = 15.82 hr ⁻¹ when the	

catalyst mass = 0.25 g, WHSV = 8 hr ⁻¹ when the catalyst mass = 0.5 g and a WHSV = 5.27 hr ⁻¹ when the catalyst mass = 0.75 g.	107
Figure 35: Selectivity to olefins [C2= to C4=] for different catalyst loadings of 0.25, 0.5 and 0.75 g.	109
Figure 36: Propylene/Ethylene ratios for different catalyst loadings of 0.25, 0.5 and 0.75g.	110
Figure 37: Catalytic conversions of hexane obtained when varying the N ₂ : Hexane dilution ratios. The reactions were carried using different nitrogen to feed ratios [N ₂ : Hexane] under the following conditions: Time on stream [TOS] = 6 hours, N ₂ : Hexane dilution ratios = [0:1, 1:1 and 2:1], feed flow rate = 0.1 ml/min, T = 550 °C, Catalyst mass = 0.25 g, P = 1 atm and a WHSV = 15.82 hr ⁻¹	111
Figure 38: Selectivity to olefins [C2= - C4=] when varying the N ₂ : Hexane dilution ratios over a period of 6 hours.	112
Figure 39: P/E ratios for different N ₂ : Hexane dilution ratios.	114
Figure 40: Catalytic conversions of hexane obtained from using HZSM-5 catalysts. All the catalytic cracking reactions were performed on a bench scale quartz-tube reactor using hexane as a model feed. The reactions were carried under these conditions: T = 550 °C, Time on stream [TOS] = 6 hours, N ₂ : Hexane dilution ratio = 1:1, feed flow rate = 0.1 ml/min, P = atm, WHSV = 15.82 hr ⁻¹ and a catalyst mass = 0.25 g.	115
Figure 41: Selectivity towards paraffins and BTEX products for HZSM-5 catalysts.	118
Figure 42: Selectivity to olefins [C2= - C4=] products for HZSM-5 catalysts.	119
Figure 43: P/E ratios for the prepared HZSM-5 catalysts with different SA ratios.	120
Figure 44: Catalytic conversions of dodecane obtained when using the synthesized zeolite with SA=71 and a commercial zeolite with SA=80. The catalytic cracking reactions were performed on a bench scale quartz-tube reactor using dodecane as a model feed. The reactions were carried under the following conditions: T = 550 °C, Time on stream [TOS] = 6 hours, N ₂ : Hexane dilution ratio = 1:1, feed flow rate = 0.1 ml/min, P = 1 atm, WHSV = 15.82 hr ⁻¹ and a catalyst mass = 0.25 g.	122
Figure 45: Selectivity towards paraffins and BTEX products formed when using the commercial catalyst with SA=80 and the prepared catalyst with SA=71.	123

Figure 46: Selectivity towards olefins [C2= to C4=] products formed when using the commercial catalyst with SA=80 and the prepared catalyst with SA=71.....	124
Figure 47: Selectivity towards paraffins and BTEX products formed when using a commercial catalyst with SA=80 and the prepared catalyst with SA=71. The catalytic cracking reactions were performed on a bench scale quartz-tube reactor using TDO as a model feed. The reactions were carried under the following conditions: T = 550 °C, Time on stream [TOS] = 6 hours, N ₂ : TDO dilution ratio = 1:1, feed flow rate = 0.1 ml/min, P = 1 atm, WHSV = 15.82 hr ⁻¹ and a catalyst mass = 0.25 g.	126
Figure 48: Selectivity towards olefins [C2= to C4=] products formed when using the commercial catalyst with SA=80 and the prepared catalyst with SA=71.....	127



LIST OF TABLES

Table 1: Comparison in Catalytic Cracking and Thermal Cracking Operating Conditions (3, 5).....	2
Table 2: Grades of zeolites with different Si/Al molar ratio (10)	35
Table 3: A list of chemicals and reagents used for synthesis of zeolites as well as their composition.....	66
Table 4: Specifications of the GC used for gas hydrocarbon analysis.....	71
Table 5: Specifications of the GC used for liquid hydrocarbon analysis.....	71
Table 6: Different dilution ratios used for nitrogen to feed flow rate	76
Table 7: Chemical compositions of the prepared HZSM-5 catalysts with different Si/Al ratios as determined by XRF	82
Table 8: Calculated peak intensities and their corresponding relative % crystallinity of the prepared zeolite samples.....	88
Table 9: NH ₃ -TPD temperature and acid quantity of HZSM-5 zeolites with different Si/Al ratios.....	90
Table 10: Calculated average macropore sizes for the prepared materials from SEM analysis.	93
Table 11: Textural properties of the prepared HZSM-5 zeolites with different Si/Al ratios	95
Table 12: Effect of temperature on catalytic cracking of n-hexane over nano-scale ZSM-5 catalysts with different Si/Al ratios and without the use of a catalyst (1)	102

THESIS OUTLINE

This thesis is broken down into six chapters and an outline is provided below. In general, the thesis contains a literature review, experiment section, results and discussion, conclusion, recommendations and future work. The literature review is separated in two chapters [1 and 2].

Chapter 1 provides an introduction to the cracking reactions, catalytic processes and the cracking reactions that take place over different zeolites, mainly the ZSM-5 zeolite catalyst. Furthermore, it discusses the catalytic cracking mechanisms over different catalysts. The advances and the current research and developments in the technology of zeolite catalysts for catalytic cracking are also discussed in this chapter.

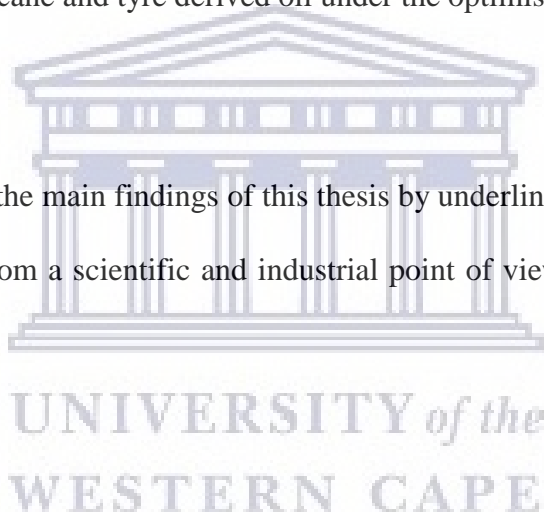
Chapter 2 provides a brief historical background on zeolites, specifically ZSM-5. The factors that affect the synthesis of zeolites, including the different methods used to synthesize and modify hierarchical zeolites have been discussed. Furthermore, the effects of the physical and chemical properties of the hierarchical zeolites on the performance of the catalyst are also discussed. The problem statement, rationale and motivation for the research, and the research aims and objectives are also included.

Chapter 3 details the experimental procedures used to prepare the ZSM-5 catalysts with different Si/Al ratios. It begins by listing all the chemicals used for synthesizing these zeolite catalysts. It then discuss in detail all the experimental procedures employed during the synthesis of these zeolite catalysts. Furthermore, a summary of the instruments and the characterization techniques used in this study such as FTIR, XRD, XRF, HRSEM, BET, NH₃-TPD and GC with their description are also discussed. Lastly, the reactor description and its set-up for the catalytic activity testing of the ZSM-5 catalysts in the catalytic cracking are briefly discussed as well.

Chapter 4 provides a thorough discussion of the obtained results during the characterization of the prepared materials. Different characterization techniques such as XRF, FTIR, XRD, NH₃-TPD, TGA, HRSEM and BET that were used in this study are also discussed.

Chapter 5 deals with optimisation of the reaction conditions and the evaluation of the catalytic performances of the synthesized materials via catalytic cracking of hexane, dodecane and tyre derived oil. It starts by investigating the effects of reaction conditions such as temperature, WHSV and nitrogen diluent: feed ratio on catalytic activity and selectivity when using a commercial catalyst with SA=80. It then provides a discussion of results on the catalytic activity and selectivity of the prepared materials when tested via catalytic cracking of hexane, dodecane and tyre derived oil under the optimised reaction conditions.

Chapter 6 provides a summary of the main findings of this thesis by underlining an overview of the activities and contributions of the results from a scientific and industrial point of view. Recommendations for future work are also outlined chapter.



CHAPTER 1: Introduction to Cracking Reactions

Chapter Overview

Chapter 1 briefly presents an introduction to the cracking reactions, catalytic processes and the cracking reactions taking place over different zeolites, particularly the ZSM-5 zeolite catalyst. It further discusses the catalytic cracking mechanisms over different catalysts. The advances and the current research and developments in the technology of zeolite catalysts for catalytic cracking are discussed.

1.0 Cracking Reactions and Processes

1.1 Cracking Reactions

Cracking is defined as a practise of producing short and useful hydrocarbon molecules by simple breaking down the longer hydrocarbons. The main method for generating light olifens is via thermal or steam cracking and currently yield up to 95% of ethylene globally and about 60% of the world's propylene as a by-product to ethylene production (1). Various petrochemical processes make use of these olefins as the main building blocks and for generating useful materials such as ethylbenzene, vinyl chloride, polyethylene, polypropylene etc (2). Nonetheless, producing these olefins using the steam cracking method requires relatively high temperatures of about 800-850 °C. This leads to enormous energy consumption, approximately 40% of the energy that is used in the refinery. A way to reduce this high usage of energy has been practiced by researchers by developing a more effective route for producing light olefins that are environmentally friendly. Catalytic cracking makes use of lower temperatures of roughly 450-650 °C during the production of light olefins. The acid strength and the optimising operating conditions of the zeolite catalyst can be used to control the yields of ethylene and propylene. Therefore, catalytic cracking is found to be a flexible route to produce both ethylene and propylene and has been considered as a best substitute for thermal cracking (3,4). Table 1 below shows the comparison in operating conditions of the catalytic and thermal cracking. Processes, mechanisms and reactions taking place in catalytic cracking over different naphtha range hydrocarbons are discussed in detail below.

Table 1: Comparison in Catalytic Cracking and Thermal Cracking Operating Conditions (3, 5).

Operating conditions	Catalytic cracking	Thermal Cracking
Temperature	450-650 °C	800-850 °C
Pressure	1 bar	70 bar
Catalysts used	Mostly zeolites	No catalyst
Feed	Mainly light and heavy naphtha [C2-C12+]	Mainly light and heavy naphtha [C2-C12+]
Product distribution	Olefins [ethylene, propylene, butenes] Aromatics [Benzene, Toluene, Xylenes]	Olefins [ethylene, propylene, butenes] Aromatics [Benzene, Toluene, Xylenes]
Mechanism	Carbenium and Haag Dessau ion mechanism	Free radical mechanism

1.2 Cracking Processes

The catalytic cracking process of pure hydrocarbons has been extensively practised to explore the chemistry of the industrial process. The supply of products that are of great economic importance to the petroleum refiner are directed by cracking and secondary reactions (5). Zeolites with strong Brønsted acidity have an important role in catalytic cracking. Breaking down of hydrocarbons with sizes that range from C₆ to the ones made up of numerous carbon atoms have been studied using mesoporous zeolites since they have strong acidity, improved surface area and high thermal stability. Refineries crack large quantities of heavy hydrocarbon feedstocks as depicted in Figure 1 below into portions that are more valuable, making the steam cracking, fluid catalytic cracking [FCC] and hydro-cracking routes to be vital in the industry. These cracking process are explained in detail in the sections below.

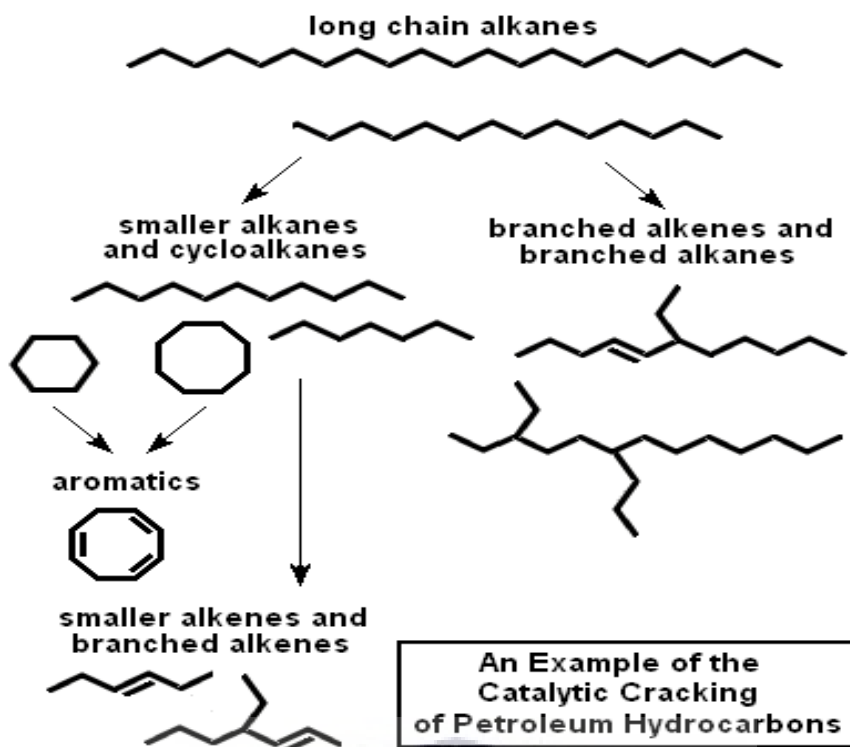


Figure 1: Catalytic cracking of long chain alkanes into shorter chains and aromatics (6).

1.2.1 Steam Cracking Process

Steam cracking processes for the activation of paraffins has been extensively studied for over 50 years. Paraffin activation takes place through steam cracking when high temperatures of 800 °C or more are used to heat-up paraffin during this process. This technique can be used to activate a large number of feeds, for as long as their boiling points are below 600 °C (7). The steam cracking process can be divided into two parts. [i] The initial cracking temperatures [i.e. 500 – 680 °C] are used to preheat the feed and the steam. [ii] The steam is fed into the high temperature reactor [i.e. 750 – 875 °C], where the steam cracking takes place. The ratio of the feed to steam and the partial pressure of the reactants can greatly influence the selectivity in the steam cracking process (8). Olefins and diolefins dominate the product profile in a steam cracking process, both which are found to be more reactive than the starting material [i.e. paraffin]. The reactor effluent is quenched at 0.02-0.1 seconds to avoid successive reactions that lead to a decrease in the yield and selectivity of the targeted products. Consequently, a combination of absorption processes and distillation is used to separate the products. Steam cracking process operates without the use of a catalyst (7,8).

Ethane, propane and gasoline are mainly used in steam crackers and FCC units as the main feedstocks to produce propylene as by-product. The kind of feedstock that is used in steam cracking can greatly affect the yield of propylene. Heavy feedstocks like hexane tend to produce more propylene than lighter feedstocks like ethane. Ethane-based feeds have been widely used recently in steam crackers. However, only ethylene is being produced in large yields and a very small yield of propylene is produced as a by-product when using ethane based feeds. Therefore, a shortage of propylene is anticipated to occur in the near future when only focusing on this kind of method. In recent years, the market and the demand for propylene has grown more than that of ethylene as illustrated in Figure 2 below (1). Furthermore, there are a few drawbacks associated with using steam cracking such as the use of high temperatures [800-850 °C] and greenhouse emissions. This leads to a search of alternative methods and technologies to increase the yield of propylene. Pyrolysis section alone makes use of roughly 65% of the total energy and 75% of the total energy loss in the plant. As a consequence of high process temperatures, these furnaces need to be out of service for decoking. FCC has been found to be the main alternative to the steam cracking method as a source of propylene production (9).

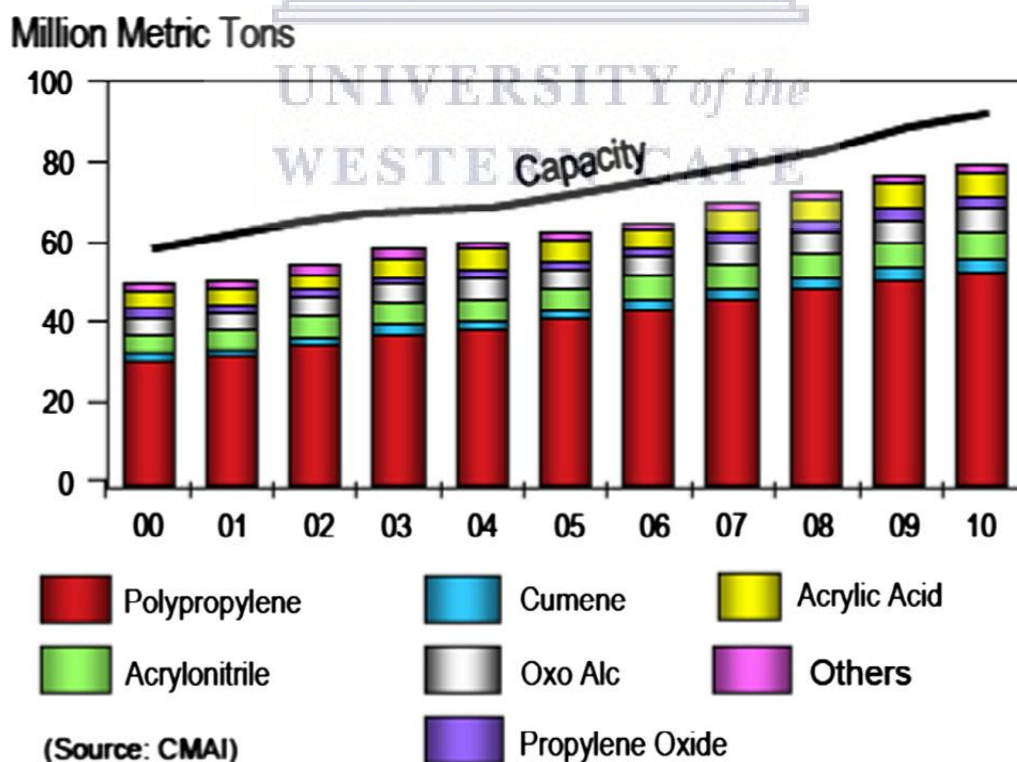


Figure 2: The demand growth of propylene (1).

A lot of research has been done to investigate different ways to enhance the efficiency of steam cracking reactions and to reduce coke formation in steam cracking. Jeong *et al* (10) investigated the catalytic pyrolysis of naphtha in a quartz reactor with 5 mm α -Al₂O₃ spheres for light olefins production. Ethylene and propylene exhibited high yields of 10 % and 5% higher values when compared to the thermal cracking at the same reaction conditions and absence of α -Al₂O₂ spheres. Karaba *et al* (11) investigated a way to improve the steam-cracking efficiency of naphtha feedstocks by mixed/separate processing. A laboratory cracking reactor was used for both blend and separate processing of naphtha feedstocks at different blending ratios and temperature range of 760 – 810 °C. Steam cracking of light naphtha exhibits ethylene yield of 24.1 wt. % at maximum temperature, whereas only 13.6 wt. % of ethylene was attained from heavy naphtha. Both the yields of ethylene and propylene displayed a decreasing trend with increasing content of heavy naphtha in blended feedstock. The results achieved suggest that there is a possibility of mutual effects between components, leading to non-linear dependence of products yields on the blending ratio.

1.2.2 Fluid Catalytic Cracking Process

Fluid catalytic cracking [FCC] is one of the most essential refinery processes in that it converts the heavy fraction of crude oil into transportation fuels. Upon the cracking route, hydrocarbons having bulky molecular sizes crack into tiny molecules over bond separations (12). Fluid catalytic cracking [FCC] is used in oil refineries to convert feedstocks such as heavy gas oils [HGO], vacuum gas oils [VGO] or residues into useful products such as liquefied petroleum gas [LPG], diesel and olefinic gases etc. It is also widely used to produce most of the world's gasoline and propylene for the polymer industry as well as a tiny fractions of raw materials for petrochemical processes (13). Refinery FCC operations currently supply roughly 30% of propylene globally, 64% comes from thermal steam cracking of naphtha and the rest by means of propane dehydrogenation route or metathesis. Usually about 2 wt.% ethylene and 3-6 wt.% propylene are obtained in a conventional FCC process (14). Y-zeolite, an inert matrix, an inert binder and an active alumina are catalysts employed in the FCC process. There are two problems faced by these catalysts, mainly it is coke deposition and the dealumination of Y-zeolite. To stimulate the catalysts in the regenerator vessel, combustion of the deposited coke is carried out and also supplies heat to the FCC reactor, where the general FCC process operates without external heating (15). Efforts are made on both the catalyst and process side to

increase the yield of propylene from the FCC process. One of the effective ways to improve the yield of propylene is by adding ZSM-5 to the FCC catalyst because it provides refiners a way to improve the fabrication output of their FCC units (2).

A common fluid catalytic cracking process involves a mixture of a heated hydrocarbon charge with a hot stimulated catalyst as it goes into the riser pipe that leads to the reactor. Within the riser pipe, the charge is mixed with a recycle stream, then vaporized and elevated to a reactor temperature of roughly 493-554 °C, by the hot catalyst. The charge is then cracked at 10 - 30 psi as the mixture moves up the riser pipe. The riser pipe is where all the cracking occurs in the current FCC process units. The produced light products are separated further making use of a fractionator (16,17). The used up catalyst is regenerated to eliminate the coke collected throughout the process. It moves over the catalyst stripper to the regenerator, where some of the deposited coke starts burning off. Depending on the conditions used, the regenerator temperature can go up from 650-760 °C. An additional fresh catalyst is then used to optimize the cracking process. Feedstocks are in the atmospheric residuum (reduced crude) to the naphtha range. Feed preparation is normally done through coking, vacuum distillation, thermal cracking, propane de-asphalting etc to eliminate high-molecular weight non-volatile materials and metallic components. Figure 3 below shows the reactor and the regenerator setup and the conditions used during the FCC process. The key variables of this process are temperature, catalyst to feedstock ratio, pressure, volume or the weight of the feedstock in the reaction zone that is charged per hour, per weight or volume of the catalyst (17).

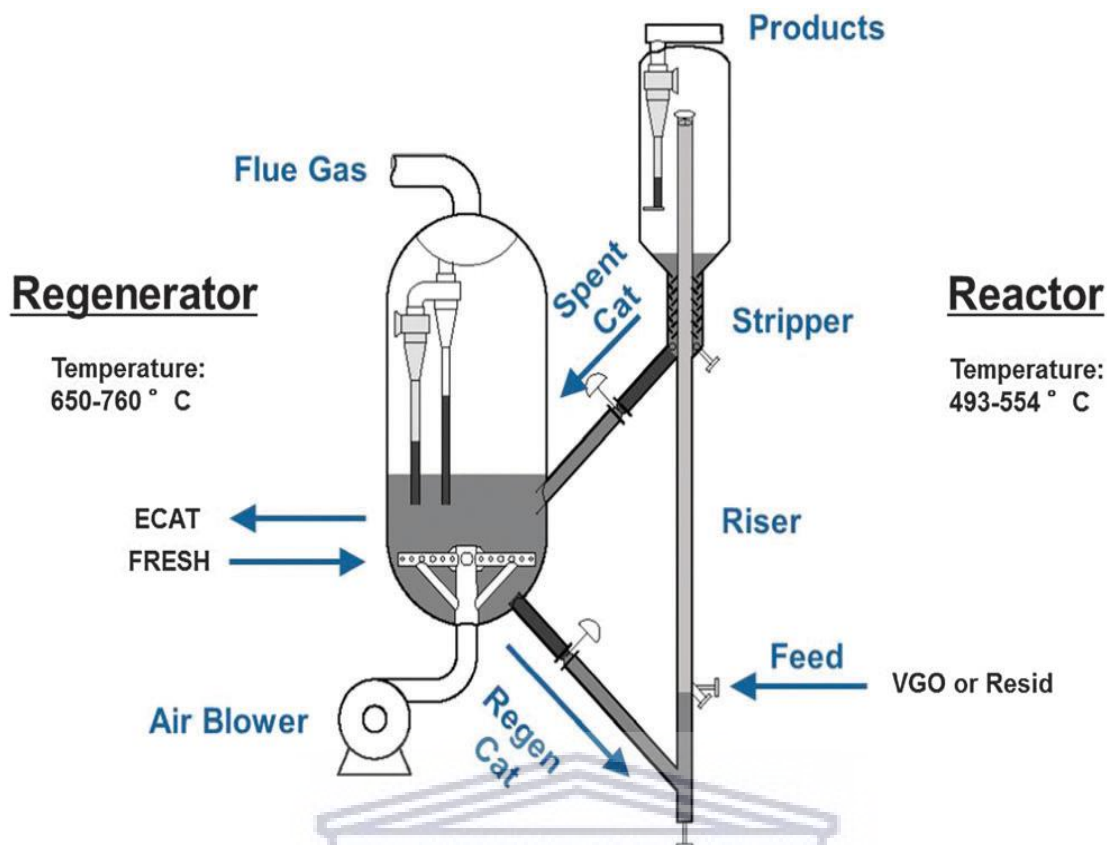


Figure 3: Reactor and regenerator operating conditions used in the fluid catalytic cracking [FCC] process (13).

The use of modified mesoporous ZSM-5 zeolites to increase the yield of light olefins, particularly propylene have been widely investigated on FCC and compared to that of the parent ZSM-5 zeolites. Aitani *et al* (18) investigated the catalytic cracking of Arabian Light vacuum gas oils [AL-VGO] over FCC catalyst having novel zeolite additives to boost propylene yield. They tested a mesoporous [Mezo-ZSM-5], TNU-9, SSZ-33 and a conventional ZSM-5 as additives to a commercial ultra-stable Y [USY] FCC equilibrium catalyst [E-Cat]. TNU-9 is a medium pore zeolite that has three dimensional 10-ring channel pore system. SSZ-33 is a large pore zeolite that consists of two intersecting 12-ring and 10-ring channels. The four catalysts are mixtures of 10 wt. % and 90 wt. % E-Cat each of ZSM-5, Meso-Z, TNU-9 and SSZ-33 additives. A fixed-bed micro-activity test [MAT] unit was used to evaluate their catalytic performance at different catalyst/oil ratios and temperatures of 520 °C. They observed that even though they used these additives, there was no decrease in the cracking activity of all the E-Cat/additives. At comparable gasoline percentage yield, the highest yield of propylene [12.2 wt. %] was reached over E-Cat/Mezo-Z as compared to 9.0 wt. % each from

E-Cat/ZSM-5 and E-Cat/TNU-9. The yield of propylene was more than doubled for the Mezo-Z that has an easily reachable pore structure and essential mesopores. The increase in the yields of propylene over Mezo-Z was enhanced by the acidity of the zeolite and its improved mass transport. For other additives, the low improvement in propylene was attributed to its higher hydrogen transfer activity.

Another example of a modified mesoporous ZSM-5 zeolite was given by Awayssa *et al* (19). They used a modified hierarchical ZSM-5 [HZSM-5] as FCC additive to investigate the yield enhancement of light olefins from catalytic cracking of Vacuum Gas Oils [VGO]. Alkaline treatment and Mn were used to modify the HZSM-5 having variable Si/Al ratios. The modified HZSM-5 was tested as FCC catalysts additives to boost the propylene yield from catalytic cracking of hydro-treated AL-VGO. A commercial USY E-Cat in a fixed-bed MAT unit at different catalyst/oil ratios and 550 °C were used to assess the performance of the alkaline treated and the Mn/HZSM-5 additives. The light olefins yield over E-Cat with a parent HZSM-5 increased to 18.1, 25.4 and 27.4 wt. % for Si/Al of 30, 80 and 280 as compared with 15.4 wt. % over E-Cat [at 75wt. % conversion]. The use of a modified Mn/HZSM-5 as an additive instigated an additional increase in the yield of light olefins. The E-Cat-Mn/HZSM-5 with Si/Al = 80, and 2.0 wt. % Mn achieved the largest light olefins yield of 29.2 wt. %. They reasoned that the decrease in the amount of strong acid sites and acid density resulted to the better fabrication of light olefins over the Mn/HZSM-5 additive. The development of hierarchical micro-meso topology also displayed a high yield ~28.3 wt. % of light olefins for the alkaline treated HZSM-5 as compared to the parent ZSM-. This was due to the hierarchical pore topology that delivered an easy movement and accessibility of bulky molecules to and from active sites (20). Consequently, it is clearly observed that the use of modified mesoporous zeolites results in improved yields of light olefins as compared to the parent ZSM-5 zeolite.

1.2.3 Hydro-Cracking Process

Hydrocracking is a process by which the hydrocarbon molecules of petroleum are broken into simpler molecules of gasoline or kerosene by adding hydrogen under high pressure and in the presence of a catalyst (21). It was mainly established for the conversion of heavy fractions into lighter transportation fuel products. It is accomplished in a suitable reactor vessel by contacting a hydrocarbon feedstock with a bifunctional

catalyst. Vacuum gas oil, which is a substantial fraction of petroleum, is used as the main feedstock. Hydrocracking conditions consist of high pressures of 75-160 bars, the presence of hydrogen and high temperatures of 230-455 °C. The products are normally fully saturated. This process is normally done in a single or several reaction vessels in series that make use of a single catalyst (22).

Hydrocracking reactions are commonly run in trickle-bed reactors where the gas-liquid phase flow is simultaneously downward via a fixed-bed of catalyst particles. The down flow mode has a low pressure-drop and the absence of flooding which makes it to be frequently used in industrial practice. Diesel and jet fuel are the main products obtained from hydrocracking, but liquefied petroleum gas [LPG] and low sulphur naphtha fractions are also produced (23,24). Different classes of acidic supports such as [i] amorphous oxides, e.g., silica-alumina, [ii] hybrid supports made up of a mixture of amorphous oxide and zeolite or [iii] crystalline zeolites, mostly ultra-stable Y-zeolites [USY], ZSM-5 and a binder have been used for the formulation of hydrocracking catalysts (25). Zeolites have good benefits such as improved selectivity, high hydrothermal stability and acidity as compared to amorphous supports since they have well-defined pore structure and high density of acid sites, resulting in high hydrocracking activity (26). In the process productivity, hydrocracking catalyst systems can be deactivated due to a number of factors in this case. These consist of the build-up of coke precursors on the internal and external configuration of the catalysts, the fast elimination of metallic poisons and complete blockage of the pores. The accessibility of reactants and products species become limited since the pore size of catalyst becomes narrowed when this occurs. This reduces the selectivity and activity properties of the catalyst. Therefore, the pore structure of the catalyst is an important factor that can be used during the hydrocracking reaction to evaluate the conversion, selectivity and stability of the catalyst (27). Hierarchical [i.e. mesoporous] zeolite catalysts with diameters that are in the range of 2-50 nm are found to demonstrate improved activity-stability properties. Since the hydrocracking catalysts are usually bifunctional, the catalytic design aims for the production of mesoporous support materials that allow synergic metal support and active interaction for ideal process. The main metals used for hydrocracking catalysts include Mo or W, usually sulfided in situ and supported by Ni, Co or platinum group metals (28).

An ongoing research work on the effect of catalyst pore sizes has been done by various researchers to improve the activity and the selectivity of the catalyst during the hydrocracking process by using a catalyst with bigger pore sizes and modified catalysts by different metals. According to Sekhar (29), greater cracking properties and removal of heteroatoms were demonstrated by Al₂O₃-supported catalysts having 7-20 nm than those with pore sizes of less than 7 nm. Song *et al* (30) confirmed a similar result by improving asphaltenes obtained from enhancing bitumen. The activity of the NiMo/Al₂O₃ catalyst was found to increase with an increase in the pore size from 5 to 29 nm. The mesoporous catalysts with larger pore sizes also demonstrated higher yields of oil products.

Another example of the modification of the pore characteristics is given by Ying *et al* (31). They also discovered that a hydrocracking conversion of 63% was obtained from using a similar catalyst with pore size of ~25 nm as compared to 54% obtained when using the same catalyst with pore size of ~10 nm. According to Puron *et al* (32), excellent liquid hydrocarbon yields from remaining oil upgrading were formed by alumina catalysts with mesopores than the microporous catalysts. These catalysts were also resistance to deactivation. The resistance can mechanically be ascribed to superior interactions of the left over oil feed with the active catalyst sites because of the removed diffusion complications. Regali *et al* (22) studied the effect of metal loading on activity, selectivity and deactivation behaviour of Pd/silica-alumina catalysts. The bifunctional catalysts consist of palladium on amorphous silica-alumina with different metal loadings [0 - 1.2 wt. %] and were compared in the hydrocracking or/- hydro-isomerization of n-hexadecane. The acidic properties of the support were influenced by the metal loading. The selectivity, the rate of deactivation and the initial activity were also found to be highly affected by the metal-acid site ratio. The initial activity revealed a strong dependence on the metal acid site ratio up to a Pd loading of 0.33 wt%, whereas at high metal loadings, the increase in activity was limited.

1.3 Catalytic Cracking Mechanism over Zeolites

Cracking reactions over acidic catalysts like zeolites normally proceed through the carbonium ion mechanism. The catalytic cracking mechanism is usually crucial at low temperatures. Acidic molecular sieves like ZSM-5 include both Lewis (non-proton acidic centres) and Bronsted [proton acidic centers] sites

(33,34). Alkanes can be activated by two mechanisms namely the classical bimolecular [oligomerization cracking] and the non-classical monomolecular (protolytic cracking), also referred to as Haag-Dessau cracking mechanism as shown in Figure 4 (35).

1.3.1 Monomolecular (Protolytic Cracking) Mechanism

In monomolecular mechanism, alkanes are protonated for the formation of carbonium ions transition states. These states can go through either C-C bond cleavage yielding alkanes, together with methane and ethane or C-H bond cleavage yielding carbenium ions and hydrogen. The carbenium ions then lead to the formation of alkanes in the $C_1 - C_3$ range through back donation of a proton to the zeolite (34). The carbonium ions go through α -cracking reactions, producing smaller paraffin and extra stable carbenium ion which can be desorbed further as a smaller alkene. Cracking on Lewis acid sites occurs through both the free radical mechanism and the carbonium ion mechanism. Lewis acid sites improve the breaking of C-C bonds, stimulate adsorption of hydrocarbons and speed up the cracking of β -bonds and the development of free radicals. The development of light olefins is favoured by the Bronsted acid sites, whereas the strong Lewis acid sites accelerate the coke formation. The formation of ethylene is possible via this mechanism as illustrated in Figure 4 below (36). This anticipated mechanism explains the large amount of methane, ethane and hydrogen that is produced during the cracking process that the classical mechanism fails to explain. Narrow pores of the zeolite catalyst, high cracking temperatures, low partial pressures and conversions of the feed hydrocarbon are parameters that favour this reaction mechanism (37,38).

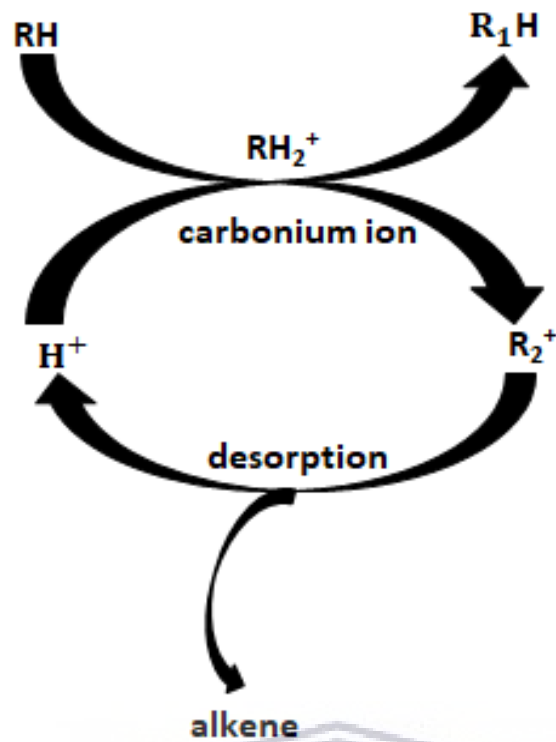


Figure 4: Haag-Dessau cracking mechanism for an alkane molecule [RH] that proceeds through a carbonium ion transition state (36).

1.3.2 Bimolecular (Oligomerization Cracking) Mechanism

In bimolecular mechanism, cracking occurs when the branched secondary and tertiary alkyl-carbenium ions that result from the feed molecule are cleaved by a particular beta-scission into smaller alkenes and alkylcarbenium ions as illustrated in Figure 5 below (36). According to this mechanism, a hydride is abstracted by a carbenium ion from an alkane and forms an additional carbenium ion, which cracks through β -scission. Carbenium ions are chain carriers with the main ones being the most steady that can generally form tertiary ions such as t-butyl cations. Alkane cracking involves alkyl group shift [isomerization] reactions, C-C bond breaking [β -scission] and simultaneous formation of C-C bond (39). Methane, ethane and ethylene are not discovered in this mechanism since it is not likely to form primary alkylcarbenium ions. Bimolecular hydride transfer reactions between feed alkanes and alkylcarbenium ions lead to chain

reactions. Thus, the yield of olefins is limited to only 50 wt% because these chain reactions yield shorter alkanes (37,38).

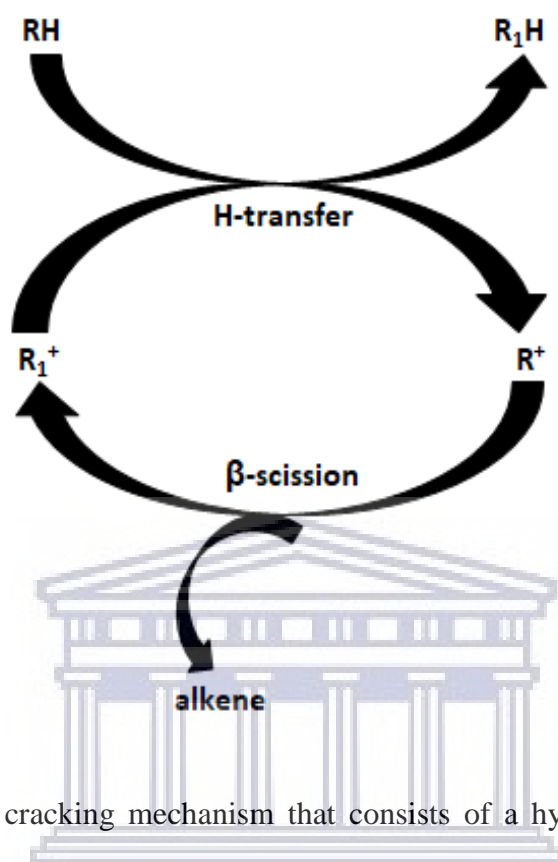


Figure 5: An alkane molecule cracking mechanism that consists of a hydride transfer step to a smaller carbenium ion $[R_1^+]$ followed by β -scission (36).

1.4 Feedstocks for Cracking Reactions

Steam cracking is commercially used in huge scale industrial units for the production of ethylene and propylene. The common petroleum resultant naphtha contains a wide variety of different hydrocarbon types. These include normal and branched paraffins, naphthenes, benzene, olefins and alkyl aromatics. Paraffins are known to crack easily and offer high yields of ethylene, whereas other compounds such as benzene are quite inflexible to the normal cracking conditions. It is also identified that a high product yield is obtained when cracking normal olefins compared to cracking iso-paraffins. Adsorptive separation techniques e.g. simulated moving bed technology, have been developed to separate olefins from paraffins and to also separate normal [straight chain] paraffins from non-normal [branched chain] paraffins and aromatics (40). Higher temperatures are required for the catalytic cracking of paraffinic naphtha as compared to the olefinic

naphtha cracking. Thermal cracking of paraffinic light naphtha activate at almost 600 °C. Thermal cracking also happens instantaneously in high temperature catalytic cracking (41). Low additional value normal paraffins having 5-11 carbons are produced as by-products from processes such as FCC unit or the conversion of methanol to olefins, generally over hydrogen transfer reactions catalysed by the acid sites. Paraffins need to be improved, separated or recirculated to the acid catalytic conversion units since they have moderately low commercial interests and low octane number. Therefore, improving the value of this paraffin fraction in order to increase the oil and organic waste management is a major challenge (42–44). On the other hand, light olefins such as ethylene, propylene or butene are high value hydrocarbons and are commonly used as building blocks for the production of clean fuels. Catalytic cracking is one of the most studied alternatives for upgrading low quality naphtha. Normal alkanes are used as model molecules during the study of catalytic cracking with the main aim to produce olefins (45).

Naphtha is a light hydrocarbon fraction product that is generated through the distillation process of crude oil and/or syncrude and it consist of a great quantity of low value saturated paraffins. Naphtha can be further separated into two streams based on hydrocarbon length and boiling range. Light naphtha has a boiling range from 30-145 °C and heavy naphtha with a boiling range from 140-205 °C. Light naphtha contains most of the hydrocarbons [paraffins, olefins and oxygenates] with six and lower carbon atoms, while heavy naphtha contains most of the hydrocarbons with about greater than six carbon atoms. The distillate obtained from crude oil distillation unit is called straight run naphtha and consists of great quantity of low value saturated paraffins. It is the leading feedstock at present, accounting a total of approximately ~50-55%. Light Cracked Naphtha obtained from the cracking of naphtha in the FCC process generally contains a significant amount of olefins. Naphtha thermal cracking has been the established method to produce light olefins (46). Ethylene and propylene are both light olefins identified to be the most essential raw materials and their demand has increased. Many industries use these light olefins as feedstocks to produce chemicals such as ethylene oxide, resins, fibres, polypropylene, polyethylene as well as other chemicals (47–49). Figure 6 below shows quantities of various feedstocks that are used worldwide in steam cracking (50). Research has now focused on creating more effective processes due to the fact that the thermal cracking route requires high reaction temperatures, high energy consumption, high CO₂ emission, low yield of roughly 25% and 35% for ethylene

and propylene, respectively (51,52) . Therefore, catalytic cracking of naphtha now appears to be the ultimate method and more efficient in energy use as compared to thermal cracking. This method allows for high yields of ethylene and propylene to be achieved using fairly low temperatures (53–56).

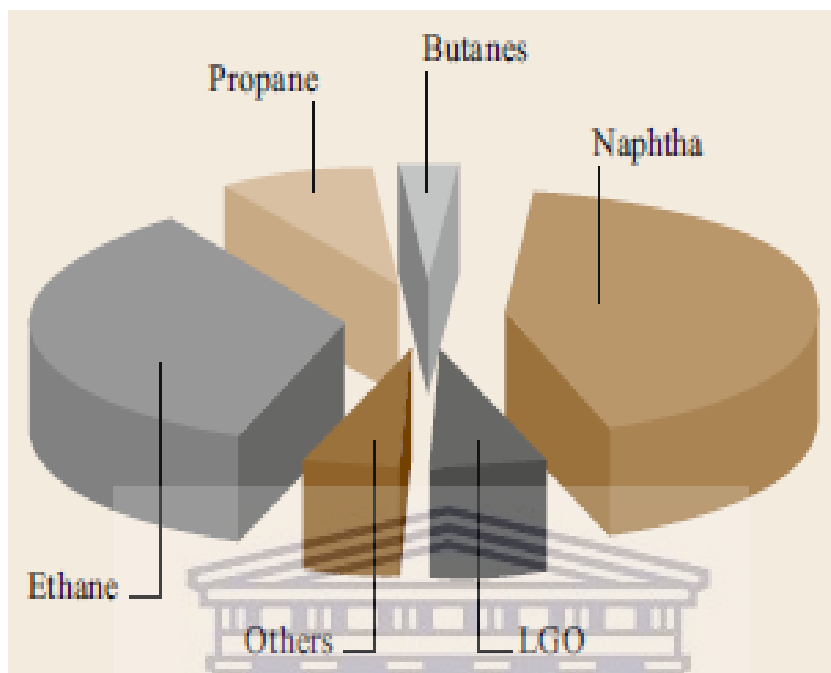


Figure 6: Quantities of various feedstocks used worldwide in steam cracking (50).

1.4.1 Cracking of Naphtha Olefins

A wide investigation to produce higher olefins which are characteristic naphtha components has been done by various researchers via catalytic cracking by use of zeolites. This has been done to enhance the FCC processes, to clarify the reaction mechanism and how catalysts perform. A report on large quantities of C₅-C₈ alkenes in Chinese FCC gasoline was given by Long *et al* (57). They confirmed how the conversion of isoparaffins and aromatics would be when using a ZSM-5 zeolite. They reported that hydrogen transfer (HT) and isomerisation reactions take place at low temperatures of about 200 °C. However, this led to the formation of cyclic olefins instead of aromatics. Selectivity towards aromatic products is found to increase with an increase in temperature. For isoparaffins, selectivity occurs at 300-350 °C. Propylene, butenes and pentenes form at temperatures of 450 °C with lesser contact times. Wang *et al* (58) studied the catalytic cracking of 1-pentene using ultra-stable Y (USY) zeolite at temperatures ranging from 250 to 350 °C. They

witnessed that during the first minute of the reaction, the HT reactions as well as the preliminary high activity of cracking decreased faster with a strong coke deposition. The double bond isomerization now then remains the main reaction. High temperatures favour desorption of coke precursors at a given TOS, leading to a low coke deposition but which then becomes more aromatic. Nawaz *et al* (59) also studied the catalytic cracking of 1-hexene using SAPO-34 catalysts to produce propylene. Kaolin was used in the synthesis as a source of Si and Al so as to modify the catalyst texture. A material having a mesostructured slit-shaped was attained when using kaolin in the synthesis. The activity and the stability of the catalyst were greatly enhanced than when comparing with the conventional SAPO-34 in the catalytic cracking of 1-hexene cracking. This is prompted by the enhanced diffusional access to the active sites. However, the selectivity towards propylene gets preserved at a particular level of conversion. At a high feed conversion of 98.2 % and temperatures of 575 °C with WHSV=14 h⁻¹ and TOS=1 min, a high selectivity of 73.9 wt% for propene was successfully achieved when using the mesostructured SAPO-34.

Another example to produce higher olefins which are characteristic naphtha components has been given by Feng *et al* (60). They studied the catalytic cracking of naphtha to light olefins using fluorinated HZSM-5 zeolite (F/HZSM-5) catalysts. These catalyst samples were synthesized through submerging the HZSM-5 (Si/Al = 46) zeolite into an aqueous NH₄F solution. They discovered that the maximum yields for ethene and propene were achieved at 600 °C with 20.2 % and 36.4 % obtained respectively. This was found when using a 0.1F/HZSM-5 zeolite that has large amounts of Brønsted acid sites of 7.3 and 4.3 % which are higher than those of a parent HZSM-5 zeolite. They also found out that modification by fluorine does not control the pore characteristics of HZSM-5 zeolites only, but also modifies the amount of acid sites as well as the density of Brønsted acid sites that could be necessary to achieve high naphtha conversions and selectivities towards light olefins (60). Wei *et al* (61) also identified that the yield of light olefins through the catalytic cracking of *n*-hexane increased when using HZSM-5 zeolites that are ion-exchanged by using alkali solution.

1.4.2 Cracking of Paraffins

Altwasser *et al* (35) studied the catalytic behaviour of the small-pore catalysts through catalytic cracking of *n*-octane using small-pore zeolites. The Brønsted acid sites of the zeolites were used as catalysts for cracking

of n-octane in a fixed-bed reactor that is constantly functioning. They chose n-octane as a model hydrocarbon since it can go through all the different kinds of β -scission reactions. High relative contributions of monomolecular Haag-Dessau cracking are revealed by the small-pore zeolites, i.e., low selectivities to branched hydrocarbons and high selectivities of C₁-C₃ hydrocarbons. Bimolecular hydrogen transfer reactions are slowed down in 8-ring zeolites, forming more olefins than paraffins. However, for small-pore zeolites, there is no observed pure monomolecular cracking but characteristic products of bimolecular cracking reactions like branched hydrocarbons were observed on small-pore catalysts. A study to investigate the catalytic roles of the pore structure and acidity in catalytic cracking of naphtha was also performed by Jung *et al* (62) via catalytic cracking of n-octane using alkali-treated MFI zeolites. A formation of mesopores and loss of strong acid sites was observed during the alkali treatment on the MFI zeolite. The short residence time and the low acidity encouraged the decrease of cracking activity, leading to lower conversion while increasing selectivity for major cracking products. The acidity was the main influence for determining the composition of the product and the level of conversion. Therefore, high yields of alkene and a high conversion were achieved by using the MFI zeolite with great quantities of strong acid sites. The production of longer alkanes, e.g., hexane and heptane were inhibited by the mesopores formed during the alkali treatment by reducing further oligomerization. Due to the fast elution of the important cracking products, the selectivity for propylene was high when using alkali-treated zeolites. However, the alkali treatment was not highly effective to boost the whole alkene selectivity. Therefore, the alkali treatment demonstrates the cracking route of n-octane in zeolite pores.

Another example of cracking paraffins has been given by Konno *et al* (63). They studied the kinetics of n-hexane cracking over ZSM-5 zeolites [MFI-type zeolite, Si/Al = 150 and 240] to explore the influence of crystal size and catalyst lifetime. The catalytic testing was examined at temperatures of 823-923 K under atmospheric pressure. The obtained results showed that the nano-zeolites produced high conversion of n-hexane with steady activity for 50 hrs as compared to the macro-zeolite. The reason for this observation is that the reaction with macro-zeolites occurs below transition conditions, whereas for nano-zeolites, the reaction occurs below reaction-limiting conditions. Due to coke deposition, the nano-zeolites short diffusion resistance and the huge external surface area decrease the impact of pore plugging. Kinetic model for

catalytic cracking of n-pentane over HZSM zeolite with Si/Al =15 was recently proposed by Aguayo *et al* (64). The catalyst preparation involved combining the HZSM-5 zeolite matrix with a mesoporous matrix of weak acidity. The kinetic tests were carried in a fixed bed reactor for 15 hrs at 350-550 °C and 1.4 bars. At high temperatures, the formation of BTX aromatics [coke precursors] and olefins and the deactivation of the catalyst were highly favoured, leading to a loss of the catalyst activity.

1.5 Effects of Hierarchical ZSM-5 on Catalytic Cracking

An interest in the research and development of hierarchical zeolites has been extensively growing, owing at least two levels of porosity so as to decrease diffusion limitations in reactions catalysed using microporous zeolites. In this practice, hierarchical means the presence of at least one additional pore system, adding to the intrinsic zeolite microporosity, normally in the mesopore size range. Several strategies and methods have been suggested and established for the introduction of porosity in conventional zeolites. A zeolite is a kind of crystalline aluminosilicates made up of various distinct micropores and intrinsic properties that are tunable. It has been applied in many petrochemical and chemical industries for reactions such as alkylation, catalytic cracking and isomerization (65). Zeolites have special properties that make them useful in the industrial processes. These properties are responsible for high acidity, shape selectivity, high surface area and thermal or/- hydrothermal stability (66). Many zeolites have been used extensively for the production of hydrocarbons such as ethylene and propylene via catalytic cracking. A ZSM-5 zeolite type has been recognized to be the most suitable catalyst for catalytic cracking due to its special pore structure and its acidity. However, ZSM-5 zeolite has its own drawbacks such as a microporous structure which may limit the movement of reactants and products to and from the active sites. Figure 7 below provides an example of a parent and hierarchical zeolite.

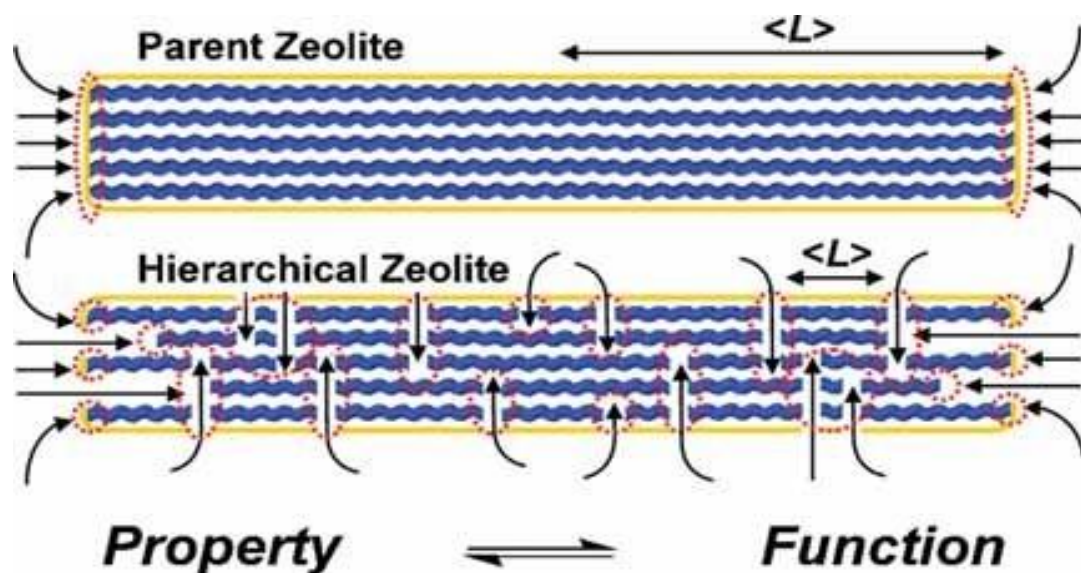


Figure 7: Pictorial representation of a parent and a hierarchical zeolite (67).

The hierarchical zeolite shows bigger pores and free movement of reactants and products from the active sites. On the other hand, the parent zeolite does not show any mesopores and not all the zeolite active sites can participate in the catalytic reaction because the mass transport to and from the active sites is being limited (67). The slow diffusion of large bulky hydrocarbons leads to the pore blockages of the zeolite and cause coke formation. For reactions to successfully occur, strong acid sites are needed. However, when there are too many strong acid sites present within the catalysts, reactants start to over-react on them and become converted into aromatic hydrocarbons or deposited carbon which leads to the deactivation of the catalysts (68). The composite of micro and mesopore is highly favoured for improving the activity and circulation of reactants and products. Hence, this above mentioned problem can be solved by developing a hierarchical pore zeolite having both micro and mesoporous structure (69). Hierarchical zeolites have enhanced mass transport properties, long catalyst lifetime and excellent product selectivities. Various methods for introducing mesopores on zeolites include post processing and templating methods, e.g. soft templates (70). These methods will be briefly discussed in chapter 2 of this work.

The use of mesoporous ZSM-5 zeolites has been widely investigated by researchers via catalytic cracking to enhance the yield and selectivity of olefins and to reduce the diffusion limitations encountered by microporous zeolites. The acidity also plays a major role in the catalytic cracking process. Hence, there has been a need to also investigate the use mesoporous zeolites with different acid sites. Mesoporous MFI

zeolites prepared using the alkali treatment were studied by Jung *et al* (62) to investigate the catalytic roles of acidity, pore structure and their activity for the cracking of n-octane at 773 K. They found out that while the product selectivity continues to be greatly affected, the mesoporous MFI demonstrates a low activity as compared to the original MFI zeolite. The alkaline treatment decreases the amount of the strong acid sites, leading to the formation of mesopores. However, the alkali-treated zeolites showed an enhanced selectivity towards propylene due to the fast elution of primary cracking products. Acidity was the prime factor responsible for the conversion level and the product selectivity, leading to a high yield when using the MFI zeolite with a massive amount of strong acid sites. Niwa *et al* (51) also studied the acidity and catalytic activity of mesoporous ZSM-5 in comparison with the zeolite ZSM-5, silica-alumina and Al-MCM-41 catalytic cracking of n-octane. The Al-MCM-41 and silica-alumina revealed huge quantities of defect sites and huge distributions of acid sites which varied significantly from the zeolite ZSM-5 and mesoporous ZSM-5. The mesoporous zeolites were found to have an activity that is similar to or a little lower as compared to that of the conventional zeolites.

Xionghou *et al* (71) studied the catalytic cracking of butene to ethylene and propylene on mesoporous ZSM-5 by desilication. An alkali treatment of parent ZSM-5 zeolite was used to prepare the mesoporous ZSM-5 which was then applied in the catalytic cracking of butene. The results obtained revealed that introducing mesopores into the parent ZSM-5 by alkali treatment could greatly improve the catalytic performances. The conversion, selectivity and the yield of ethylene and propylene when using the mesoporous ZSM-5 zeolite were greatly enhanced as compared to when using the parent ZSM-5. When the treated concentration of NaOH solution was 0.1-0.2 M, the highest yields of 81.76% ethylene and 79.35% propylene were produced respectively. This was due to the bigger pores, the improved access to acid sites and zeolite structure. Therefore, mesoporous ZSM-5 zeolites with increased accessibility of acid sites are found to be useful in catalytic cracking and can greatly enhance the yield and selectivity of olefins.

The use of modified mesoporous zeolites has also been investigated and then compared to their parent zeolites. Yajun *et al* (72) compared the catalytic cracking results of n-hexane over HF-ZSM-5 and the parent ZSM-5 zeolite. Initially, a high catalytic performance was observed during the catalytic cracking of n-hexane

when using the parent ZSM-5 but the conversion rate decreased very fast, especially after the 6th hour of the reaction. This was due to that there were only micropores that existed within the parent ZSM-5 catalyst. The acid sites got covered by the deposited carbon that mounted up in the micropores, leading to the deactivation of the catalyst. However, after treating the zeolite with HF-NH₄F solution, the catalytic performance had a remarkably improvement but also decreased as the HF concentration was increased. This was due to that the treatment of the ZSM-5 zeolite with HF-NH₄F solution created mesopores and macropores, while the micropores were still retained within the zeolite structure at low HF concentrations. However, a facile synthesis route for producing hierarchical ZSM-5 zeolite was developed by Coppens *et al.* (73) using TPAOH as the SDA. The Si/Al ratio and the recrystallization time were varied to adjust the mesoporous size. Sodium hydroxide treatment was also used to obtain a mesoporous ZSM-5 followed by washing with hydrochloric acid. Enhanced catalytic activity was revealed from the hierarchical ZSM-5 because it has higher molecule diffusion efficiency.

Hierarchical ZSM-5 materials have also been prepared and tested for their activity in the conversion of long chain hydrocarbons and bulky molecules. A mesoporous HZSM-5 zeolite that is made-up by carbon templating was also compared with a conventional HZSM-5 in one study for catalytic cracking of *n*-hexadecane. A noticeable increased activity was established when using the mesoporous HZSM-5, leading to a conversion of 52% for *n*-hexadecane than when comparing the conventional zeolite that only had a conversion of 17%. The cracking activity of these two zeolites further improved when they got impregnated with platinum, with the mesoporous HZSM-5 again displaying even higher activity than that of the conventional HZSM-5 (74). Hoan *et al* (75) designed hierarchical ZSM-5 materials for improving the production of LPG olefins in the catalytic cracking of Triglycerides. They fabricated a series of hierarchical ZSM-5 zeolites namely, composites ZSM-5, nanosized ZSM-5 and a mesoporous ZSM-5. The composite ZSM-5 and nanosized ZSM-5 were prepared using the direct-synthetic routes for a comparative purpose. The mesoporous materials were prepared using post-synthetic modifications that involve subsequent acid washing and base treatment. They observed that the subsequent acid washing step of alkaline treated ZSM-5 was necessary to enhance the catalytic performance. Great yields of the desired products, i.e., LPG olefins and gasoline were demonstrated by the mesoporous ZSM-5 zeolite compared to the parent ZSM-5 at almost

complete conversion of (ca. 90 wt. %). Selectivity towards the LPG olefins was also improved over all the hierarchical ZSM-5 materials, mostly high for composite ZSM-5 [ca. 94 wt. %]. Therefore, it is evident from the literature that modifying the ZSM-5 zeolite by incorporating secondary mesoporosity can effectively enhance the catalytic performance in terms of activity and selectivity in the catalytic cracking of various hydrocarbon feeds.

1.6 Tuning the Distribution of Al for the Production of Propylene

A capable strategy has been suggested in adding to the incorporation of heteroatoms and hierarchization treatment. It involves affecting the circulation of Al atoms as well as acid centers amongst different crystallographic locations within a particular zeolite framework (76). The influence of distributing Al in the framework of ZSM-5 was investigated by Sazama *et al* (77) through monitoring the conditions of the zeolite synthesis. This was done by performing catalytic cracking of 1-butene by using ZSM-5 zeolites that have comparable Si/Al framework ratios and crystal sizes. However, these zeolites have relative concentrations of close and single framework Al atoms that are not the same. They found out that the catalytic cracking of butenes and octenes is supported by the distant single Al atoms whereas the HT reactions that lead to the formation of aromatics are enhanced by close Al atoms.

Wu *et al* (78) made a comparison between a template-free ZSM-5 with a ZSM-5 zeolite fabricated using aid of TPA⁺. The template-free ZSM-5 was also improved by impregnating with tetramethyl orthosilicate (TMOS). This is done to remove the acid sites that are on the crystal surface. During the synthesis, TPA⁺ supported ZSM-5 reveals a better position of acid sites at the channel intersections, in agreement with the position of TPA⁺. In contrast, the template-free ZSM-5 displays a remarkable higher amount of Al placed in pore channels. These results agree with the ones previously reported by groups of Dedecek, Kubota and Tatsumi about the influence of synthesis conditions on ZSM-5 (79,80). Consequently, at a butene conversion of ~ 93% the template-free ZSM-5 leads to a rise of 5 wt. % [from ca. 46 to 51 wt. %] in the yield to propylene plus ethylene. Modifying with TMOS reduced the conversion of butene and caused an increase in ethylene and propylene yield.

A slight dealumination process was proposed by Jin *et al* for adjusting the acidity of ZSM-5 that is also relevant to Y and Beta zeolites (81). The method was then named “dry steaming dealumination” since this kind of treatment does not require extra steam or chemicals. The dealumination was done at temperatures above 400 °C by using the self-adsorbed water on the zeolite. As a result, it is easier to control the operating variables and treatment procedure compared to the conventional steaming process. Ibáñez *et al* (82) investigated the outcome of this modification through catalytic cracking of 1-butene. They noticed that strong acid sites and tetrahedral framework of Al species that are situated inside the micropores and some extra-framework species distorted as dealumination took place. Moreover, the density of the acid sites was moved to the intersections of the zeolite micropores with weaker acidity. This leads to the selective suppression of HT reactions, with the corresponding increase in selectivity towards propylene. The selectivity towards propylene got boosted up to 69 % by a 500 °C steamed catalyst, with a decrease of 34 % in coke deposition than when using a parent ZSM-5 zeolite with Si/Al = 15. Therefore, the use of modified mesoporous zeolites has been found to be the best materials for catalytic cracking in order to improve the selectivity towards propylene.

1.7 Conclusion

The use of mesoporous zeolites for catalytic cracking of paraffins and intermediate olefins is a promising method to enhance the yield of light olefins, particularly ethylene and propylene. The best advantage of using mesoporous materials is the fact that bulky molecules are able to move to and from the active sites of the intracrystalline zeolite. The existence of bigger intracrystalline pores in zeolites allows cracking of heavy molecules to occur inside the mesopores (83). In this study, the use of hierarchical macro-/mesoporous zeolites ZSM-5 zeolite crystals with variable Si/Al ratios have been investigated through catalytic cracking of hexane, dodecane and tyre derived oil to enhance selectivity to propylene. Catalytic cracking makes use of lower temperatures of roughly 450-650 °C during the production of light olefins and leads to more favourable propylene to ethylene ratios. Furthermore, catalytic cracking processing of light naphtha offers an opportunity to produce high value hydrocarbons with high octane number. Therefore, catalytic cracking is found to be a flexible route to produce both ethylene and propylene and has been considered as a best substitute for thermal cracking (83).

1.8 References

1. Sadrameli S.M. Thermal/catalytic cracking of hydrocarbons for the production of olefins: as state-of-art review. *Therm Crack Rev.* 2015;(140):102–105.
2. Siddiqui M.A.B, Aitani A.M, Saeed M.R, Al-Khattaf S. Enhancing the production of light olefins by catalytic cracking of FCC naphtha over mesoporous ZSM-5 catalyst. *Top Catal.* 2010;(53):1387–1393.
3. Sadrameli S.M. Thermal/catalytic cracking of liquid hydrocarbons for the production of olefins: A state-of-the-art review II: Catalytic cracking review. *Fuel.* 2016;(173):285–297.
4. Sattler J. J. H. B, Ruiz-Martinez J, Santillan-Jimenez E, Weckhuysen B.M. Catalytic dehydrogenation of light alkanes on metals and metal oxides. *Chem Rev.* 2014;(114):10613–10653.
5. Farkaš A, Rožić M, Barbarić-Mikočević ž. Catalytic and Thermal Cracking of Pure Hydrocarbons: Mechanisms of Reaction. *J Hazard Mater.* 2005;(41):25–33.
6. Wang Y, Yokoi T, Namba S, Kondo J.N, Tatsumi T. Catalytic cracking of n-hexane for producing propylene on MCM-22 zeolites. *Appl Catal A, Gen.* 2015;(504):192–202.
7. Gärtner C.A, Veen A.C Van, Lercher J.A. Oxidative Dehydrogenation of Ethane : Common Principles and Mechanistic Aspects. *ChemCatChem.* 2013;(5):3196–3217.
8. Jiang G, Zhang L, Zhao Z, Zhou X, Duan A, Xu C, Gao J. Highly effective P-modified HZSM-5 catalyst for the cracking of C₄ alkanes to produce light olefins. *Appl Cat A, Gen.* 2008;(340):176–182.
9. Akah A, Williams J, Ghrami M. An Overview of Light Olefins Production via Steam Enhanced Catalytic Cracking. *Catal Surv from Asia.* 2019;(23):265-276.
10. Jeong S.M, Byun Y.C, Chae J.H, Lee W. Coke Formation on the Surface of α -Al₂O₃ in the Catalytic Pyrolysis of Naphtha. *Korean Journ. of Chem Eng.* 2001;(18):842–847.
11. Karaba A, Dvořáková V, Patera J, Zámostný P. Improving the steam-cracking efficiency of naphtha

- feedstocks by mixed / separate processing. *J Anal Appl Pyrolysis*. 2020;(146):104–768.
12. He M.Y. The development of catalytic cracking catalysts: acidic property-related catalytic performance. *Catal Today*. 2002;(73):49–55.
 13. Vogt E.T.C, Weckhuysen B.M. Fluid catalytic cracking : recent developments on the grand old lady of zeolite catalysis. *Chem Soc Rev*. 2015;(44): 7342–7370.
 14. Ceerqueira H.S, Caeiro G, Costa I, Ribeiro F.R. Deactivation of FCC catalysts. *J Mol Catal A Chem*. 2008;(292):1–13.
 15. Tonetto G.M, Ferreira M.L, Atias J.A.A, de Lasa H.I. Effect of steaming treatment in the structure and reactivity of FCC catalysts. *AIChE J*. 2006;(52):754–768.
 16. Guan H, Ye L, Shen F, Song Z. Journal of the Taiwan Institute of Chemical Engineers Economic operation of a fluid catalytic cracking process using self-optimizing control and reconfiguration. *J Taiwan Inst Chem Eng*. 2019;(96):104–113.
 17. Speight, J.G, Ozum B. Petroleum Refining Processes. *Appl Catal A, Gen*. 2002;15(197):25–33.
 18. Siddiqui M.A.B, Aitani A.M, Saeed MR. Enhancing propylene production from catalytic cracking of Arabian Light VGO over novel zeolites as FCC catalyst additives. *Fuel*. 2011;(90):459–466.
 19. Awayssa O, Aitani A, Al-Yassir N, Al-Khattaf S. Modified HZSM-5 as FCC additive for enhancing light olefins yield from catalytic cracking of VGO. *Applied Catal A, Gen*. 2014; (477):172-183.
 20. Mandal S, Das A.K, Yadav A, Yadav M, Bhatnagar A, Dongara R, Venkata V, Bhaskara S, Rama S, Katravulapalli M. Fluid catalytic cracking (FCC) process for manufacturing propylene and ethylene in increased yield. *United States Patent*. 2014;(2):1-9.
 21. Weitkamp J. Catalytic Hydrocracking-Mechanisms and Versatility of the Process. *ChemCatChem*. 2012;(4):292–306.
 22. Regali F, Francesca L, Maria A, Montes V, Boutonnet M, Järås S. Effect of metal loading on activity,

- selectivity and deactivation behavior of Pd /silica-alumina catalysts in the hydroconversion of n-hexadecane. *Catal Today*. 2014;(223):87–96.
23. Bouchy C, Hastoy G, Guillon G, Martens J.A. Fischer-Tropsch waxes upgrading via hydrocracking and selective hydroisomerization. *Oil Gas Sci Technol*. 2009;(64):91–112.
24. Galadima A, Muraza O. Journal of Industrial and Engineering Chemistry Hydrocracking catalysts based on hierarchical zeolites : A recent progress. *J Ind Eng Chem*. 2018;(61):265–280.
25. Rossetti I, Gambaro C, Calemma V. Hydrocracking of long chain linear paraffins. *Chem Eng J*. 2009;(154):295–301.
26. Xu R, Pang W, Yu J, Huo Q, Chen J. Chemistry of zeolites and related porous materials: Synthesis and structure. *John Wiley Sons*. 2009;(58):361–372.
27. Nasser G.A, Kurniawan T, Tago T, Bakare I.A, Taniguchi T. Cracking of n-hexane over hierarchical MOR zeolites derived from natural minerals. *J Taiwan Inst Chem Eng*: 2016;(61):20-25.
28. Looi P.Y, Mohamed A.R, Tye C.T. Hydrocracking of residual oil using molybdenum supported over mesoporous alumina as a catalyst. *Chem Eng J*. 2012;(181–182):717–724.
29. Sekhar M.V.C. Pore Structure Engineered Catalysts for Hydrocracking Heavy Feeds. *Studies in Surface Science and Catalysis*. 1988. (38); 383–392.
30. Nihonmatsu T, Nomura M. Effect of Pore Structure of Ni-Mo/Al₂O₃ Catalysts in Hydrocracking of Coal Derived and Oil Sand Derived Asphaltenes. *Ind. Eng. Chem. Res*. 1991;(30):1726–1734.
31. Ying Z, Gevert B, Otterstedt J, Sterte J. Large-Pore Catalysts for Hydroprocessing of Residual Oils. *Ind. Eng. Chem. Res*. 2000;(34):1566–1571.
32. Puron H, Pinilla J.L, Fuente J.A.M De, Milla M. Hydrocracking of Maya Vacuum Residue with NiMo Catalysts Supported on Mesoporous Alumina and Silica-Alumina. *Energy Fuels*. 2013;(27):3952-3960.

33. Farkaš A, Rožić M, Barbarić-Mikočević Ž. Catalytic cracking of hydrocarbons over modified ZSM-5 zeolites to produce light olefins: A review. *J Hazard Mater.* 2005;(398):25–33.
34. Akah A, Al-Ghrami M, Saeed M, Siddiqui M.A.B. Reactivity of naphtha fractions for light olefins production. *Int J Ind Chem.* 2017;(8):221-233.
35. Altwasser S, Welker C, Traa Y, Weitkamp J. Catalytic cracking of n-octane on small-pore zeolites. *Microporous and Mesoporous Materials.* 2005;(83):345–356.
36. Kotrel S, Kno H, Gates B.C. The Haag-Dessau mechanism of protolytic cracking of alkanes. *Microporous and Mesoporous Materials.* 2000;(36):11–20.
37. Jentoft F.C, Gates B.C. Solid-acid-catalyzed alkane cracking mechanisms : evidence from reactions of small probe molecules. *Topics in Catalysis.* 1997;(4):1–13.
38. Anderson B.G, Schumacher R.R, Duren R Van, Singh A.P, Santen R.A Van. An attempt to predict the optimum zeolite-based catalyst for selective cracking of naphtha-range hydrocarbons to light olefins. *J Mol Cat A: Chemical.* 2002;(181):291–301.
39. John T.M, Wojciechowski B.W. On Identifying the Primary and Secondary Products of the Catalytic Cracking of Neutral Distillates. *Journal of Catalysis.* 1975;(37):240–250.
40. Foley T.D, Sohn S.W. Ethylene production by steam cracking of normal paraffins. *United States Pat.* 2012;(2):3–9.
41. Lee J.H, Kang S, Kim Y, Park S. New Approach for Kinetic Modeling of Catalytic Cracking of Paraffinic Naphtha. *Ind. Chem. Eng.* 2011;(50):4264–4279.
42. Liu J, Zhao S, Chen X, Shen B. Upgrading FCC gasoline through adsorption separation of normal hydrocarbons. *Fuel.* 2016;(166):467–472.
43. Huang X, Li H, Xiao W, Chen D. Insight into the side reactions in methanol-to-olefin process over HZSM-5 : A kinetic study. *Chem. Eng. Journ.* 2016;(299):263–275.

44. Tian P, Wei Y, Ye M, Liu Z. Methanol to Olefins (MTO): From Fundamentals to Commercialization. *ACS Catalysis*. 2015;(5):1922-1938.
45. Buchanan J.S. The chemistry of olefins production by ZSM-5 addition to catalytic cracking units. *ACS Catalysis*. 2000;(55):207–212.
46. Siddiqui M.A.B, Aitani A.M, Saeed M.R, Al-Khattaf S. Enhancing the production of light olefins by catalytic cracking of FCC naphtha over Mesoporous ZSM-5 catalyst. *Top Catal*. 2010;(53):1387–1393.
47. Mei C, Wen P, Liu Z, Liu H, Wang Y, Yang W, Xie Zaiku, Hua W, Gao Z. Selective production of propylene from methanol : Mesoporosity development in high silica HZSM-5. *Journal of Catalysis*. 2008;(258):243–249.
48. Farkaš A, Rožić M, Barbarić-Mikočević ž. A ZSM-5-based catalyst for efficient production of light olefins and aromatics from fluidized-bed naphtha catalytic cracking. *Hazard Mater*. 2005;(124):25–33.
49. Bortnovsky O, Sazama P, Wichterlova B. Cracking of pentenes to C₂-C₄ light olefins over zeolites and zeotypes role of topology, acid site strength and concentration. *Appl Cat*. 2005;(287):203–213.
50. Zhu G, Xie C, Li Z, Wang X. Catalytic Processes for Light Olefin Production. *Prac. Adv. in Petro. Process*. 2017;(5):149–168.
51. Suzuki K, Aoyagi Y, Katada N, Choi M, Ryoo R, Niwa M. Acidity and catalytic activity of mesoporous ZSM-5 in comparison with zeolite ZSM-5, Al-MCM-41 and silica-alumina. *Catalysis Today*. 2008;(132):38–45.
52. Komatsu T, Ishihara H, Fukui Y, Yashima T. Selective formation of alkenes through the cracking of n- heptane on Ca²⁺ -exchanged ferrierite. *Applied Catalysis A, General*. 2001;(214):103–109.
53. Krannila H, Haag W.O, Gates B.C. Monomolecular and Bimolecular Mechanisms of Paraffin Cracking : n-Butane Cracking Catalyzed by HZSM-5. *Journal of Catalysis*. 1992;(135):115-124.

54. Babitz S.M, Williams B.A, Miller J.T, Snurr R.Q, Haag W.O, Kung H.H. Monomolecular cracking of n-hexane on Y , MOR , and ZSM-5 zeolites. *Applied Catalysis A: General*. 1999;(179):71-86.
55. Corma A, Orchilles A.V. Current views on the mechanism of catalytic cracking. *Microporous Mesoporous Materials*. 2000;(35-36):21–30.
56. Katada N, Kageyama Y, Takahara K, Kanai T, Ara H, Niwa M. Acidic property of modified ultra stable Y zeolite: increase in catalytic activity for alkane cracking by treatment with ethylenediaminetetraacetic acid salt. *J Mol Cat A: Chemical*. 2004;(211):119–130.
57. Long, H, Wang, X, Sun, W, Guo X. Conversion of N-Octene Over Nanoscale HZSM-5 Zeolite. *Catal Letters*. 2008;(126):378–382.
58. Wang B, Manos G. Deactivation Studies During 1-Pentene Reactions Over HUSY Zeolite. *Chem Eng J*. 2008;(142):217–223.
59. Nawaz Z, Tang X, Zhu J, Wei F, Naveed S. Catalytic Cracking of 1-Hexene to Propylene Using SAPO-34 Catalysts with Different Bulk Topologies. *Chinese J Catal*. 2009;(30):1049–1057.
60. Feng X, Jiang G, Zhao Z, Wang L, Li X, Duan A, Liu J, Xu C, Gao J. Highly Effective F-Modified HZSM-5 Catalysts for the Cracking of Naphtha To Produce Light Olefins. *Energy Fuels*. 2010;(24):4111–4115.
61. Al-Yassir N, Wei F. Multifunctional Catalysis used in Thermo-Catalytic Cracking of Hydrocarbon Feedstock for the Production of Light Olefins. Concordia, Canada. 2007;(22):260–296.
62. Jung J.S, Park J.W, Seo G. Catalytic cracking of n-octane over alkali-treated MFI zeolites. *Applied Catalysis ,: General*. 2005;(288):149–157.
63. Konno H, Okamura T, Kawahara T, Nakasaka Y, Tago T, Masuda T. Kinetics of n -hexane cracking over ZSM-5 zeolites-Effect of crystal size on effectiveness factor and catalyst lifetime. *Chem Eng J*. 2012;(207–208):490–496.

64. Cordero-lanzac T, Aguayo A.T, Gayubo A.G, Castaño P, Bilbao J. Simultaneous modeling of the kinetics for n-pentane cracking and the deactivation of a HZSM-5 based catalyst. *Chem Eng J.* 2018;(331):818–830.
65. Farkaš A, Rožić M, Barbarić-Mikočević ž. Innovations in hierarchical zeolite synthesis. *J Hazard Mater.* 2005;(264):25–33.
66. Farkaš A, Rožić M, Barbarić-Mikočević ž. A new method to construct hierarchical ZSM-5 zeolites with excellent catalytic activity. *J Hazard Mater.* 2005;(21):25–33.
67. Verboekend B.D, Groen J.C, Pe J. Interplay of Properties and Functions upon Introduction of Mesoporosity in ITQ-4 Zeolite. *Adv Funct. Mat.* 2010; (20): 1441–1450.
68. Ji Y, Yang H, Yan W. Strategies to Enhance the Catalytic Performance of ZSM-5 Zeolite in Hydrocarbon Cracking: A Review. *Catalysts.* 2017;(7):367-390.
69. Chen F, Ma L, Cheng D, Zhan X. Synthesis of hierarchical porous zeolite and its performance in n-heptane cracking. *Catalysis Communications.* 2012;(18):110–114.
70. Xu S, Zhang X, Cheng D, Chen F, Ren X. Effect of hierarchical ZSM-5 zeolite crystal size on diffusion and catalytic performance of n -heptane cracking. *Front.Chem. Sci. Eng.* 2018;(12):780-789.
71. Farkaš A, Rožić M, Barbarić-Mikočević ž. Butene catalytic cracking to ethylene and propylene on mesoporous ZSM-5 by desilication. *J Hazard Mater.* 2005;(12):25–33.
72. Ji Y, Yang H, Yan W. Catalytic cracking of n-hexane to light alkene over ZSM-5 zeolite: Influence of hierarchical porosity and acid property. *Mol Catal.* 2018;(448):91-99.
73. Wang J, Yue W, Zhou W, Coppens M. Microporous and Mesoporous Materials TUD-C : A tunable , hierarchically structured mesoporous zeolite composite. *Microporous Mesoporous Materials.* 2009;(120):19–28.
74. Kustova M.Y, Rasmussen S.B, Kustov A.L, Christensen C.H. Direct NO decomposition over

- conventional and mesoporous Cu-ZSM-5 and Cu-ZSM-11 catalysts : Improved performance with hierarchical zeolites. *Applied Catalysis B: Environmental*. 2006;(67):60–67.
75. Vu X.H. Designing Hierarchical ZSM-5 Materials for Improved Production of LPG Olefins in the Catalytic Cracking of Triglycerides. *Adv. Mat Scie & Eng*. 2019;(2019):1-7.
76. Blay V, Louis B, Miravalles R, Yokoi T, Peccatiello K.A, Clough M, Yilmaz B. Engineering Zeolites for Catalytic Cracking to Light Olefins. *ACS Catal*. 2017;(7):6542–6566.
77. Sazama P, Dedecek J, Gabova V, Wichterlova B, Spoto G, Bordiga S. Effect of Aluminium Distribution in the Framework Of ZSM-5 on Hydrocarbon Transformation. Cracking of 1-butene. *J Catal*. 2008;(254):180–189.
78. Wu T, Yuan G, Chen S, Xue Y, Li S. Synthesis of ZSM-5 and Its Application in Butylene Catalytic Cracking. *J Fuel Chem Technol*. 2017;(45):182–188.
79. Yokoi T, Mochizuki H, Namba S, Kondo J. N, Tatsumi T. Control of the Al Distribution in the Framework of ZSM-5 Zeolite And Its Evaluation by Solid-State NMR Technique and Catalytic Properties. *J Phys Chem*. 2015;(119):15303–15315.
80. Pashkova V, Sklenak S, Klein P, Urbanova M, Dedecek J. Location of Framework Al Atoms in the Channels of ZSM-5: Effect of The (Hydrothermal) Synthesis. *Chem-A Eur J*. 2016;(22):3937–3941.
81. Jin L, Hu H, Zhu S, Ma B. An Improved Dealumination Method For Adjusting Acidity of HZSM-5. *Catal Today*. 2010;(149):207–211.
82. Ibanez M, Epelde E, Aguayo A.T, Gayubo A.G, Bilbao J, Castano P. Selective Dealumination of HZSM-5 Zeolite Boosts Propylene by Modifying 1-Butene Cracking Pathway. *Appl Catal A: Gen*. 2017;(543):1–9.
83. Edilene D, Ferracine S, Carvalho K.T.G, Silva D.S.A, Urquieta E.A. Carbon-Templated Mesopores in HZSM - 5 Zeolites : Effect on Cyclohexane Cracking. *Catal Letters*. 2020;(2):2–30.

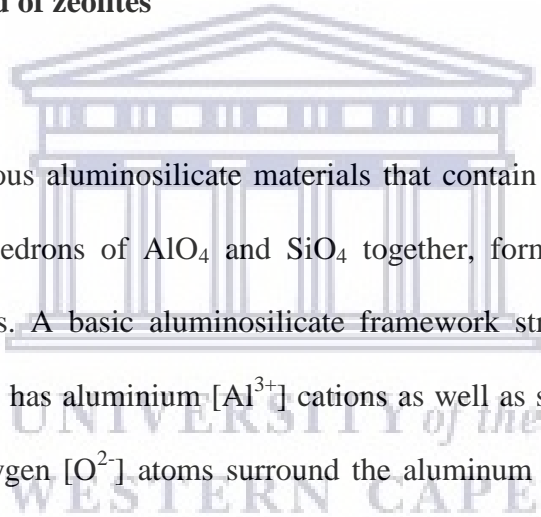
CHAPTER 2: Introduction to Zeolite Science and Practice

Chapter Overview

Chapter 2 provides a brief historical background on zeolites, specifically ZSM-5. The factors that affect the synthesis of zeolites, including the different methods used to synthesize and modify hierarchical zeolites have been discussed. Furthermore, the effects of the physical and chemical properties of the hierarchical zeolites on the performance of the catalyst are also discussed. The research aims, objectives, motivation of research and outline are also included.

2.0 A brief historical background of zeolites

2.1 Zeolites



Zeolites are crystalline, microporous aluminosilicate materials that contain pores of molecular sizes. They are made from connecting tetrahedrons of AlO_4 and SiO_4 together, forming crystalline structures with different framework arrangements. A basic aluminosilicate framework structure is used to make up all zeolites. This framework structure has aluminium [Al^{3+}] cations as well as silicon [Si^{4+}] cations that have a tetrahedral arrangement. Four oxygen [O^{2-}] atoms surround the aluminum and silicon atoms, having each [O^{2-}] inside the Al-O and Si-O bonds that connect two cations. This is shared between two tetrahedrons resulting to a macromolecular three-dimensional framework of SiO_2 and AlO_2 tetrahedral building blocks as shown in Figure 8. In this arrangement, each tetrahedron comprises four oxygen [O^{2-}] atoms that surround an Al or a Si cation, causing a formation of a silicate with a three-dimensional tetrahedral structure and a Si:O ratio of 1:2 (1). A net negative charge arises from the tectosilicate framework due to Si^{4+} ions being substituted by Al^{3+} ions [Figure 9] and this is usually positioned in single oxygen anions that are attached to some aluminium cation. In most cases, counter ions such as alkaline earth metals [Na^+ , K^+ , Ca^{2+} etc] normally balance the resultant negative sites. In other zeolites, Li^+ , Ba^{2+} and Sr^{2+} counter ions are also found (1). These ions are found on the zeolites external surface with weak electrostatic bonds that are confined with the aluminosilicate structure (2,3). These mobile non-framework counter ions are usually exchangeable

and are found in cavities which result from the 3-dimensional framework of Si-O/Al-O bond tetrahedra framework. These cavities become channels when they are aligned and H₂O molecules can be found within the cavities, hence hydration can be done on zeolites using low temperatures (4,5).

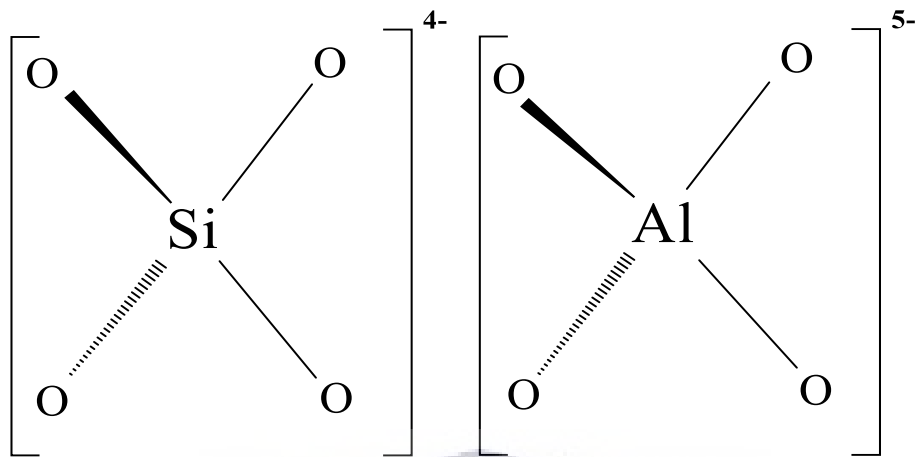


Figure 8: Unit building blocks formed by molecules of SiO₄ and AlO₄ (5).

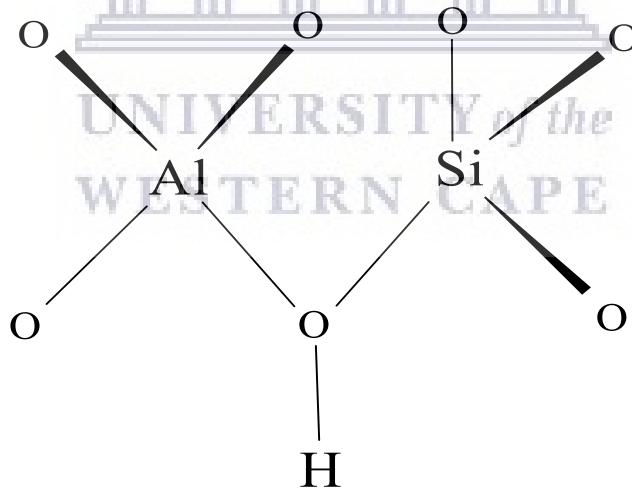


Figure 9: A part of a zeolite formed by a tetrahedral arrangement of the Si-O and Al-O bonds (5).

Zeolites have structures that reveal consistent arrangements of pores [ca. 3-15 Å] as well as porous crystals when observed on molecular scale. Many zeolites occur naturally but they can also be produced synthetically into many different kinds. The most widely used zeolites in the world are the synthetic varieties (6). More

than 40 natural zeolites so far have been found worldwide and over 150 zeolites that have been synthesized. The most regularly mined and used natural zeolites include mordenite, phillipsite, chabazite, stilbite, analcime, clinoptilolite and laumontite. Mazzite, barrerite, offretite and paulingite are the uncommon natural zeolites. The major synthetic zeolites include zeolite A, X, Y, Faujasite, ZSM-5 and mordenite (7).

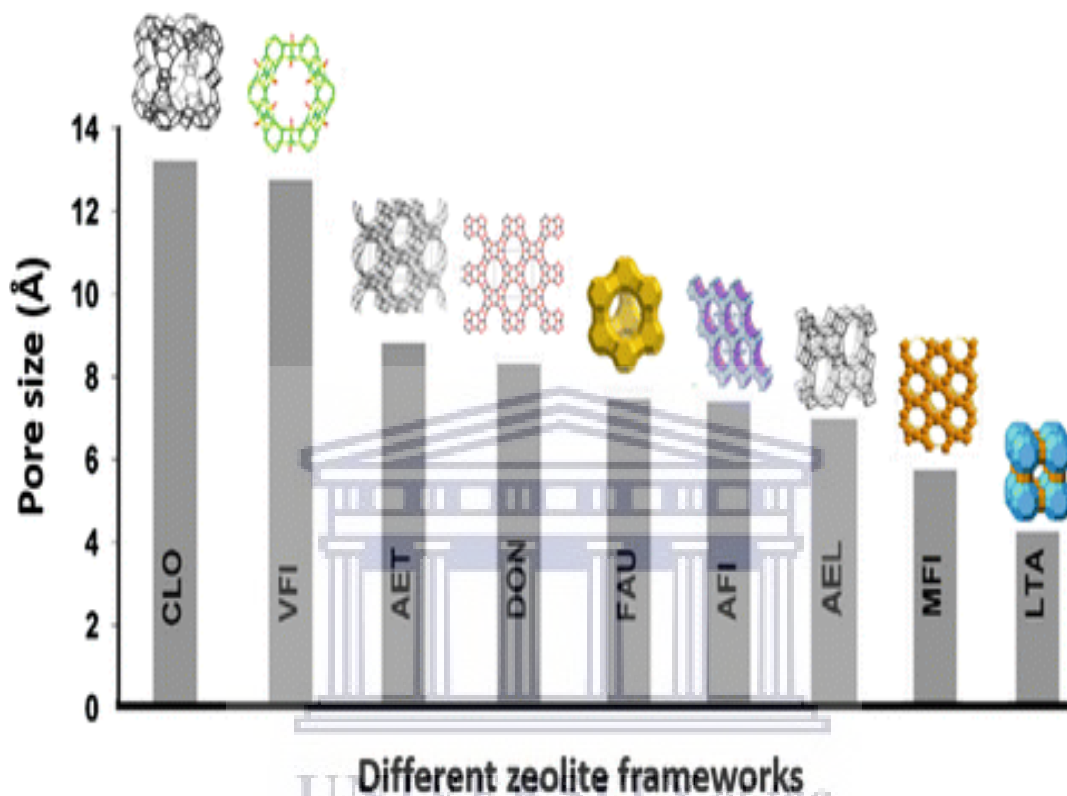


Figure 10: Most widely used zeolite framework types and their ring sizes (8).

Zeolites are usually represented as a family of open-framework aluminosilicate materials that consist of orderly dispersed micropores in molecular dimensions. Figure 10 shows the most widely used zeolite framework types and their pore sizes, with each given a three-letter code by the International Zeolite Association. The names of zeolites belong to the corresponding framework type. For example, LTA means Linde Type A, [Zeolite A], MFI means Mobil Five [Zeolite ZSM-5 and Silicate-1], FAU means Faujasite [zeolites X and Y] etc. Other widely used zeolite framework types include Mordenite [MOR], Chabazite [CHA] and Sodalite [SOD]. Based on the Si/Al molar ratio, these zeolites are classified/graded as low, intermediate and high silica zeolites as presented in Table 2 below (8–10).

Table 2: Grades of zeolites with different Si/Al molar ratio (10)

Zeolite grade	Si/Al molar ratio	Some common mineral names and their framework codes
Low silica	< 2	Analcime (ANA), cancrinite (CAN), Na-X (FAU), natrolite (NAT), phillipsite(PHI), sodalite (SOD)
Intermediate silica	2-5	Chabazite (CHA), faujasite (FAU), mordenite (MOR), Na-Y (FAU)
High silica	> 5	ZSM-5 (MFI), zeolite- β (BEA)

An MFI synthetic zeolite named as ZSM-5 from a pentasil family of zeolites is one of the best known and most commonly used zeolite type (11). It is the best used zeolite as compared to the other catalysts for hydrocarbon catalytic cracking due to its great advantages. These advantages include high surface areas, strong acid sites, good ion-exchange ability and high thermal/hydrothermal stability (12). The ZSM-5 zeolite is the catalyst used in this study and will be discussed in great length.

2.2 Zeolite ZSM-5

Zeolite ZSM-5 is a microporous material having a three-dimensional pore system with dimensions of 0.54-0.57 nm and is easy to synthesize. It is a typical molecular sieve and an important class of zeolite catalyst with a Mobil Five [MFI] topological structure. It was initially prepared in 1976 by the Mobil Oil scientists Argauer and Landolt (13). It is found to be one of the best catalysts due to the fact that it can withstand high temperatures and pressure (14). Furthermore, its catalytic performance can be improved by simply incorporating other functional components and metal oxide promoters. ZSM-5 as a catalyst has high intrinsic acidic strength and shape-selective medium-pore which allows it to have excellent catalytic properties (13–15). It is commonly applied to liquid and gas separation, petrochemical processing and fine chemical production, in reactions such as cracking, hydrocracking, oligomerization and aromatization (16,17).

A ZSM-5 structure is made of several pentasil units that are bonded together through oxygen bridges creating pentasil chains. About eight five-membered rings having vertices within the rings make up a

pentasil unit. An oxygen atom is expected to bond between these vertices of Al or Si. Corrugated sheets consisting of 10-ring holes are formed when the pentasil chains are interconnected by oxygen bridges. An Al or Si as vertices is found in each 10-ring hole having an O that is assumed to be attached between each vertex just like the pentasil units. A straight structure composed of 10-ring channels is formed when oxygen bridges bond with each of the corrugated sheets. These channels run parallel to the corrugations and sinusoidal 10-ring channels perpendicular to the sheets (18). The sheets have adjacent layers that are occupied by a reversal point and the pore sizes of the channels that run parallel with the corrugations are estimated to be 5.4-5.6 Å (19). Figure 11 below shows a molecular structure of a ZSM-5 zeolite.

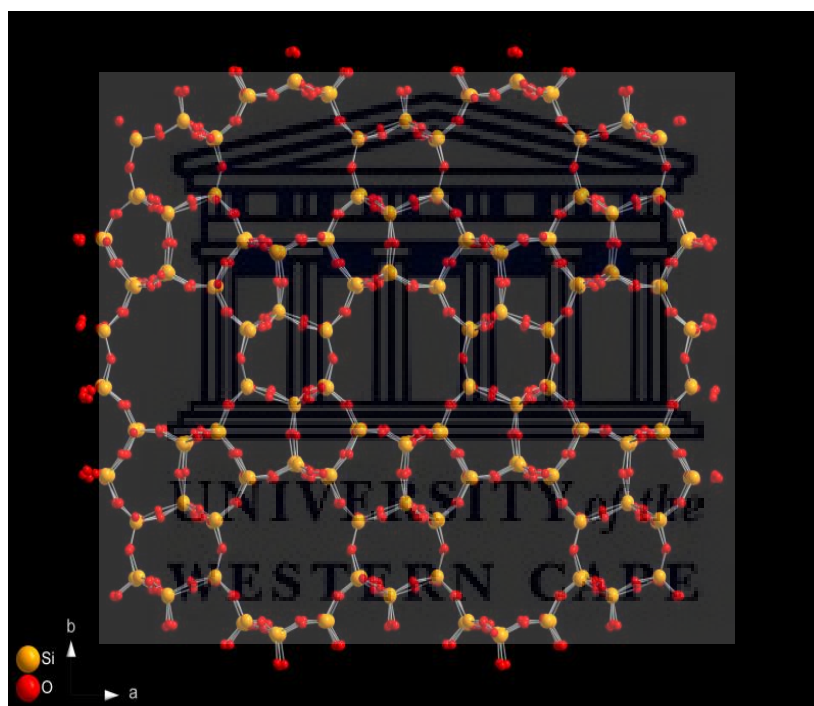


Figure 11: A ZSM-5 zeolite molecular structure displaying well-defined channels and pores within the zeolite (5).

2.3 Synthesis of zeolites

The formation mechanism of zeolites has been studied at a great extent for a long period of time and great progress has been made with respect to zeolite synthesis methods. Zeolite synthesis involves finding the conditions that are suitable enough for the formation of their structures from mixtures that contain the silica [SiO₂] and the alumina [Al₂O₃] source. This is due to the fact that zeolites are porous materials containing aluminosilicate compositions. Mineralizing agents are normally added to the solution because the silica and

alumina solubility in water is low. This causes the mixture to solubilize and leads to formation of Si-O-Si and Si-O-Al bonds. A hydrothermal process is normally used for synthesizing zeolites, making use of silica and alumina source as reagents as well as structure directing templates such as quaternary ammonium salts and mineralising agents (20,21). Zeolite formation depends on the parameters such as aging, temperature and the seeding process. The formation depends on the exact composition of the synthesis gel including pH, water content, Si/Al ratio, silica and aluminum source, type of template, template concentration and ionic strength (22). The factors affecting zeolite synthesis are discussed in further detail in the following section.

2.4 Factors that affect zeolite synthesis

During the hydrothermal synthesis, the zeolite synthesis is usually challenging and affected by different factors. These factors include temperature and pressure, reactant sources, batch composition, Si/Al ratio, water content and seeding as observed in Figure 12 below. Other factors may also include alkalinity, pH, organic templates, aging, inorganic cations, nucleation and growth (23,24). Some of the main factors which cause an influence in the type of zeolite obtained after the synthesis are highlighted below.

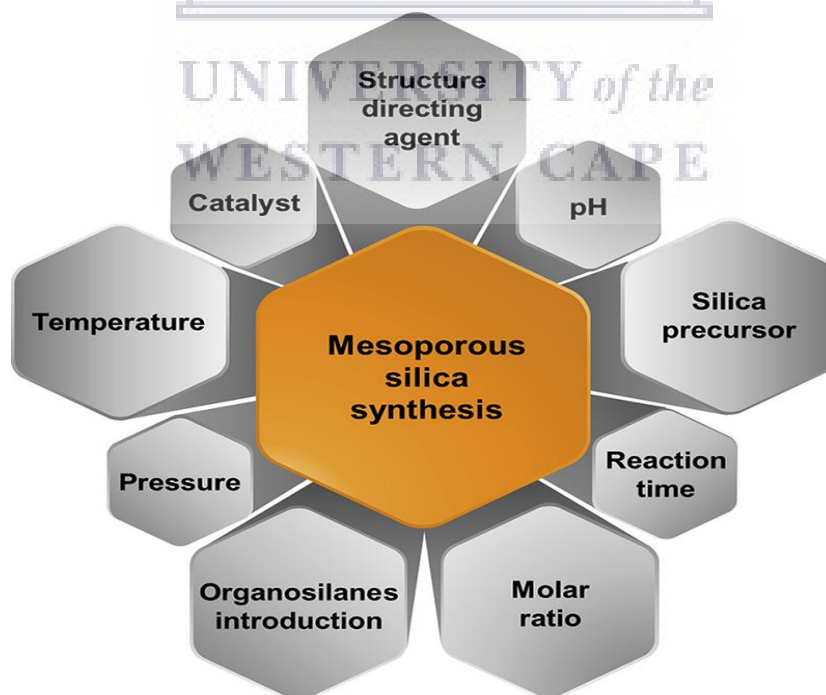


Figure 12: Different factors that affect the zeolite synthesis (25).

2.4.1 Si and Al reagents

Suitable silica reagents are defined as any silica sources that can be solubilized under hydrothermal conditions. They have common reagents that include fumed silica, sodium and potassium silicates, colloidal silica, precipitated silica, and alkoxy silanes such as tetraethyl orthosilicate. To remove the formed alcohol from alkoxy silanes, a hydrolysis step followed by the evaporation step is normally required under basic or acidic conditions to convert it into silica. The suitable alumina reagents are defined as any alumina sources that can be solubilized under hydrothermal conditions. Aluminum metal, aluminum hydroxide, gibbsite, neutral aluminas such as aluminum metal, meta-kaolin, acidic aluminas such as aluminum sulfate, basic aluminas such as sodium and potassium aluminates, boehmite aluminum nitrate, aluminum chloride and aluminum alkoxides such as aluminum isopropoxide and aluminum *sec*-butoxide are all common examples of suitable alumina sources. To achieve perfect homogeneity and reactivity of the starting synthesis gel, the neutral aluminas are normally dissolved in the hydroxide reagents before being added to the remaining ingredients. Upon deciding on what alumina reagent should be used, there are effects that need to be accounted for such as acidity, alkalinity, additional cations and any alcohol that may be formed.

2.4.2 SiO₂/Al₂O₃ molar ratio [Si/Al]

The SiO₂/Al₂O₃ molar ratio is vital in the hydrothermal synthesis process. It is believed to be associated exactly to the acidity, catalytic activity and the sorption of the zeolite materials as well as their thermal/hydrothermal and chemical stability. Zeolite types such as type A [LTA], X [FAU] and hydroxysodalite [SOD] have low Si/Al ratio [Si/Al ≤ 5]. These types are made from reaction mixtures having strong alkalinity and a low SiO₂/Al₂O₃ molar ratio. The zeolites types such as beta [BEA], ZSM-5 [MFI], and ZSM-11 [MEL] are referred to as high Si/Al ratio zeolites [Si/Al > 5]. A gel containing a high SiO₂/Al₂O₃ molar ratio and weak alkalinity or in neutral F⁻ medium is used to make these types of zeolites. Flanigen et al. (26) reported zeolites that are synthesized from a SiO₂/Al₂O₃ molar ratio [Si/Al > 10] comprising a variation of pore sizes from 0.4 to 0.8 nm. These types are found to be organophilic and hydrophobic, and include a variant of zeolites Y, beta and ZSM-5. According to Jihong (27) the required final product is not guaranteed by changing the Si/Al ratio within the original reaction mixture, unless if the

synthesis is in effective conditions for a particular zeolite. Therefore, the Si/Al molar ratio in the first reaction does not have a quantitative correlation with the one in the final product (23,28,29).

2.4.3 Organic Structure Directing Agent

Organic structure-directing agents [OSDAs] are used to control the development of certain kinds of channels and pores during the synthesis of zeolites (30). Zeolites are normally prepared from aqueous gel solutions that contain different heteroatom sources, inorganic and/or organic cations that act as structure directing agents [SDA], and the mobilizing agents e.g., hydroxyl or fluoride anions (31). To synthesize the new zeolite frameworks, the use of organic structure directing agents OSDAs is found to be one of the most important approaches. In zeolite synthesis, OSDAs are mainly used to make the development of a zeolite that would not form if it may not be used. Furthermore, the OSDAs have an impact on the gel chemistry to cause different precursors to form once they are used as a gel modifier. These different precursors go on to crystallize a framework material. In several circumstances, the OSDA is the template around which the species of silica and alumina within the gel preparation first organize and then condense to form a zeolite with cages and/ or channels of the framework that match the size of the OSDA.

Effective OSDAs have important parameters such as size, rigidity, shape and hydrophobicity. Zeolites containing bigger cages and channels are formed by larger OSDAs due to that they are combined in the pores of the zeolite (32). Flanigen (33) proposed that the inorganic cations comprise a structure directing role that is restricted and they also have an impact in the ordering of water molecules in a solution. Water molecules are also found to generate areas of micro-organisation that lead to nucleation centres when they are subsequently displaced by the silicate and the aluminate species. The formation of zeolites is highly influenced by templates or SDAs (20) by:

1. Influencing the gelation or/- nucleation process.
2. Making a chemical potential of the lattice to be lower.
3. Contributing to the stability through H-bonds and other weak interactions.
4. Using geometry to control the way a specific structure forms.

2.4.4 Effect of the Water Concentration

Producing zeolite catalysts following the hydrothermal method always require the use of water as a solvent in the presence of SDA. Water is found as a perfect solvent for solubilizing the silica, alumina, inorganic and SDA cations in the presence of hydroxide and fluoride mineralizing agents. Water normally acts as a [i] accelerator of chemical reactions, [ii] space filler, [iii] hydrolyser and reformer of the M-O-M bond [where M and O denote metal atom and oxygen, respectively], and [iv] viscosity maintaining agent. For the zeolite materials, crystal growth as well as nucleation is believed to be influenced by these non-solvent influences of water. At the surface of the growing crystal, water is a vital factor in the basic condensation reaction between silica and the alumina species. To increase the yield of the synthesis for large scale zeolites and to ease the mass transfer of the synthesis gel, H_2O/Si levels of greater than 25 are used to accomplish this (32). The structure directing ability of the template can be influenced by the amount of water used during the preparation of zeolites with high silica. This leads to the formation of different zeolites structures when the same SDA is used (34). Hydrothermal and steam assisted methods are the most widely used to synthesize zeolites using water as a solvent.

Steam assisted crystallization [SAC] also known as a dry gel conversion [DGC] method, is one of the most preferred procedures for the preparation of hierarchical zeolites. Unlike the hydrothermal technique, water vapour is used in this method to treat the dry gel so that in the crystallization process, the zeolite precursors have proximity. This can help increase the zeolite yield and form the preferred phase (35–37). Some benefits of using DGC include good control over particle size and texture, low energy and SDA consumption, and it can also maintain the synthesis gel composition, especially for the $Si/O_2/Al_2O_3$ molar ratio in the final materials. An amorphous mixed oxide is used in this technique, prepared as a dry gel and then treated under hydrothermal conditions with the use of steam and a structure directing agent. During the steaming process, the crystallization of the zeolite has been recommended to go through an orientated additional route, which involves the collection and orientation of small crystallites that lead to the formation of bigger crystals. This technique is different from the hydrothermal synthesis of zeolites according to this proposed mechanism (35). On the other hand, hydrothermal synthesis technique refers to reactions taking place beyond room temperature with 1 bar of pressure in an aqueous solution and closed system. It is classified into two

synthetic reactions namely, subcritical and supercritical. Supercritical synthesis consist of very high temperatures, roughly 1000 °C and pressure of up to 3000 bar, whereas the temperatures in subcritical synthesis are only in the range of 100-240 °C. Hydrothermal synthesis of zeolites is normally done using sealed Teflon-lined steel autoclaves (24). The synthesis is usually performed in a basic [high pH] medium by mixing together amorphous reactants that have silica and alumina with a cation source. The reaction mixture in an aqueous solution is heated in Teflon-lined steel autoclaves at high temperatures, normally above 100 °C for a specific zeolite. The reactants remain amorphous for a period of time [induction period] after raising the synthesis temperature, and then the crystalline zeolite product is detected after this period. An equal mass of zeolite crystals basically replaces all the amorphous material. The zeolite crystals are then improved by filtering followed by washing and then drying (38). The advantages of hydrothermal technique include low energy consumption, low air pollution and easy control of the solution and high reactivity of reactants (24).

2.4.5 Crystallization temperature and time

Temperature and time are the most essential and required crystallization conditions for a specific type of a zeolite. This is due to the fact that every anticipated zeolite phase has a distinct temperature range at which it can be synthesized (23). Crystallization temperature can strongly affect nucleation and the growth of crystals. The temperature is directly proportional to the crystal growth rate and the nucleation rate. Therefore, increasing temperature will lead to an increase in both factors. However, crystallinity will normally increase with an increase in crystallization time. In the work developed by Ciric (39), Kacirek and Lachert (40), they found out that the growth mechanism and the nucleation in the formation of a zeolite is influenced by crystallization temperature. Nevertheless, Zhdanov and Samulevich (41) explained that as the crystallization temperature increase, the growth and the nucleation rates also increase.

The crystallization conditions, temperature and time affect the final product formed. Ostwald's rule of successive phase transformation states that the initial metastable product forms first, which can then convert into a more stable and usually undesirable product with time. More thermodynamically stable, low porosity zeolites or non-porous dense phases such as quartz and cristobalite are more likely to form when high temperatures and longer periods of time are introduced. An amorphous or a partial crystalline product may

be formed when crystallization is very short. On the other hand, impurities may start to form when the crystallization time is too long. Crystallization time may also be longer when the synthesis temperatures are low. At high temperatures, denser phases may begin to crystallize at a short period of time even before the desired product is recovered (32).

2.5 Hierarchical zeolites

Hierarchical zeolites refers to the all the materials that contain micropores having two classes of pores (32). These hierarchical porous structures exhibit at least one extra pore system as an example of a secondary porosity. As established by the IUPAC classification, the extra porosity is normally in the mesopore size range having diameters starting at 2-50 nm or macropores larger to even greater than 50 nm. The purpose of this arise from the fact that hierarchical zeolites aim to promote entrance of large molecules to active sites of the catalyst while they also sustain the acidity and the crystallinity of the original zeolites (42,43). Studies have been conducted for the catalytic cracking of hydrocarbons using different zeolite types as catalysts. Among these catalysts, the suitable and most commonly used zeolite is an acidic type known as ZSM-5. However, the zeolite ZSM-5 has its own drawbacks. It has acid sites that are not in use, a long diffusion pathway and a modest microporous structure that allows it to possible be deactivated by deposited carbon (12). For hydrocarbon cracking reactions to occur, strong acid sites are needed for such reactions to be successful. However, when there are too many strong acid sites present within the catalyst, reactants start to over-react on them and become converted into aromatic hydrocarbons or deposited carbon which leads to the deactivation of the catalyst (12). Furthermore, a highly acidic zeolite life-time decreases because the high acidity leads to coke formation to increase on the surface of the catalyst, which may block its micropores and cause deactivation. Lastly, the distribution and the transfer of reactants and products inside the pores becomes limited because of the zeolite crystal size being bulky as compared to its micropores (44). Figure 13 below shows blocked bulky products bouncing back on a normal zeolite with only micropores but having free access on the hierarchical zeolite with both micro- and mesopores. Therefore researchers have thoroughly investigated the use of a ZSM-5 as the best candidate in catalytic cracking of hydrocarbons and

have endeavoured to improve its catalytic activity through various modifications of its porosity, acidity and crystal structure. The cracking of hydrocarbons has now been practised by various groups of researchers by making use of mesoporous ZSM-5 zeolites.



Figure 13: A parent zeolite with micropores and a hierarchical zeolite with both micro- and mesopores (45).

Hierarchical zeolites have been used regularly in reactions such as catalytic cracking, aromatization, condensation, alkylation, isomerization, condensation and conversion of methanol to hydrocarbons [MTH] (46,47). Introducing mesopores in zeolites have two direct effects such as [i] increasing the available surface area to larger molecules and [ii] it reduces the intra-crystalline diffusion length. Hierarchical zeolites generally display properties such as less coke formation and conversion of large reactants with greater activities and selectivity. These properties are all related with the easy access to the active sites and a reduced contact time for intra-crystalline diffusion. When hierarchical zeolites are used as adsorbents or separation media, they tend to reveal improved adsorption kinetics compared to conventional zeolites (48).

2.6 Methods used to synthesise hierarchical zeolites

There has been an extensive growth of interest in the research of hierarchical zeolites over the past years. Researchers have done substantial work on different synthetic strategies to prepare hierarchical zeolites and developing a variety of methods to synthesise them. This leads to the development and publication of numerous literatures every year (48,49). Hierarchical structures can be obtained using two major techniques known as the top-down and bottom-up approaches.

In **top-down approach**, post-synthetic methods are classified into three groups as [i] demetallation [desilication and dealumination], [ii] delamination and assembly and [iii] mixed techniques also known as dissolution/recrystallization are used to present an extra porosity into conventional zeolite crystals. This is done by using destructive and extractive processes to eliminate the zeolite crystals that were already formed (32). The post synthetic methods that represent the top-down approach and most regularly studied are the desilication and the dealumination approach. In this approach, microporous zeolites are initially used and then at a later stage modified synthetically to form hierarchical zeolite structures (50). Dongmin *et al* (51) performed desilication by alkali treatment to enhance the heavy oil cracking ability of ZSM-5. The results obtained reveal that desilication by NaOH, NaOH/ $[\text{NH}_4]_3\text{PO}_4$ and NaOH/Al $[\text{NO}_3]_3$ solutions can all generate a mesoporous structure to ZSM-5 zeolite. The highest mesoporous surface area was demonstrated by the ZSM-5/ NaOH/ $(\text{NH}_4)_3\text{PO}_4$ -F. After the hydrothermal synthesis, a low relative crystallinity and less acidic sites were demonstrated by the ZSM-5/ NaOH than the parent ZSM-5. However, the NaOH/ $(\text{NH}_4)_3\text{PO}_4$ and NaOH/Al $(\text{NO}_3)_3$ modified ZSM-5 samples maintained a good hydrothermal stability. A higher catalytic activity was exhibited by NaOH/ $[\text{NH}_4]_3\text{PO}_4$ and NaOH/Al $[\text{NO}_3]_3$ modified ZSM-5 samples than the ZM-5/ NaOH and parent ZSM-5 in catalytic cracking of vacuum gas oil [VGO]. Especially for NaOH/ $[\text{NH}_4]_3\text{PO}_4$ modified ZSM-5 sample, an increase in conversion of VGO from 78.91 to 85.13 % and an increase in the yield of propylene from 15.01 to 18.83 % were observed. Hartanto *et al* (52) studied the effect of alkaline treatment in the properties of hierarchical ZSM-5 prepared by post-synthesis desilication. An aqueous solution of NaOH was used to treat the ZSM-5 zeolite with different concentrations of 0.25, 0.5, 1.0 and 2.0. The highest crystallinity was achieved by NaOH 0.25M. The increase in NaOH concentration caused the particles of ZSM-5 to decrease in crystallinity severely. Furthermore, the mesopore

is extremely reduced at high concentrations, forming macropores. The occurrence of micropore and mesopore in all samples indicates that the alkaline treatment succeeded to form hierarchical ZSM-5 using different NaOH solution. Meng *et al* (53) studied the effect of dealumination of HZSM-5 by acid treatment on catalytic properties in non-hydrocracking of diesel. Modified HZSM-5 zeolites having different concentrations of HCl and different acid types were created. After dealumination by H₃PO₄ and HCl treatment, the mesopores were prepared successfully in the HZSM-5 zeolites and the acid sites were rearranged. The hydrochloric acid treated sample [HZ-1.0HA] demonstrated the best gasoline yield and diesel non-hydrocracking activity.

In the **bottom-up approach**, three preparation strategies known as [i] hard templating, [ii] soft templating and [iii] non-templating methods are used when preparing hierarchical zeolite systems. Constructive and consecutive crystallization processes are always used during the creation of hierarchical zeolites. During the procedure of the zeolite development, it is already taken into attention to implement an extra pore system when using this approach. To accomplish this, a second function is added into the crystallization system by using [i] a different template as compared to the microporous [SDA], [ii] a template that can function in various ways [iii] a growth-modifying additive, or [iv] between at least two closely related crystal systems, use an intergrowing approach, and [v] a targeted-oriented aggregation process of preformed zeolite [nano] crystals. The soft-templating method was used in this study and is explained in detail in the following section. The top-down and bottom-up approaches are schematically represented in Figure 14 below.

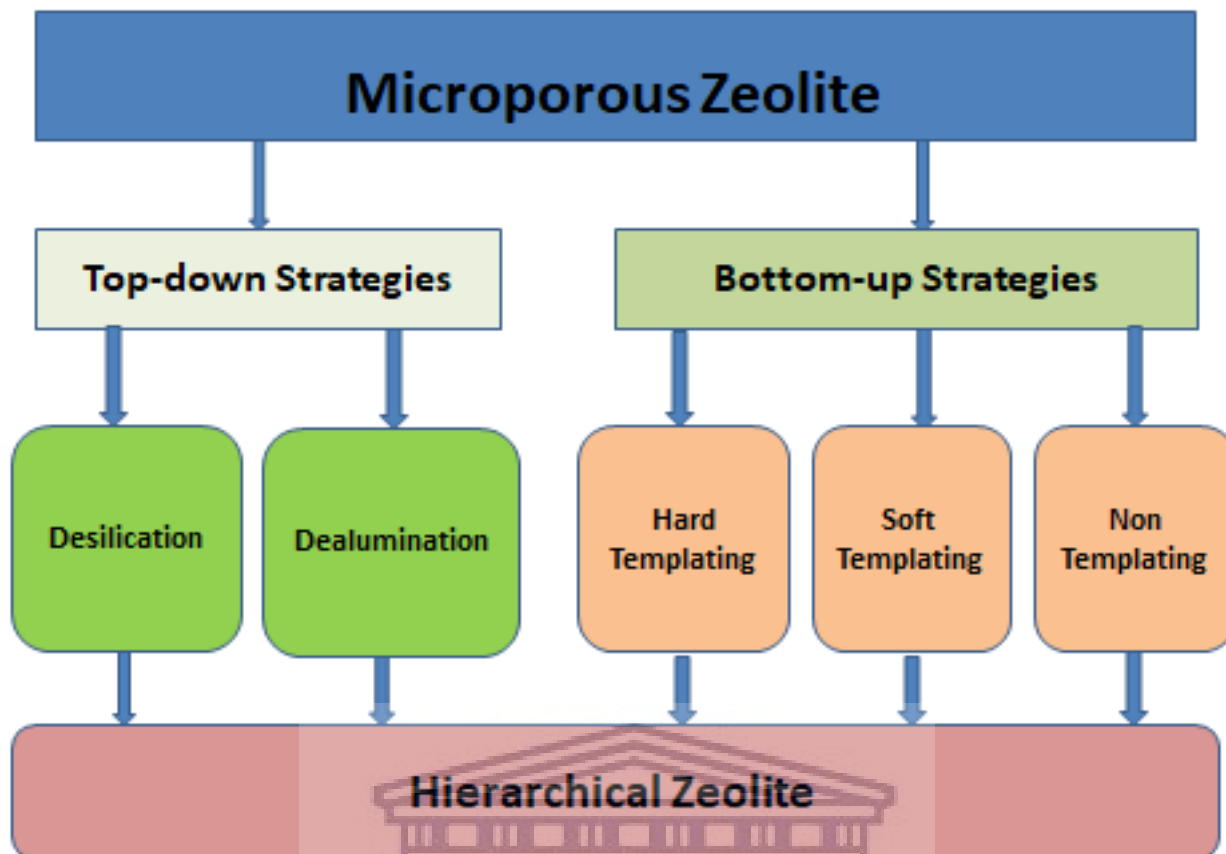


Figure 14: A diagram representing different hierarchical zeolite development approaches (54).

2.6.1 The bottom-up approaches

2.6.1.1 Hard-templating

When preparing hierarchical zeolites, hard-templating technique [also known as solid-templating] normally makes use of hard templates since they make it easy to generate mesoporosity by simple calcining them out after synthesis (55). Figure 15 below shows how the phosphate/phosphonate materials with accessible mesopores are obtained after removing the template by calcination/solvent extraction in both soft-templating and hard-templating approaches. Two conditions for this method are usually used: [i] using tiny carbon particles that are amorphous, e.g. splitting carbon black elements that have sizes of about a ten of nanometres within the zeolite synthetic gel. During the crystallization period of a zeolite, the carbon particles combine with the produced crystals and create mesopores just after the calcination step (56). However, during crystallization process, other zeolites are not persistent enough to accommodate impurity and so they limit

the achievement of this approach to MFI zeolites (57). [ii] Restricting the zeolite growth inside the empty spaces of the porous carbon (58).

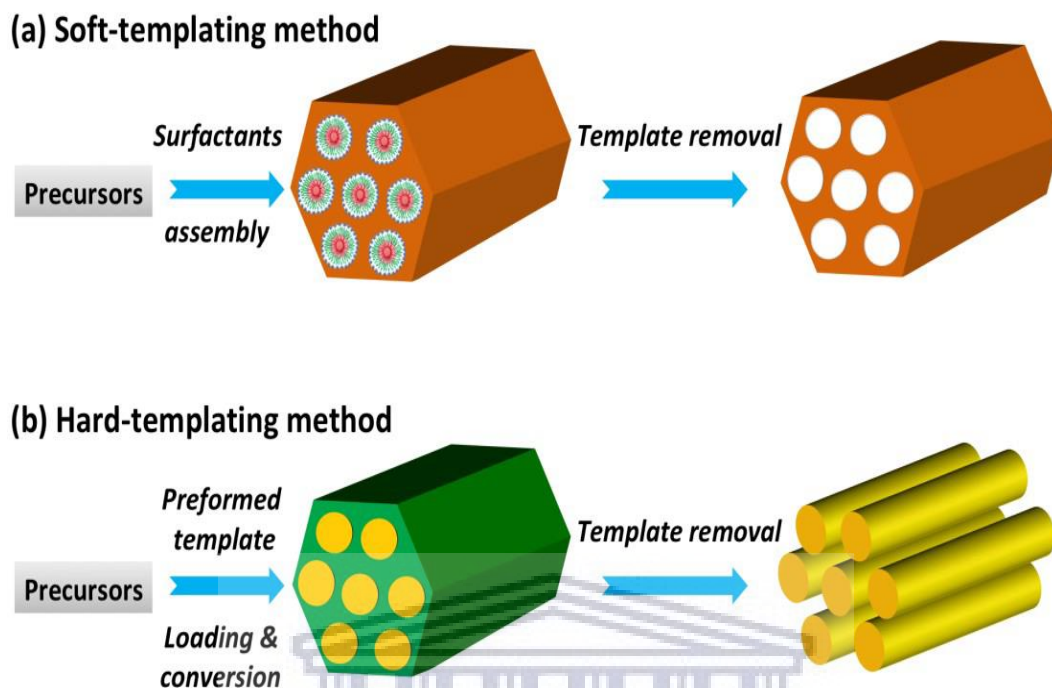


Figure 15: Schematic representation of template removal from soft-templating and hard-templating method (59).

Carbon black, carbon nanotubes and/or carbon nanofibers, carbon aerogel and other diverse well-ordered mesoporous carbon replicas are generally used as hard templates (15,60). Depending on the association and the arrangement of the templates during the synthesis route, carbon templates have an advantage of generating an extensive range of mesoporous structures, from being greatly well-organized and interconnected (56). Soltanali *et al* (61) synthesized mesoporous beta catalysts in the presence of carbon nanostructures as hard templates for use in the methanol to olefin [MTO] process. Carbon nanotubes, carbon nanofiber and graphene oxide templates were used to prepare three beta catalyst samples to study the effect of carbon nanostructures as hard templates. Another sample was also prepared in the absence of nanostructured carbon templates. The catalytic activity of the prepared catalysts was compared in the MTO conversion reaction at WHSV of 8.0 h^{-1} , atmospheric pressure and temperatures of $400 \text{ }^\circ\text{C}$. Graphene oxide was found to be the best active template on the pore size and mesoporosity of the Beta catalyst. The performance and lifespan of the catalyst were enhanced by increasing the mesoporosity.

2.6.1.2 Soft-templating

A facile soft-template method refers to supramolecular units like self-assembled arrangements of structure-directing molecules like surfactants, leading to mesopores of up to 30 nm. It is used to synthesize highly ordered mesoporous carbon nanoparticles [MCNs] with well-controlled morphology from spherical to rod-like structures (62). Surfactant molecules that are organized well within a supramolecular micelle are used to form either mesopores or both mesopores and micropores when following this method. It is usually divided into primary and secondary soft templating and hydrothermal synthesis is mostly used as a preparation method. Designed surfactants are normally employed to bring together the most important building units in a way that will create intra- or inter-crystalline mesopores in primary soft templating (63). Under the conditions of zeolite synthesis, the surfactant micelle is flexible when comparing it with the hard templates and that is why the micelle is referred to a “soft template”. The molecular operation of the functional groups as well as the geometrical packaging parameter of the surfactant is a benefit to the surfactant molecule to control the structure. Supporting extracts like swelling agents [normally trimethylbenzene], inorganic salts and co-surfactants are used to control the packaging parameter (64–66). In the soft templating approach, two functions are being fulfilled by the surfactants [i] for the formation of a zeolite, the hydrophilic part acts as a structure directing agent [*e.g.* di- or multi or multi-quaternary ammonium surfactants] or anchors the surfactant into the zeolite [organosilane surfactants] while the hydrophobic part acts as a mesoporegen (67,68). Secondary soft templating approach makes use of commercially available surfactants such as cetyltrimethylammonium bromide [CTAB].

Figure 16 below shows a proposed micro-emulsion mechanism. During the experiment, soft templates cetyltrimethylammonium bromide [CTAB] and tetrabutylammonium hydroxide [TBAOH] for the micro- and meso- structures were used, respectively. The macroporosity was created by adding ethanol during the synthesis. The steam-assisted route was used to achieve the mesoporous framework crystallization into zeolite. During the thermal treatment, adding ethanol in the mixed solution is believed to form an ‘oil-in-water’- like micro-emulsion. The droplets of ‘oil’ in the system could possibly lead to the formation of the macropores in the zeolite particles. An ‘ethanol-in-water’ micro-emulsion is believed to form under correct volume ratios of ethanol/water from 13:4 to 10:7 in this case. This is done with support of a surfactant,

CTAB, with the hydrophobic groups of the surfactant being extended into the ethanol droplets whereas the hydrophilic ends exist in the water phase. When the zeolite seeds are comprised into the emulsion above, the hydrophilic species, together with the zeolite sub-units and silica precursors should remain in the water phase. The hydrophilic inorganic precursors and free CTAB are believed to form a mesoporous structure. Ethanol and water evaporate during the gelation and drying process. This allows the self assembly route to make the mesoporous structure more ordered. The mesoporous framework crystallization, the macropore formation and the self assembly of the mesoporous structure may occur at once during the drying and steaming processes. The mesoporous framework crystallization and the self assembly may be incomplete after the steaming process and therefore, might continue and complete during the calcining step (69). This micro-emulsion mechanism has been adopted and used in the current study for the formation of hierarchical zeolites with different Si/Al ratios.

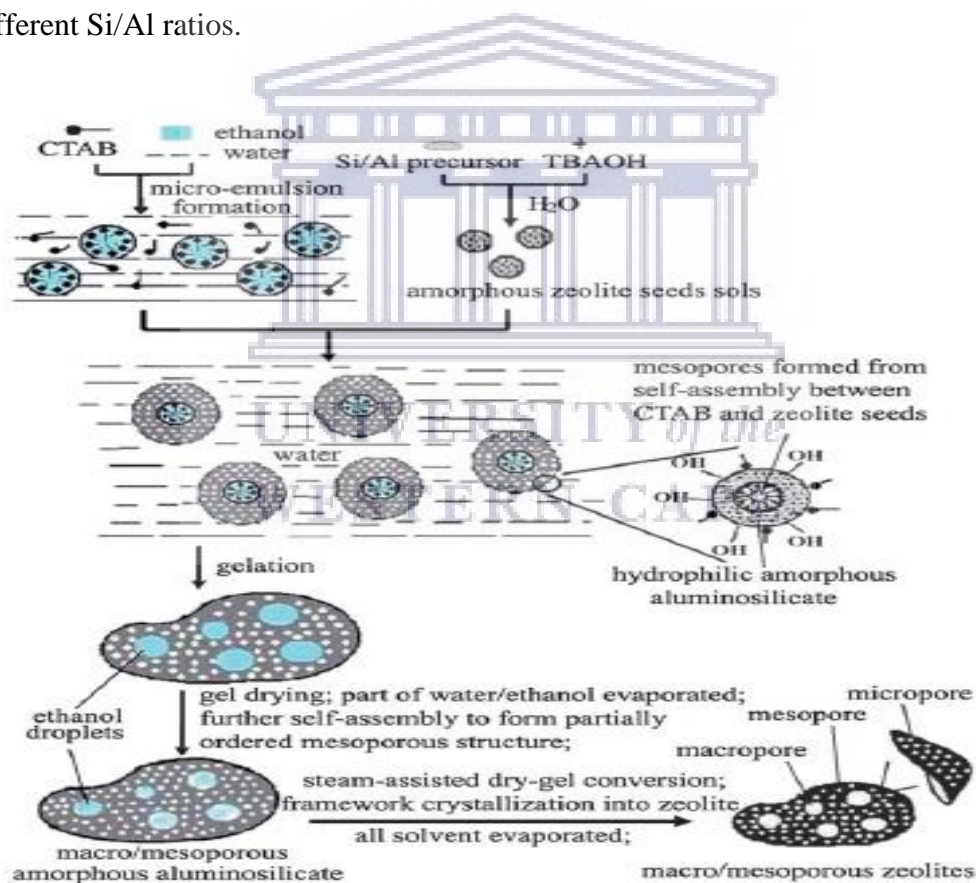


Figure 16: The fabrication of hierarchically porous tri-modal zeolites using a proposed micro-emulsion mechanism (69).

2.6.1.3 Non-templating

Non-templating method only makes use of microporous structure-directing agents and does not take into account any hard/soft templates when forming mesopores in zeolites. The production of zeolite single crystal domains with mesopores that are intracrystalline as well as the synthesis directly by nanocrystal assembly having interstitial spacing as mesopores are some of the non-templating methods used to produce hierarchical zeolites. The development of precursor nanoparticles and their growth to zeolite crystals takes place in the non-templating approach since it involves critical control over zeolite crystallization. A dry gel conversion [DGC] or a conventional hydrothermal treatment is commonly preferred by the nanocrystal assembly of hierarchical structures and a synthetic environment that prefers nucleation over the crystal growth is essential (50). In the course of hydrothermal synthesis, the adjustment of aggregation, crystal growth and nucleation helps to control self-assembly of nanocrystals during the formation of hierarchical zeolites having additional mesoporosity. Inter-growing crystallization procedure can also be done with the routine of DGC technique like steam-assisted crystallization instead of using the hydrothermal crystallization. Under thermal or mechanical stress, it is likely to lose the extra mesoporosity. Most of the time, this mesoporosity is unstable and is influenced by the degree of intergrowth. Excessive crystal twinning is one of the promising techniques used to form hierarchy by generating the extra porosity through zeolite synthesis (70). Shestakova *et al* (71) investigated the influence of template free-free conditions, seed-assisted synthesis of hierarchical ZSM-5 zeolite on its particle morphology, texture and crystallinity. They proposed a promising technique to reduce the template intake by three times during the fabrication of ZSM-5. They established that [i] the crystallinity of the resulting zeolite ZSM-5 was affected by the crystallinity and the concentration of the seed, [ii] the phase purity of the zeolite was affected by the concentration of NaOH in the reaction mixture and [iii] and increase in the $\text{Al}_2\text{O}_3/\text{SiO}_2$ molar ratio from 0.01 to 0.04 in the reaction mixture with $\text{Na}_2/\text{SiO}_2 = 0.3$ leads to a decrease in the crystallinity of the sample. The synthesized zeolite has a significant mesopore volume of $0.100 \text{ cm}^3/\text{g}$ that indicates its hierarchical pore structure as compared to the commercial sample which has bulky intergrowths of crystals.

2.7 Influence of physical and chemical properties of hierarchical zeolites on catalysis

Zeolite materials are classified as microporous materials. They exhibit a number of unique properties when they are applied in catalysis. These properties include large surface areas, strong acidic centres, high thermal stability and a well-defined system of micropores. Regardless of the advantages they possess, these materials also show diffusion limitations when branched molecules or large molecules are used in the reaction (72–74). Diffusion limitations results from the relative rigid zeolite framework and cause active sites to be difficult to access when reactants larger than the pore sizes are present in the microporous zeolite catalysts (32,57). Not all of the zeolite active sites participate in the catalytic reaction because the mass transport to and from the active sites is being limited. Only 10% and below at the edge of the large crystal might take part when there is this diffusion controlled regime. Furthermore, diffusion limitation leads to a short life span of the catalyst due to its influence on coke formation and hence catalyst deactivation. Diffusion limitations are generally experiential for solid materials that contain micropores. The transport to different reagents to and from the active sites is reduced by low diffusivities (49). Hierarchical zeolites that possess at least two levels of porosity, mainly in the mesoporous range are considered to improve these limitations. Generally, hierarchical zeolites should easily allow access of large reactants to catalytically active sites, but also maintaining the crystallinity and the acidity of the original zeolite (50,74). Therefore, an ongoing research has been done to develop more effective methods to synthesize microporous and mesoporous materials.

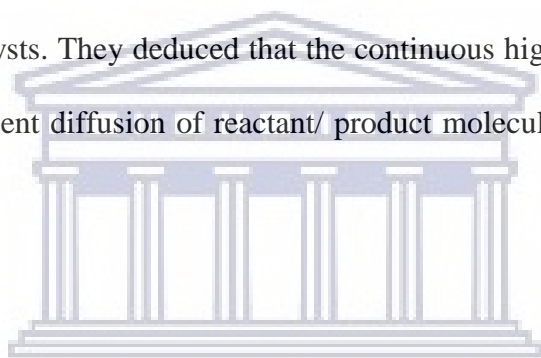
Hierarchical zeolites are prepared using two major techniques known as “top-down” which include dealumination, demetallation and recrystallization and “bottom-up” which include soft templating, hard templating and non-templating (74). The physical and chemical properties of hierarchical zeolites such as surface area, porosity, acidity and crystallinity are affected when prepared using these different methods. Removal of framework atoms such Al [dealumination] and Si [desilication] from the structure is one of the common approaches used to synthesize mesoporous zeolites by generating a secondary porosity in the zeolites. However, the use of these methods has a main disadvantage of destroying the zeolite structure during the processing and does not permit accurate control of the density, size and shape of mesopores (75). During the “desilication” method, the attained hierarchical material is characterized by the occurrence of the

secondary system of mesopores within each grain, but still retaining its acidic properties and microporous character. However, the structure and acidic properties of the attained materials gets affected during the introduction of an extra pore system during the desilication process (76). Secondly, it regularly leads to a loss of microporosity. For example, for zeolite ZSM-5 with Si/Al ratio of 42, the specific surface area of mesopores was found to be $272 \text{ m}^2/\text{g}$ and 50% of the porosity lost was recorded [the pore volume decreased from $0.17 \text{ cm}^3/\text{g}$ to $0.09 \text{ cm}^3/\text{g}$]. Therefore, the desilication method needs to be performed in a way that will produce an extra mesoporosity with little or no loss of the micropore volume and no side effect on the acidic properties of the produced materials (77). On the other hand, during the “dealumination” method, the removal of the aluminum atom is guided by incomplete breakdown of the zeolite structure and the development of vacancies. These vacancies create an extra porosity, mostly in the mesoporous range in the microporous structure of zeolite. However, serious changes may occur in acidic properties of the zeolite when removing the aluminum atoms. This depends on the applied method of dealumination. Furthermore, dealumination could possible lead to poor association and diffusion of the produced pores, followed by serious damage of crystalline properties in adverse processing conditions (78). This has motivated the searching for new methods of generating mesoporosity.

The bottom-up technique escapes these drawbacks and makes use of hard, soft and template free methods. However, in hard templating, a solid template is added during the synthesis to generate limited spaces around where the growing zeolite crystallizes. The hard template materials are then extracted using high temperature combustion, leaving mesoporous voids behind. Furthermore, it makes use of expensive templates that are commercially unprofitable. The use of template-free method has a few environmental and economic advantages such as speeding up the development of the preferred phase, reducing the amount of the used molecular template, and makes it easier to control the morphology and size of the resulting zeolite crystals. However, it is not an easy task to generate a controllable macro-/and mesoporosity without making use of the necessary templates. Therefore, this makes the soft-template method to be the best one so far due to its economic and environmental advantages, leading to its widespread use. The advantages include abundant and inexpensive template use; it does not destroy the zeolite structure and it is easier to control

the morphology and the creation of mesopores when using soft-templates during the fabrication of hierarchical zeolites (49,79).

Researchers have been preparing mesoporous zeolites while maintaining its microporosity by using the soft-templating method since it is easier to control the mesopores and the morphology of the zeolites. The synthesis of hierarchical tri-modal porous ZSM-5 zeolites, Hp-ZSM with a controllable macroporosity was reported by Junjiang *et al* (69), synthesized via steam-assisted conversion route in the presence of ethanol. The prepared materials were a new kind of hierarchical porous ZSM zeolite [Hp-ZSM] having well defined macro-/meso-/ microporous structures, a mesoporous ZSM-5 [meso-ZSM-5], a conventional ZSM-5 and an aluminum doped MCM-41 type [Al-MCM-41]. The catalytic performance of these materials was tested on catalytic cracking of benzaldehyde. The Hp-ZSM revealed high hydrothermal stability and high activity when compared to the other catalysts. They deduced that the continuous high activity of the Hp-ZSM could be attributed to the free and efficient diffusion of reactant/ product molecules that pass through the macro- and mesoporous network.



2.8 Problem Statement

ZSM-5 zeolites are attractive in the research industry due to their unique alumina crystalline structure and high surface areas. They are extensively used in various crude oil and chemical refinery processes and also in the petroleum and petrochemical industries as heterogeneous catalysts since they impose strong acidity, are highly thermal and hydrothermal stable, have superior shape selectivity and uniform micropores (17,80). However, the ZSM-5 zeolite catalyst suffers from low diffusion restrictions of the bulky reactants and products. This is caused by their small pore size which leads to slow transportation of bulky reactants and products to and from the active sites causing blockage within the zeolite crystalline when involved in the process. In the process of catalytic cracking, the diffusion of products becomes a challenge due to the microporous structure of ZSM-5. As a result, coke formation takes place due to the products being blocked in the micropores of the ZSM-5. These regular micropores have sizes normally from 0.54-0.57 nm, leading to transport limitations in catalytic applications (81). ZSM-5 zeolite catalysts also have acid sites that are not

in use, a long diffusion pathway and a modest microporous structure may cause it to possibly be deactivated by deposited carbon. Furthermore, a highly acidic zeolite life-time decreases because the high acidity leads to coke formation to increase on the surface of the catalyst, which may block its micropores and cause deactivation (12). This leads to a restriction of reactions catalysed by zeolites in many industries such as cracking, oxidation, isomerization, esterification as well as alkylation because they cannot function at their best potential. A lot of complex side reactions such as aromatization, polymerization and alkylation take place during cracking, causing coke to be formed on the catalyst. This reduces the conversion rate and product selectivity (14,82). The proposed study involves the fabrication of zeolite ZSM-5 that has variable Si/Al ratios with mesopores and macropores which are inter-connected with a microporous network. This should increase the pore sizes of the ZSM-5 and reduce the amount of coking that leads to the deactivation of the catalyst. The main aim for this is to enhance the yield of olefins, particularly propylene by improving diffusion of reactants and products to and from the catalysts, thereby also minimizing side reactions that lead to unwanted products and coke precursors (69).

2.9 Rationale and motivation for the research

Ethylene and propylene are light olefins greatly used for their importance as feedstocks for producing useful materials. These materials include ethylbenzene, vinyl chloride, ethylene oxide, polyethylene and polypropylene as well as other materials. The production of these light olefins has been achieved via steam cracking of various hydrocarbons for a number of years (83,84). The steam cracking of hydrocarbons has been used as the main route for the production of light olefins such as ethylene and propylene that are vital as feedstocks in the petrochemical industry and supplies more than 57% of global propylene as a by-product to ethylene production. Another important source of propylene that produces roughly 35% of propylene globally as a by-product to gasoline production is the fluid catalytic cracking [FCC] unit (85,86). However, steam cracking method makes use of high reaction temperatures roughly 800-880 °C which require huge amount of energy intake. This leads to large amounts of CO₂ emissions which is undesirable to the environment and could possible cause global warming. Furthermore, steam cracking has other drawbacks

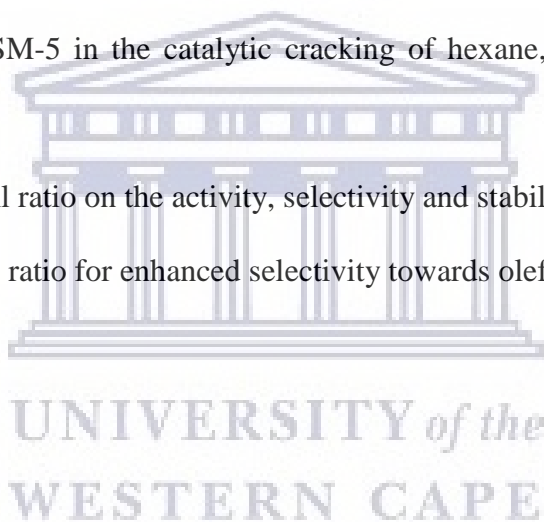
such as restricted control over propylene to ethylene ratios in the olefins that arise from steam crackers whereas the propylene demand is increasing at a fast rate as compared to ethylene (87,88). Hence, researchers have tried to find ways to develop an environmentally friendly technology to improve the production of light olefins. The catalytic cracking of the hydrocarbon feedstocks over zeolite catalysts occurs at lower temperatures of 500-650 °C as compared to the steam cracking, and leads to more favourable propylene to ethylene ratios (83). Zeolites, specifically ZSM-5 have been used to investigate catalytic cracking of several types of hydrocarbons for the production of light olefins including the naphtha range. They are useful in cracking, hydrocracking and are also widely used in the petroleum and the petrochemical industry due to that they have high thermal/hydrothermal stability, well-defined microporosity and shape selectivity (16,17). However, zeolites encounter the difficulty of restricted diffusion since they are microporous materials. Creating mesopores and/or macropores that are inter-connected within the microporous network of a zeolite but retaining its catalytic activity has been the best technique to overcome the problem. Therefore, increasing the pore sizes in the synthesized ZSM-5 will reduce the amount of coking that leads to fast deactivation. This study focuses on the synthesis of hierarchical macro and/or mesoporous ZSM-5 zeolite crystals with variable Si/Al ratios in order to enhance selectivity to propylene in the catalytic cracking of hexane, dodecane and tyre derived oil [TDO] to produce light olefins (69).

UNIVERSITY of the
WESTERN CAPE

2.10 Research aims and objectives

The aim of this project is to synthesise hierarchical macro/mesoporous ZSM-5 zeolite crystals with variable Si/Al ratios and test them as catalytic cracking catalysts. With this aim, the following objectives are required to be achieved:

- Synthesis of hierarchical ZSM-5 with variable Si/Al ratio [30, 60, 90, 150, and 300] using steam assisted hydrothermal method.
- To establish the effect of Si/Al ratio of ZSM-5 on its acidity, surface area, porosity, morphology and crystallinity.
- Characterization of the prepared catalyst using [FTIR], [XRD], [XRF], [NH₃-TPD], [TGA], [HRSEM], [BET] and [GC].
- Catalytic evaluation of ZSM-5 in the catalytic cracking of hexane, dodecane and tyre derived oil [TDO].
- Establish the effect of Si/Al ratio on the activity, selectivity and stability of the catalyst.
- Finding the optimum Si/Al ratio for enhanced selectivity towards olefins.



2.11 References

1. Armbruster T, Gunter M.E. Crystal structure of natural zeolites. *Reviews in Mineralogy and Geochemistry*. 2001;(45):1–67.
2. Farkaš A, Rožić M, Barbarić-Mikočević Ž. Ammonium exchange in leakage waters of waste dumps using natural zeolite from Krapina region, Croatia. *J Hazard Mater*. 2005;(117):25–33.
3. Widiastuti N, Wu H, Ang H.M, Zhang D. Removal of ammonium from grey water using natural zeolite. *Desalination*. 2011;(277):15–23.
4. Sponer J.E, Sobalik Z, Leszczynski J, Witchterlova B. Effect of metal coordination on the charge distribution over the cation binding sites of zeolites. A combined experimental and theoretical study. *J Phys Chem*. 2001;(105):8285–8290.
5. Farkaš A, Rožić M, Barbarić-Mikočević ž. A Review of the Chemistry, Structure, Properties and Applications of Zeolites. *J Hazard Mater*. 2005;(7):25–33.
6. Cundy C.S, Cox P.A. The hydrothermal synthesis of zeolites: History and development from the earliest days to the present time. *Chem Rev*. 2003;(103):663–701.
7. Farkaš A, Rožić M, Barbarić-Mikočević ž. Fly Ash Zeolites. *J Hazard Mater*. 2005;(78):25–33.
8. Schwanke A.J, Balzer R, Pergher S. Microporous and Mesoporous Materials from Natural and Inexpensive Sources. *Handb Ecomater*. 2017;(109):1–22.
9. Li Y, Li L, Yu J. Applications of Zeolites in Sustainable Chemistry. *Chemistry*. 2017;(3):928–949.
10. Jha B, Singh D.N. A Review on synthesis, characterization and industrial applications of fly ash zeolites. *Journal of Mataterials Education*. 2011;(33):65–132.
11. Meng L, Mezari B, Goesten M.G, Wannapakdee W, Pestman R, Gao L, Wiesfeld J, Hensen E. J. M. Direct synthesis of hierarchical ZSM-5 zeolite using cetyltrimethylammonium as structure directing agent for methanol-to-hydrocarbons conversion. *Catal. Sci. Technol*. 2017;(7):4520–4533.

12. Ji Y, Yang H, Yan W. Strategies to Enhance the Catalytic Performance of ZSM-5 Zeolite in Hydrocarbon Cracking: A Review. *Catalysts*. 2017;(7):367-390.
13. Jacobs P.A, Flanigen E.M, Jansen J.C, H van B. Introduction to Zeolite Science and Practice. Elsevier. *Stud Surf Sci Catal*. 2001;(137):1-77.
14. Narayanan S, Vijaya J.J, Sivasanker S, Ragupathi C, Sankaranarayanan T.M, Kennedy L.J. Hierarchical ZSM-5 catalytic performance evaluated in the selective oxidation of styrene to benzaldehyde using TBHP. *J Porous Mater*. 2016;(23):741-752.
15. Niu X.R, Li J, Zhang L, Lei Z.T, Zhao X.L, Yang C.H. ZSM-5 functionalized in situ with manganese ions for the catalytic oxidation of cyclohexane. *RSC Adv*. 2017;(7):50619-50625.
16. Sang S, Chang F, Liu Z, He C, He Y, Xu L. Difference of ZSM-5 zeolites synthesized with various templates. *Catal Today*. 2004;(93-95):729-734.
17. Xue T, Liu H, Zhang Y, Wu H, Wu P, He M. Synthesis of ZSM-5 with hierarchical porosity: In-situ conversion of the mesoporous silica-alumina species to hierarchical zeolite. *Microporous Mesoporous Materials*. 2017;(242):190-199.
18. Čejka J, H van B. Zeolites and Ordered Mesoporous Materials: Progress and Prospects. *Stud Surf Sci Catal*. 2005;157.
19. Catlow C.R.A, Bell R.G, Gale J.D, Lewis D.W. Modeling of Structure and Reactivity of Zeolites. 1995;(97):87-100.
20. Mohiuddin E, Markarfi I, Mdleleni M.M, Sincadu N, Key D, Tshabalala T. Synthesis of zeolites from South African kaolin clay for use as catalysts in the petrochemical industry. *Appl Clay Sci*. 2016;(119):213-221.
21. Winnie M. Mokhonoana M.P. Hierarchical zeolites: Novel supports for hydrocracking catalysts. *School of Physical and Mineral Sciences*. 2016;1-134

22. Koekkoek A.J.J, Hensen E.J.M, Santen R.A. Hierarchical ZSM-5 zeolite catalysts for the selective oxidation of benzene. *Inorganic Materials & Catalysis*. 2011;(55):189-205.
23. Farkaš A, Rožić M, Barbarić-Mikočević ž. A review on sustainable synthesis of zeolite from kaolinite resources via hydrothermal process. *J Hazard Mater*. 2005;(28):25–33.
24. Johnson E.B.G, Arshad S.E. Hydrothermally synthesized zeolites based on kaolinite: A review. *Appl Clay Sci*. 2014;(97–98):215–221.
25. Mitran R, Deaconu M, Matei C, Berger D. Mesoporous Silica as Carrier for Drug-Delivery Systems. *Nanocarriers for Drug Delivery*. 2019. (11):351–374.
26. Zimmermann N, Luis J, Perez S, Haranczyk M. High-Throughput Assessment of Hypothetical Zeolite Materials for Their Synthesizability and Industrial Deployability. *ChemRxiv*. 2019;(2):1–33.
27. Jhong Y. Studies in Surface Science and Catalysis. Introduction to zeolites. *Elsevier, Amsterdam*. 2007;(168):39–103.
28. Hu Y, Liu C, Zhang Y, Ren N, Tang Y. Microwave-assisted hydrothermal synthesis of nanozeolites with controllable size. *Microporous Mesoporous Materials*. 2009;(119):306–314.
29. Johnson E.B.G, Arshad SE. Hydrothermally synthesized zeolites based on kaolinite: A review. *Appl Clay Sci*. 2014;(97–98):215–221.
30. Simancas R, Djamal D, Noemi V, Maria T.N, Angel C, Jorda J, German S, Corma A, Rey F. Modular Organic Structure-Directing Agents for the Synthesis of Zeolites. *Science*. 2010;(330):1219–1222.
31. Trinh T.T, Tran K, Zhang X, Santen A Van. The role of a structure directing agent tetramethylammonium template in the initial steps of silicate oligomerization in aqueous solution. *Phys Chem Chem Phys*. 2015;(17):21810–21818.
32. Gebbink B.K. Hardacre C. Zeolites in Catalysis. Series Editors. *Chem Soc Rev*. 2017;(1):6-9.
33. Flanigen E.M. “A review and new Perspectives in Zeolite Crystallization,” in Molecular Sieves. *Am*

Chem Soc. 1973;(121):10–119.

34. Yu J, Ceika J, H. van B, Corma A. “Synthesis of zeolites,” in Introduction to zeolite science and practice. *Stud Surf Sci Catal.* 2007;(168):39–103.
35. Song W, Liu Z, Liu L, Skov L, Song N. A solvent evaporation route towards fabrication of hierarchically porous ZSM-11 with highly accessible mesopores. *RSC Adv.* 2015;(5):31195–31204.
36. Du Q, Guo Y, Wu P, Liu H, Chen Y. Facile synthesis of hierarchical TS-1 zeolite without using mesopore templates and its application in deep oxidative desulfurization. *Microporous Mesoporous Materials.* 2019;(275):61–68.
37. Chao P, Chen W, Lin Y, Hsu H, Asakura H. Preparation of partial crystalline mesoporous zeolite TS-1 for epoxidation of unsaturated fatty acid ester. *Catal Today.* 2020;(355):180–187.
38. Cundy C.S, Cox P.A. The hydrothermal synthesis of zeolites: Precursors, intermediates and reaction mechanism. *Microporous Mesoporous Materials.* 2005;(82):1–78.
39. Ciric J. Kinetics of zeolite A crystallization. *J Colloid Interface Sci.* 1968;(28):315–324.
40. Kacirek H, Lechert H. Rates of crystallization and a model for the growth of sodium-Y zeolites. *J Phys Chem.* 1976;(80):1291–1296.
41. Zhdanov S.P, Samulevich N.N. Nucleation and crystal growth of zeolites in crystallizing aluminosilicate gels: Proceedings of the Fifth International Conference on Zeolites. *Stud Surf Sci Catal.* 1980;(69):3-18.
42. Farkaš A, Rožić M, Barbarić-Mikočević ž. Catalysts in hydrocarbon refining. *J Hazard Mater.* 2005;(117):25–33.
43. Jin L, Liu S, Xie T, Wang Y, Guo X, Hu H. Synthesis of hierarchical ZSM-5 by cetyltrimethylammonium bromide assisted self-assembly of zeolite seeds and its catalytic performances. *React Kinet Mech Catal.* 2014;(113):575–584.

44. Alipour S.M. Recent advances in naphtha catalytic cracking by nano ZSM-5: A review. *Chinese J Catal.* 2016;(37):671–680.
45. Zhou J, Liu Z, Li L, Wang Y, Gao H, Yang W, et al. Hierarchical mesoporous ZSM-5 zeolite with increased external surface acid sites and high catalytic performance in o-xylene isomerization. *Chinese J Catal.* 2013;34(7):1429–1433.
46. Gao Y, Zheng B, Wu G, Ma F, Liu C. Effect of the Si/Al ratio on the performance of hierarchical ZSM-5 zeolites for methanol aromatization. *RSC Adv.* 2016;(87):83581–83588.
47. Na J, Liu G, Zhou T. Synthesis and Catalytic Performance of ZSM-5 / MCM-41 Zeolites With Varying Mesopore Size by Surfactant-Directed Recrystallization. *Catal Letters.* 2013;(143)267–275.
48. Liu Z, Hua Y, Wang J, Dong X, Tian Q, Han Y. Recent progress in the direct synthesis of hierarchical zeolites: Synthetic strategies and characterization methods. *Mater. Chem. Front.* 2017;(1):2195–2197.
49. Feliczak-Guzik A. Hierarchical zeolites: Synthesis and catalytic properties. *Microporous Mesoporous Materials.* 2018;(259):33–45.
50. Farkaš A, Rožić M. and Barbarić-Mikočević ž. Innovations in hierarchical zeolite synthesis. *J Hazard Mater.* 2005;(264):25–33.
51. Han D, Chen Y, Li C. The hydrothermal stability of the alkali - treated ZSM-5 and its catalytic performance in catalytic cracking of VGO. *Chem Papers.* 2019;(73):215–220.
52. Hartanto D, Wardhana D.O.K, Utomo W.P, Ni Y.L. The effect of alkaline treatment on the properties of hierarchical ZSM-5 prepared by post-synthesis desilication. *J Chem.* 2019;(12):939–946.
53. Meng X, Lian Z, Wang X, Shi L, Liu N. Effect of dealumination of HZSM-5 by acid treatment on catalytic properties in non-hydrocracking of diesel. *Fuel.* 2020;(270):117–426.
54. Jia X, Khan W, Wu Z, Choi J, Yip A.C.K. Modern synthesis strategies for hierarchical zeolites : Bottom-up versus top-down strategies. *Adv Powder Technol.* 2019;(30):467–484.

55. Tao Y, Kanoh H, Kaneko K. ZSM-5 Monolith of Uniform Mesoporous Channels. *J Am Chem Soc.* 2003;(125):6044–6045.
56. Jacobsen C.J.H, Madsen C, Houzvicka J, Schmidt I, Carlsson A, Lyngby D. Mesoporous Zeolite Single Crystals. *J Am Chem Soc.* 2000;(122):7116–7117.
57. Na K, Choi M, Ryoo R. Recent advances in the synthesis of hierarchically nanoporous zeolites. *Microporous Mesoporous Materials.* 2013;(166):3–19.
58. Li B, Sun B, Qian X, Li W, Wu Z, Sun Z, Qiao M, Duke M, Zhao D. In-Situ Crystallization Route to Nanorod-Aggregated Functional ZSM-5 Microspheres. *J Am Chem Soc.* 2013;(135):1181–1184.
59. Mei P. Synthesis of Phosphorus-Based Mesostructured / Mesoporous Materials Synthesis of Phosphorus-Based Mesostructured / Mesoporous Materials. *Adv Sci Eng.* 2018;(7):1-171.
60. Ryoo H.S.C. Microporous and Mesoporous Materials. *Int Zeolite Assoc.* 2012;(151):107–112.
61. Soltanali S, Towfighi J. Synthesis of mesoporous beta catalysts in the presence of carbon nanostructures as hard templates in MTO process. *Microporous Mesoporous Materials.* 2019;(2):169–175.
62. Li M, Xue J. Journal of Colloid and Interface Science Ordered mesoporous carbon nanoparticles with well-controlled morphologies from sphere to rod via a soft-template route. *J Colloid Interface Sci.* 2012;(377):169–175.
63. Park W, Yu D, Na K, Jelfs K.E, Slater B, Sakamoto Y, Ryong R. Hierarchically Structure-Directing Effect of Multi-Ammonium Surfactants for the Generation of MFI Zeolite Nanosheets. *Chem Mater.* 2011;(23):5131–5137.
64. Beck J.S, Vartuli J.C, Roth W.J, Leonowicz M.E, Kresge C.T, Schmitt K.D, Chu C.T-W, Sheppard E.W, McCullen S.B, Higgins JB, Schlenker JL. A New Family of Mesoporous Molecular Sieves Prepared with Liquid Crystal Templates. *J. Am. Chem. Soc.* 1992;(14):10834–10843.

65. Zhao D, Huo Q, Feng J, Chmelka BF, Stucky GD. Nonionic Triblock and Star Diblock Copolymer and Oligomeric Surfactant Syntheses of Highly Ordered , Hydrothermally Stable , Mesoporous Silica Structures. *J. Am. Chem. Soc.* 1998;(120):6024–6036.
66. Raman N.K, Anderson M.T, Brinker C.J. Template-Based Approaches to the Preparation of Amorphous , Nanoporous Silicas. *Chem Mat.* 1996;(8):1682–1701.
67. Choi M, Na K, Kim J, Sakamoto Y, Terasaki O, Ryoo R. Stable single-unit-cell nanosheets of zeolite MFI as active and long-lived catalysts. *Nature.* 2009;(461):246–249.
68. Farkaš A, Rožić M, Barbarić-Mikočević ž. Amphiphilic organosilane and seed assisted hierarchical ZSM-5 synthesis: Crystallization process and structure. *J Hazard Mater.* 2005;(221):25–33.
69. Li H, Jin J, Wu W, Chen C, Li L, Li Y, Zhao W, Gu J, Chen G, Shi J-L. Synthesis of a hierarchically macro-/mesoporous zeolite based on a micro-emulsion mechanism. *J Mater Chem.* 2011;(21):193-195.
70. Wang Z, Li C, Cho H.J, Kung S-C, Mark A. Snyder W.F. Direct, single-step synthesis of hierarchical zeolites. *A J Mater Chem A.* 2015;(3):1298–1305.
71. Shestakova D.O, Sashkina K.A, Parkhomchuk E.V. Template-Free Synthesis of Hierarchical Zeolite ZSM-5. *Pet Chem.* 2019;(59):838–844.
72. Chal R, Gørardin C, Bulut M, Donk S Van. Overview and Industrial Assessment of Synthesis Strategies towards Zeolites with Mesopores. *ChemCatChem.* 2011;(3):67–81.
73. Wei Y, Parmentier T.E, Jong K.P De, Zec J. Tailoring and visualizing the pore architecture of hierarchical zeolites. *Chem Soc Rev.* 2015;(44):7234–7261.
74. Hartmann M, Machoke G, Schwieger W, Hartmann M. Catalytic test reactions for the evaluation of hierarchical zeolites. *Chem Soc Rev.* 2016;(45):3313–3330.
75. Serrano D.P, Escola J.M, Pizarro P. Synthesis strategies in search for hierarchical zeolites. *Chem Soc*

Rev. 2013;(42):4004-4035.

76. Koohsaryan E, Anbia M. Nanosized and hierarchical zeolites: A short review. *Chinese J Catal.* 2016;(37):447–467.
77. Bonilla A, Pe J. Mesoporous ZSM-5 zeolite catalysts prepared by desilication with organic hydroxides and comparison with NaOH leaching. *Appl Catal A, Gen.* 2009;(364):191–198.
78. Triantafillidis C.S, Vlessidis A.G, Evmiridis N.P. Dealuminated H-Y Zeolites : Influence of the Degree and the Type of Dealumination Method on the Structural and Acidic Characteristics of H-Y Zeolites. 2000;(39):307–319.
79. Pérez-Ramírez J, Christensen CH, Egeblad K, Christensen CH, Groen JC. Hierarchical zeolites: enhanced utilisation of microporous crystals in catalysis by advances in materials design. *Chem Soc Rev.* 2008;(37):2530-2542.
80. Wang Y, Song J, Baxter N.C, Kuo G.T, Wang S. Synthesis of hierarchical ZSM-5 zeolites by solid-state crystallization and their catalytic properties. *J Catal.* 2017;(349):53–65.
81. Farkaš A, Rožić M, Barbarić-Mikočević ž. Butene catalytic cracking to ethylene and propylene on mesoporous ZSM-5 by desilication. *J Hazard Mater.* 2005;(12):25–33.
82. Zhou J, Hua Z, Shi J, He Q, Guo L, Ruan M. Synthesis of a hierarchical micro/mesoporous structure by steam-assisted post-crystallization. *Chem - A Eur J.* 2009;(15):12949–12954.
83. Farkaš A, Rožić M, Barbarić-Mikočević ž. Catalytic cracking of hydrocarbons over modified ZSM-5 zeolites to produce light olefins: A review. *J Hazard Mater.* 2005;(398):25–33.
84. Siddiqui M.A.B, Aitani A.M, Saeed M.R, Al-Khattaf S. Enhancing the production of light olefins by catalytic cracking of FCC naphtha over Mesoporous ZSM-5 catalyst. *Top Catal.* 2010;(53):1387–1393.
85. Chau, C, Schiller, R, Ziebarth M. Maximize petrochemicals in the FCCU to boost refinery margins,

improve gasoline pool quality. *Hydrocarb Process*. 2016;(2):45–55.

86. Sadrameli S.M. Thermal/catalytic cracking of liquid hydrocarbons for the production of olefins: A state-of-the-art review II: Catalytic cracking review. *Fuel*. 2016;(173):285–297.
87. Yoshimura Y, Kijima N, Hayakawa T, Murata K, Suzuki K, Mizukami F, Matano K, Konishi T, Oikawa T, Saito M, Shiojima T, Shiozawa K, Wakui K, Sawada G, Sato K, Matsuo S, Yamaoka N. Catalytic cracking of naphtha to light olefins. *Catal Surv Japan*.2001;4(2):157–167.
88. Rane N, Kersbulck M, Santen R.A Van, Hensen E.J.M. Cracking of n- heptane over Brønsted acid sites and Lewis acid Ga sites in ZSM-5 zeolite. *Microporous Mesoporous Materials*. 2008;(110): 279–291.



CHAPTER 3: Experimental Procedure for Catalyst Synthesis, Characterisation and Testing

Chapter Overview

The chapter begins by outlining all the chemicals used for the synthesis of the ZSM-5 catalysts with variable Si/Al ratios. It then discusses all the experimental procedures employed during the synthesis of these zeolite catalysts in detail. Furthermore, a summary of the instruments as well as the characterization techniques used in this study such as FTIR, XRD, XRF, HRSEM, NH₃-TPD, TGA, BET and GC with their description are also discussed. Lastly, the reactor description and its set-up for the evaluation of the prepared ZSM-5 materials catalysts in the catalytic cracking reaction are explained in detail.

3.0 Experimental Section

3.1 Chemicals used for synthesis

Table 3 below shows all the chemicals and reagents used in all the procedures in this study to synthesis the zeolites. All the chemicals used were supplied by Sigma Aldrich and used as they are with no further purifications.

Table 3: A list of chemicals and reagents used for synthesis of zeolites as well as their composition

Chemicals	Assay (%)
Sodium aluminate	50-56 (Al ₂ O ₃), 40 – 45 (Na ₂ O)
Tetrabutylammonium hydroxide	40 in H ₂ O
Tetraethyl orthosilicate	98
Hexadecyltrimethylammonium bromide	99
Ethanol	99.8
Ammonium Nitrate	99

3.2 Synthesis of materials

The procedures below were employed during the synthesis of hierarchical ZSM-5 zeolites with variable Si/Al ratios.

3.2.1 Synthesis of ZSM-5 zeolite solution

All the ZSM-5 zeolites were prepared via a steam-assisted hydrothermal synthetic approach making use of stoichiometric quantities of sodium aluminate [NaAlO₂], TBAOH and TEOS. For example, to synthesize ZSM-5 with Si/Al ratio of 60 in the batch mixture, approximately 8.25 ml of distilled water was used to disperse 0.0784 g of NaAlO₂ under continuous stirring in a 100 ml beaker. While stirring continuously, 2.74 ml of TBAOH aqueous solution was then added dropwise, resulting in a clear solution. 6.2 ml of TEOS was then added to the solution and the stirring continued for another 2 hours. The stirrer was stopped and the solution was left to rest overnight with no further stirring or any movement (1).

3.2.2 Synthesis of hierarchical ZSM-5 zeolite with different Si/Al ratios.

Hierarchical zeolite ZSM-5 with different Si/Al ratios of 30, 60, 90, 150 and 300 were synthesized employing the following procedure. Approximately 1g of CTAB powder was dispersed in 7 ml distilled water under continuous stirring using a 100 ml beaker. 10 ml of pure ETOH was then added to this solution while stirring forming a transparent solution. This prepared solution was then added under dropwise stirring to the zeolite ZSM-5 solution prepared in the above procedure 3.2.1, leading to a formation of white gel crystals and then left to continue stirring for 24 hours. After stirring for 24 hours, a mixture of thick white gel crystals was formed and dried for another 24 hours at 60 °C using an oven. A dry white powder [4.12 g] was obtained after drying, crushed and grinded into a fine white powder using a mortar and a pestle. A process known as recrystallization was then performed where the zeolite powder was heated at high temperatures of 150 °C with little addition of distilled water [5.24 ml] for 48 hours using a plastic Teflon flask placed inside a large stainless steel autoclave. Distilled water was then used to thoroughly wash the obtained product, which was then filtered and dried in air overnight. The final product obtained was then calcined at 550 °C for 6 hours to remove organic agents, producing a Na-ZSM-5. The other ratios were obtained by varying the amount of NaAlO₂ in procedure 3.2.1 (1).

3.2.3 Modification of ZSM-5 with Si/Al ratio of 30

The modified Si/Al ratio of 30 was prepared following the same procedure as 3.2.1 and 3.2.2 but with some modifications in procedure 3.2.2. The only difference was that the recrystallization process was performed at different temperatures and time. At first, the zeolite powder was heated at high temperatures of 150 °C with little addition of distilled water for 72 hours this time. Secondly, at 150 °C for 120 hrs, and lastly at 180 °C for 120 hrs using a plastic Teflon flask placed inside a large stainless steel autoclave.

3.2.4 ZSM-5 ion exchange from sodium form to hydrogen form

Ion exchange of Na-ZSM-5 was performed at 80 °C using a 1M solution of NH_4NO_3 under reflux. Typically, 50 ml of the NH_4NO_3 solution was used for every 1g of the zeolite and stirred for 24 hours in a round bottom flask to obtain NH_4^+ - ZSM-5. The obtained product was then thoroughly washed with distilled water, filtered and dried in air overnight. A ZSM-5 in hydrogen form was finally produced by calcining the NH_4^+ -ZSM-5 at 550 °C for 3 hrs to decompose ammonium ions (2).

3.3 Characterization of Materials

3.3.1 X-ray fluorescence [XRF] spectroscopy

X-ray fluorescence [XRF] method [Instrument PANalytical, Rh tube, 2.2 Kw] was performed in the study to determine the Al_2O_3 and the SiO_2 contents in the prepared zeolite materials. A major element analysis was done and the chemical composition results were determined and displayed in oxide form for each element.

3.3.2 Fourier-Transform Infra-Red Spectrometry [FT-IR]

FT-IR spectroscopic analysis was done in this study using a Perkin Elmer Spectrum 100 series Attenuated Total Reflection [ATR] FT-IR spectrometer to evaluate the functional groups present in the synthesized zeolite materials. The zeolite powder was first grinded into a fine powder using a mortar and pestle, and then 0.01 g of the sample was placed on the ATR diamond crystal plate in the sample slot. Basically, the spectroscopy requires that the sample of interest to be in good contact with the crystal, therefore a force

gauge was used and set to 65 [arb. units]. The spectra for all the samples were recorded from 400-1800 cm^{-1} wavenumber region at room temperature.

3.3.3 X-ray Diffraction [XRD]

X-ray diffraction analysis was done in this study using a multi-purpose X-ray diffractometer, manufactured from BRUKER AXS [Germany] with a D8 Advance diffractometer, a Lynx Eye [Position sensitive detector] used to record diffraction data at a typical speed of 0.5 sec/step and a Cu-K α radiation ($\lambda K\alpha_t = 1.5406 \text{ \AA}$) tube in a 2θ range of 0.5 to 130°. The XRD analysis was done to determine the crystal structure, phase purity and the crystal size of the synthesized zeolite materials. The XRD patterns were all taken from 0 – 60 within a 2θ (degree) range defined by the user with a size of 0.034° in 2θ . The XRD patterns were then used to calculate the crystallinity of the prepared zeolite materials.

3.3.4 High Resolution Scanning Electron Microscopy [HRSEM]

HRSEM analysis was employed in the study to establish the surface morphology as well as the elemental composition of the prepared zeolite catalysts. SEM images were obtained using an AURIGA Field Emission High Resolution Scanning Electron Microscope with a SmartSEM imaging software, supplied by Zeiss Company from Germany. The microscope uses 5 KeV for measuring images and a 20 KeV used for energy dispersive x-ray spectroscopy [EDS]. For the analysis, aluminum stubs onto which carbon tabs were placed were used to mount the samples. All the samples were then carbon coated prior to analysis.

3.3.5 NH₃-Temperature programmed desorption [NH₃-TPD]

NH₃-TPD analysis was performed in this study using an Autochem II Micromeritics chemisorption analyser to evaluate the strength as well as the amount of acid sites in the prepared ZSM-5 zeolites. A quartz U-tube reactor and quartz wool were used to perform the NH₃-TPD experiments, whereby a small piece of quartz wool was placed inside the U-tube reactor to support the catalyst. The experiment was performed by loading 0.1 g of the catalyst inside the U-tube reactor, on top of the quartz wool. This was then activated by simple increasing the heat to 500 °C and holding for 20 minutes under helium flow at 30 ml/min. The catalyst was then allowed to cool down to 120 °C under flowing helium [He], then after the gas was switched to 5% ammonia [NH₃] to balance helium. NH₃ was then absorbed at 120 °C for 60 minutes at a flow rate of 10

ml/min. Physically adsorbed NH_3 was then removed by flowing helium once more over the catalyst, then the chemically bonded NH_3 was desorbed. In this case, the temperature was ramped up to $800\text{ }^\circ\text{C}$ at a rate of $10\text{ }^\circ\text{C}/\text{min}$ while the flow rate was kept constant at $25\text{ ml}/\text{min}$

3.3.6 Thermogravimetric analysis [TGA]

Thermogravimetric analysis [TGA] was performed in this study to determine the thermal stability and the fraction of the volatile components on the prepared zeolite catalysts. This is done by monitoring the weight change that take place while a sample is heated at a constant rate. A Perkin Elmer STA 6000 Simultaneous thermal analyser was used to obtain the TGA profiles of the prepared materials. The samples were heated at a constant rate of $10\text{ }^\circ\text{C}/\text{min}$ from 30 to $900\text{ }^\circ\text{C}$ in argon.

3.3.7 Brunauer Emmett and Teller [BET]

BET multipoint method was used in this study to determine the pore-size distribution as well as the pore volumes and surface area measurements of the synthesised catalysts. A Micromeritics 3 Flex. Surface Area and Porosity Analyser was used to obtain the N_2 adsorption and desorption isotherms at $-196\text{ }^\circ\text{C}$. Prior to N_2 physisorption, approximately 0.3 g of the sample was degassed for 1 hour at $90\text{ }^\circ\text{C}$ and then the temperature was taken up to $400\text{ }^\circ\text{C}$ for another 4 hours using an inert gas to remove the remaining water inside the catalysts pores.

3.3.8 Gas Chromatography [GC]

Hydrocarbon products [liquids and gases] produced were analysed using an offline Gas Chromatography [GC] Table 4 and 5 below shows the specifications of the used GC for both gas and liquid analysis.

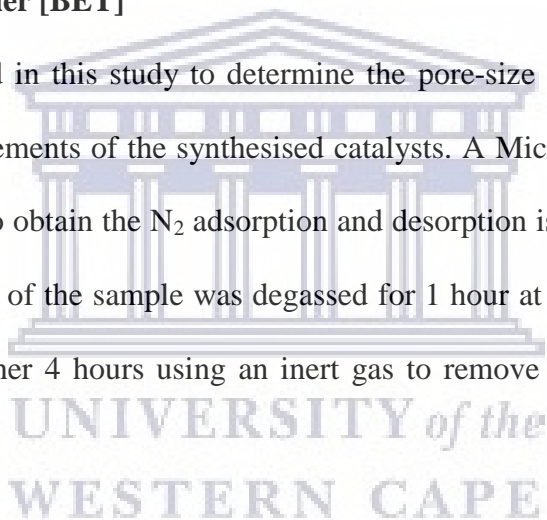


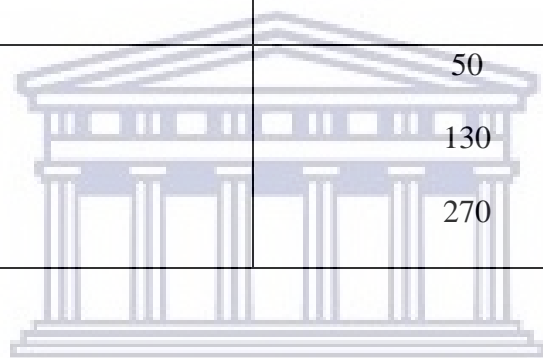
Table 4: Specifications of the GC used for gas hydrocarbon analysis

Instrument	Bruker 450-GC	
Column	BR-Alumina-Na ₂ SO ₄ , 50m x 0.53 mm ID x 10 µm	
Detector Temperature	FID @ 375 °C	
Carrier Gas	Helium	
Injection Temperature	220 °C	
Oven Temperature Program		
Rate (°C/min)	Final Temperature (°C)	Hold Time (min)
	50	10
8	190	2.5

Table 5: Specifications of the GC used for liquid hydrocarbon analysis

Instrument	Bruker 450-GC
Column	RTX®-100-DHA – 100m x 0.25 mm ID x 0.5 µm stationary phase
Detector	FID @ 350 °C
Carrier Gas	Helium
GC injector program	

Injection Temperature	250 °C	
Injection Mode	Split less	
Injection Volume	1.0 µl	
Oven Temperature Program		
Rate (°C/min)	Final Temperature (°C)	Hold Time (min)
	0	15
1	50	0
2	130	0
4	270	0



UNIVERSITY *of the*
WESTERN CAPE

3.4 Catalyst testing

3.4.1 The reactor description and set-up

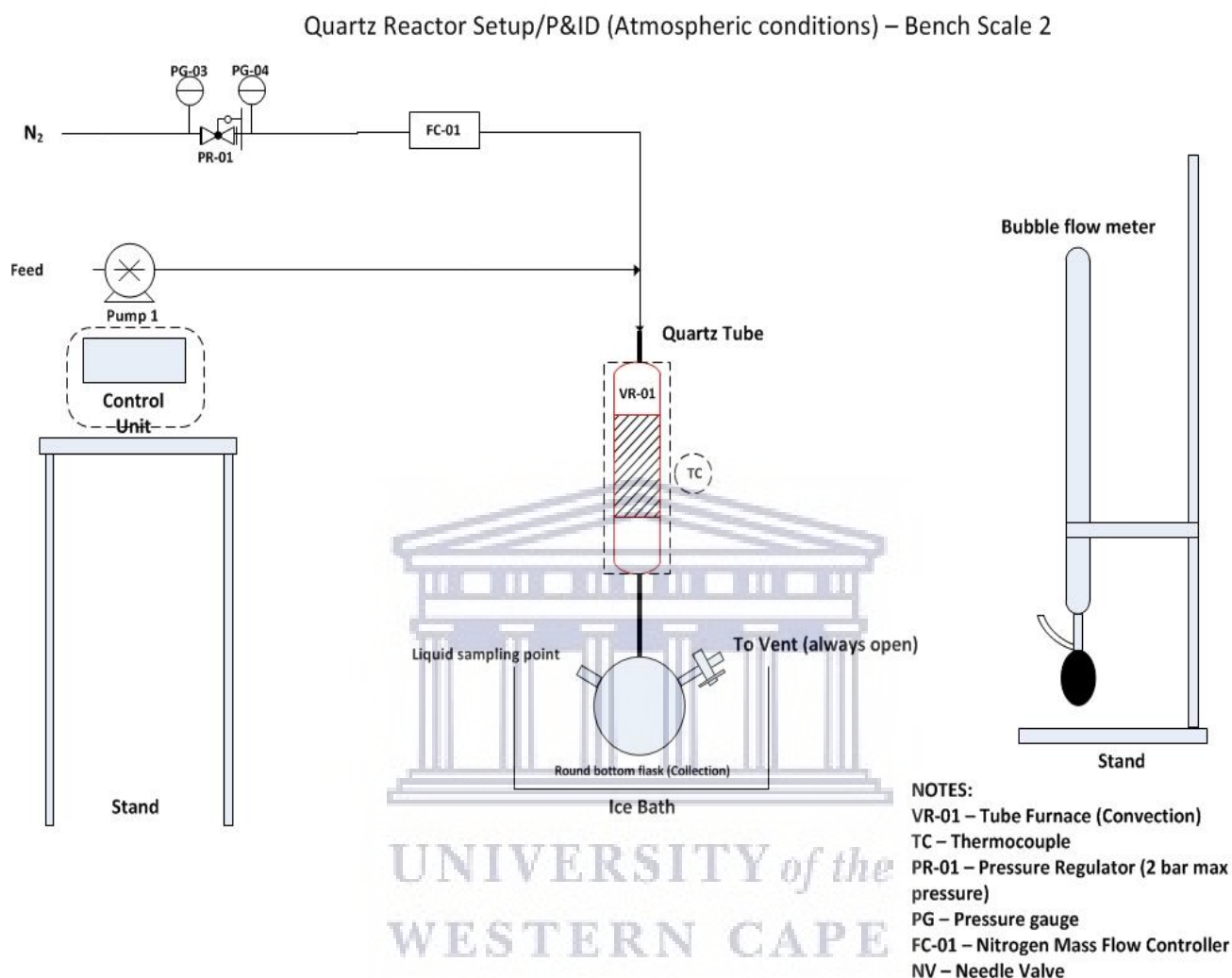


Figure 17: Reactor description and setup.

Catalytic cracking of hexane was performed over a ZSM-5 zeolite catalyst on a bench-scale quartz tube reactor. A small amount of quartz wool was placed inside the reactor as a catalyst support. The required amount of the ZSM-5 catalyst was then inserted inside the quartz tube reactor and then the reactor is placed inside a heating furnace. The quartz wool was also packed at the bottom and top of the furnace openings so as to keep the temperature constant and to prevent heat from escaping. The furnace has a thermocouple which is placed next to the catalyst. A control unit box was then used to set the temperature to be used throughout the reaction. The feed [hexane] used during the reaction was filled up inside a syringe which was then connected to a pump. The pump was used to set and control the feed flow rate. The pump was

connected to the inlet of the reactor via a Teflon tube. Another tube was fitted to the top inlet of the reactor for the nitrogen is flow. A Bronkhorst High-Tech mass flow was used to set and control the nitrogen flow rate. A round bottom flask was connected at the bottom outlet of the reactor to collect liquid products. The round bottom flask has two outlets; one is used to collect the liquid products and a second vent to insert a Tedler bag that collects the gas products. An ice bath was placed under the round bottom flask to keep the liquid samples cool and to avoid them from evaporating. A bubble flow meter was also connected at the second vent and is used to measure the flow rates of the nitrogen and gas products. The flow rate of nitrogen was varied to study the effect of nitrogen: feed ratio. The weight hourly space velocity [WHSV], which is defined as the weight in grams of feed that passes over a gram of catalysts per hour was used to adjust the contact time. The calculations for the WHSV are shown below:

$$WHSV = \frac{\text{mass of feed}}{\text{mass of catalyst}}$$

Density of the feed is used to calculate its mass as shown below:

$$m = \rho \times v$$

Where;

0.659 g/ml is the density of hexane at 25 °C

Since the volume is given by the flow rate of the feed, the mass of the feed is determined as shown below:

$$mass_{C_6} = 0.659 \frac{g}{ml} \times 0.1 \text{ ml/min}$$

$$mass_{C_6} = 0.0659 \text{ g/min}$$

Conversion from mass per minutes to mass per hours is given by:

$$mass_{C_6} = 0.0659 \frac{g}{min} \times \frac{60 \text{ min}}{1 \text{ hr}}$$

$$mass = 3.954 \text{ grams/hr}$$

When 0.25 g of the catalyst is used, the WHSV is calculated as:

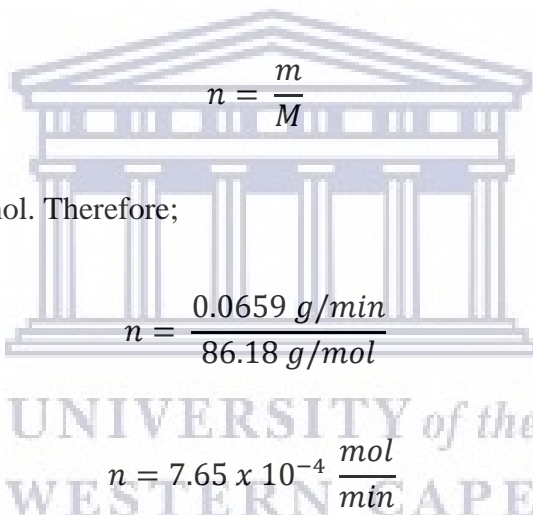
$$WHSV = \frac{3.954 \text{ g/hr}}{0.25 \text{ g}}$$

$$WHSV = 15.82 \text{ hr}^{-1}$$

The WHSV is therefore 16 hr^{-1}

0.0659 g/min is the amount of Hexane to be flown, taken from the above calculations and needs to be converted to mol/min.

To obtain the different dilution ratios of feed to nitrogen ratios [1:1, 2:1, and 3:1], calculations for flow rate of nitrogen were performed as shown below:


$$n = \frac{m}{M}$$

Molar mass of hexane = 86.18 g/mol. Therefore;

$$n = \frac{0.0659 \text{ g/min}}{86.18 \text{ g/mol}}$$
$$n = 7.65 \times 10^{-4} \frac{\text{mol}}{\text{min}}$$

The flow rate for each dilution with the molar ratio is obtained using $PV = nRT$ as shown below:

$$nN_2 = nC_6H_{14}$$

Thus $7.65 \times 10^{-4} \text{ mol/min}$ is for one mole ratio of feed to one mole ratio of nitrogen (1:1).

Using the ideal gas constant, $R = 8.314 \text{ Pa m}^3\text{K}^{-1}\text{mol}^{-1} \times 298 \text{ K}$, we get:

$$V = \frac{nRT}{P}$$

$$V = \frac{7.65 \times 10^{-4} \frac{\text{mol}}{\text{min}} \times 8.314 \text{ Pa m}^3\text{K}^{-1}\text{mol}^{-1} \times 298 \text{ K}}{101325 \text{ Pa}}$$

$$V = 1.87 \times 10^{-5} \frac{m^3}{min}$$

Multiplying the volume by 1 000 000 since there are 1 000 000 ml in m³ gives;

$$V = 18.7 \frac{ml}{min}$$

Table 6 below shows other dilution ratios obtained by simple multiplying the above volume for 1:1 by the factor of each dilution ratio.

Table 6: Different dilution ratios used for nitrogen to feed flow rate

Dilution Ratio	Feed at 0.10 ml/min in grams	Nitrogen
1:1	0.0659 g/min	18.7 ml/min
2:1	0.0659 g/min	37.4 ml/min
3:1	0.0659 g/min	56.1 ml/min

3.4.2 Experimental procedure

The catalytic cracking of hexane was performed on a bench-scale quartz tube reactor according to the setup discussed in section 3.4.1 above. Initially, 0.25g-0.75 g of the catalyst was loaded into the reactor with quartz tube inside it. The heating furnace was then set-on to the desired temperatures of 450-550 °C. Nitrogen was then flown at low flow rate ~ 10 ml/min to keep the reacting environment inert while ramping up the temperature. When the desired temperature is reached, the flow rate is then set to be the desired flow of 18.7-56.1 ml/min. The gas flow rate was monitored hourly to verify whether the initial flow rate is still maintained. All the reactions were performed at atmospheric pressure. The pump is then set-on to pump the

required amount [0.1 ml/min] of the feed into the reactor. Firstly, the pump has to be primed until it reaches the head of the Teflon tube and that of the reactor. The reaction is timed from when the first drop of feed enters the reactor. The reaction was then run for 6 hours in total and the products [liquids and gases] were collected every hour of the run and analysed on the GC. The selectivity and the conversion was calculated using equation 1 and 2 below.

$$\text{Selectivity of olefins (\%)} = \frac{\% \text{ content of olefins in product}}{\text{conversion(\%)}} \times 100 \quad \text{equation 1}$$

$$\text{Conversion (\%)} = \frac{\text{Feed}_{\text{in}} - \text{Feed}_{\text{out}}}{\text{Feed}_{\text{in}}} \times 100 \quad \text{equation 2}$$

3.4.3 Product analysis

The product spectrum was divided into two parts which are the [i] gas and [ii] liquid hydrocarbon products. Both hydrocarbon products were analysed on offline GCs.

To identify the produced gas and liquid hydrocarbons, a gas and a liquid standard obtained from PetroSA were used to calibrate the GCs. A GC trace of the gas and liquid standard used for calibration are provided in Figures 18 and 19 respectively. The gas calibration demonstrates products that are obtained in the C₁-C₅ range. The liquid calibration demonstrates the products obtained in the C₃-C₁₉ range. Products in the liquid samples from C₃-C₅ range were grouped together with the gases. Afterwards, all the hydrocarbon products having the same carbon number were also grouped together. The GC was calibrated using pure hexane which was used as a feed in most reactions carried out in this work. A trace of pure hexane calibration is provided in Figure 20 respectively. This was used to calculate the percentage conversion of hexane by identifying the retention time at which it elutes.

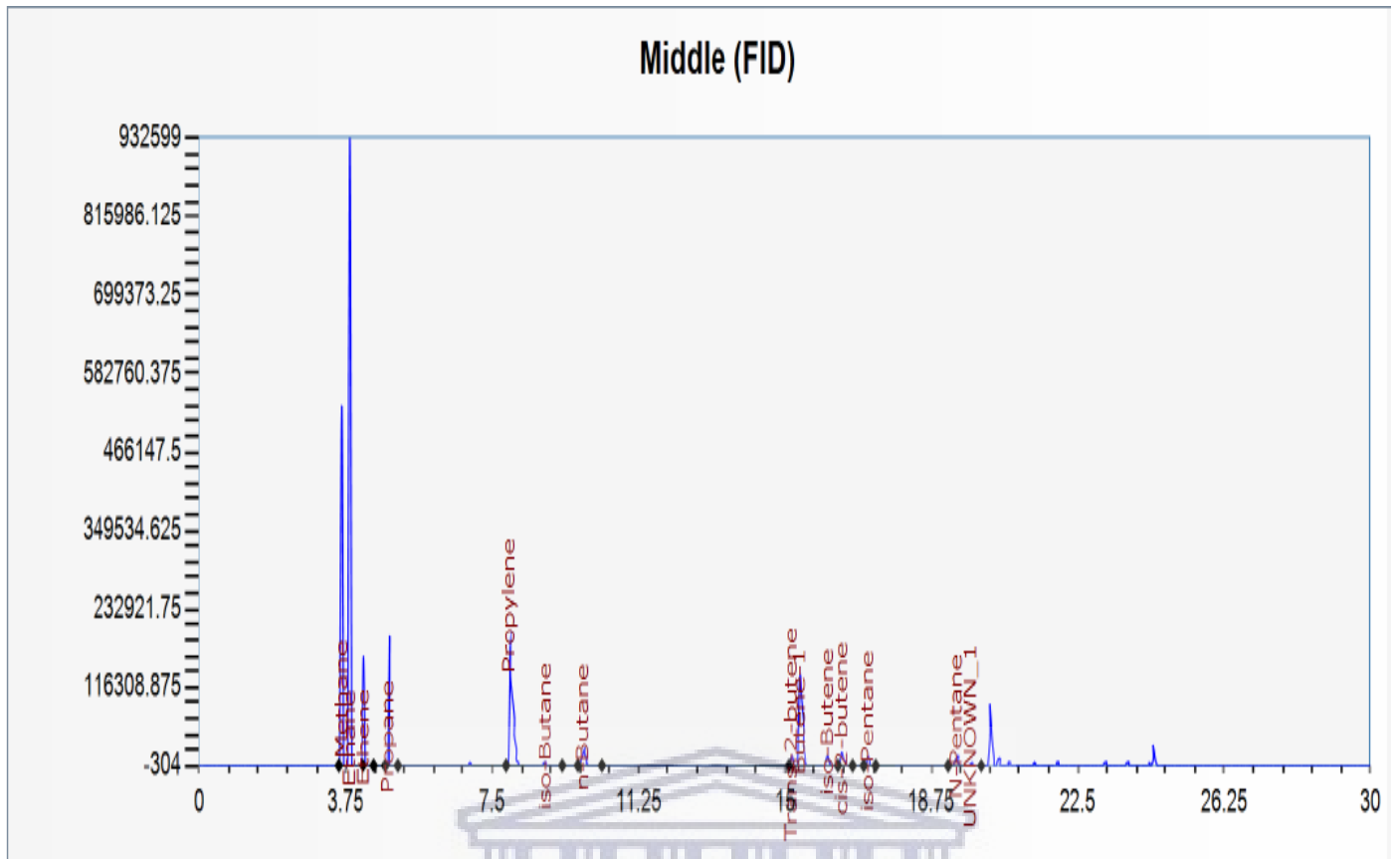
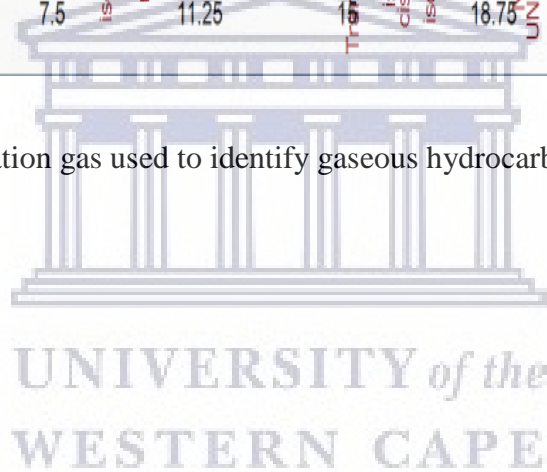


Figure 18: GC trace of the calibration gas used to identify gaseous hydrocarbon products.



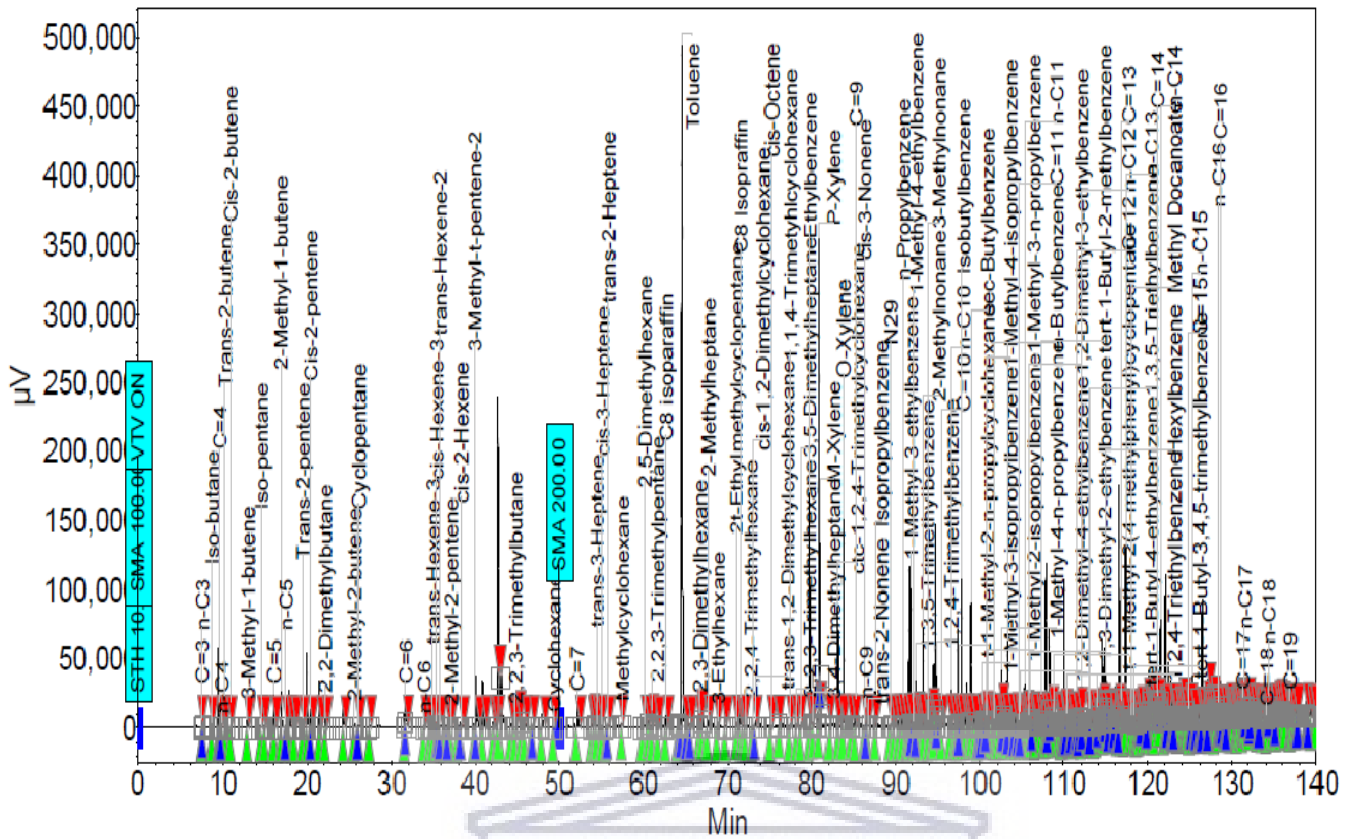


Figure 19: GC trace of the calibration used to identify liquid hydrocarbon products.

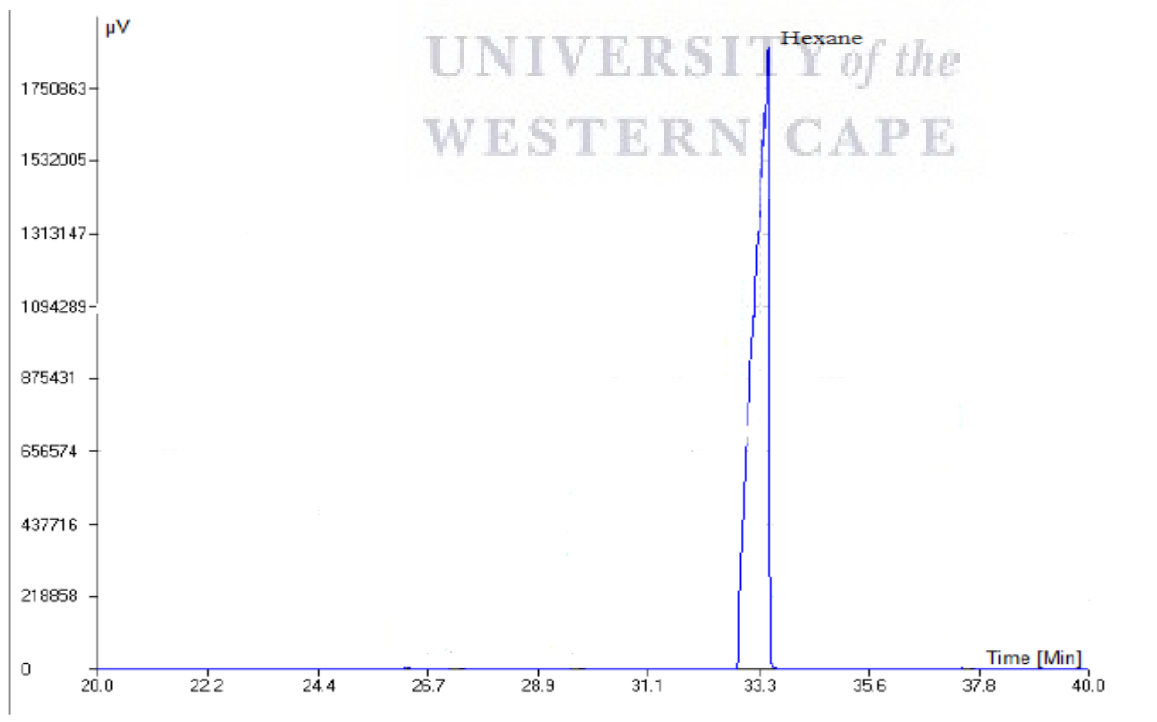


Figure 20: GC trace of the calibration of pure hexane.

3.5 References

1. Li H, Jin J, Wu W, Chen C, Li L, Li Y, Zhao W, Gu J, Chen G, Shi J-L. Synthesis of a hierarchically macro-/mesoporous zeolite based on a micro-emulsion mechanism. *J Mater Chem*. 2011;(21):19395-19401.
2. Shirazi L, Jamshidi E, Ghasemi M.R. The effect of Si/Al ratio of ZSM-5 zeolite on its morphology, acidity and crystal size. *Cryst Res Technol*. 2008;(43):1300–1306.



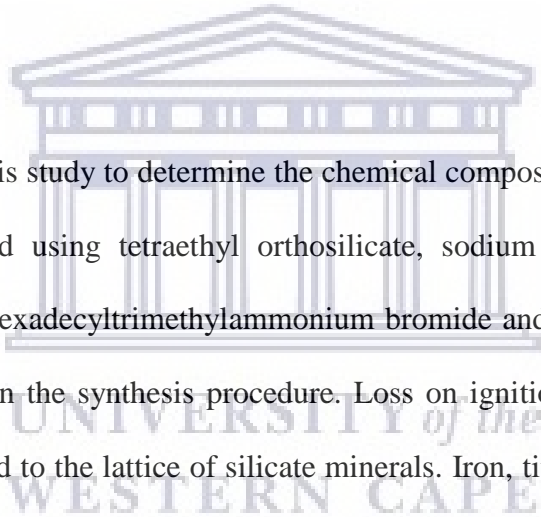
CHAPTER 4: Results and discussion of Catalyst Characterization

Chapter Overview

This chapter provides a thorough discussion on the characterization of the prepared materials. The prepared H-ZSM-5 catalysts had targeted Si/Al ratios with the initial batch mixture ratio of the prepared material labelled as SA=30, SA=60, SA=90, SA=150 and SA=300. Different characterization techniques such as FTIR, XRD, XRF, NH₃-TPD, TGA, HRSEM and BET were used in this study to confirm that the desired material was synthesized successfully, with the intended Si/Al ratios.

4.0 Catalyst Characterization

4.1 X-Ray Fluorescence [XRF]



XRF analysis was performed in this study to determine the chemical compositions of the prepared materials. These materials were synthesized using tetraethyl orthosilicate, sodium aluminate, ammonium nitrate, tetrabutylammonium hydroxide, hexadecyltrimethylammonium bromide and ethanol. The materials contain different Si/Al ratios dependent on the synthesis procedure. Loss on ignition [L.O.I] is the weight loss or gain, including the water combined to the lattice of silicate minerals. Iron, titanium, sodium and calcium are other elements that are found present in the synthesized materials. However, no iron, calcium or titanium were used during the synthesis of these materials and could be minor impurities that are present in the starting materials. These amounts are very low and are considered as negligible. Sodium is detected in the ratio of 30, 90 and 300 but in very low amounts. This means the iron exchange mostly successful, except for SA=30 which displays about 0.36 % of sodium. Table 7 displays the chemical compositions of the prepared HZSM-5 catalysts as determined by X-ray fluorescence [XRF]. The targeted ratios of the prepared catalysts are displayed in Table 7 as expected ratios. However, the actual ratios were calculated using the results [oxide contents] obtained by XRF analysis and also displayed in table 7. The calculated actual ratios were found to be close to the expected ratios, meaning that the catalysts were successfully prepared with different Si/Al ratios. However, the expected SA=90 was found to be slightly lower. This could be due to less amount

of SiO₂ being incorporated into the structure during the synthesis of the material. This is also an indication as to why this ratio has the lowest crystallinity from the XRD results. It is also observed that the Al₂O₃ content decreases as the Si/Al ratio increases whereas the SiO₂ content remains almost the same. This is expected as only the alumina content was varied during the synthesis. However, the SA=30 is found to have the lowest SiO₂ content. The calculated ratios will then be used throughout the study as the actual materials.

Table 7: Chemical compositions of the prepared HZSM-5 catalysts with different Si/Al ratios as determined by XRF

		Oxides Contents [wt. %]							
Expected ratios	Actual ratios	Al ₂ O ₃	SiO ₂	Fe ₂ O ₃	TiO ₂	Na ₂ O	CaO	L.O.I	Sum of Conc.
SA=30	SA=36	3.66	78.37	0.01	0.02	0.36	0.01	17.51	99.95
SA=60	SA=71	2.21	92.75	0.02	0.02	-	0.02	4.49	99.50
SA=90	SA=77	1.99	90.35	0.02	0.01	0.01	0.01	6.70	99.08
SA=150	SA=177	0.89	92.87	0.08	0.01	-	0.02	5.63	99.49
SA=300	SA=345	0.46	93.59	0.01	0.01	0.01	0.01	5.59	99.68

4.2 Fourier Transform Infrared Spectroscopy [FTIR]

FTIR Spectroscopy was used to evaluate the functional groups present in the synthesized zeolite as well as to reveal the crystalline properties of these materials. Figure 21 represents the infrared absorption spectra of the prepared zeolite catalysts with variable Si/Al molar ratios. FTIR spectra are recorded in the range of 1800-400 cm⁻¹. In Figure 21, all the variable Si/Al ratios show the expected peaks at the region of 446, 551, 807, 1065 and 1236 cm⁻¹ respectively except SA=36, revealing that the synthesized zeolites has a Mordenite Framework Inverted [MFI] type structure. The absorption peaks at 446 cm⁻¹, 551 cm⁻¹ and 807 cm⁻¹ are characteristic peaks attributed to the Si-O bending vibration, pentasil framework vibration and Si-O-Si symmetric vibration respectively (1). The intensity bands at around 446 cm⁻¹ also represent T-O bends which

correspond to siliceous material. The intensity of the transmittance bands that are found at 446 cm^{-1} and 551 cm^{-1} also reflects the crystallinity of ZSM-5 zeolites and is assigned to the five-membered rings of MFI zeolites (2,3). More evidence for the ZSM-5 structure appears at the stretching vibration of T-O [T =Si, Al] bands at 1065 cm^{-1} for internal asymmetric stretch and at 1236 cm^{-1} for external asymmetric stretch (1,4). However, the SA=36 does not show any peaks at 551 cm^{-1} and 1236 cm^{-1} regions. This suggests that the expected ZSM-5 structure was not successfully formed.

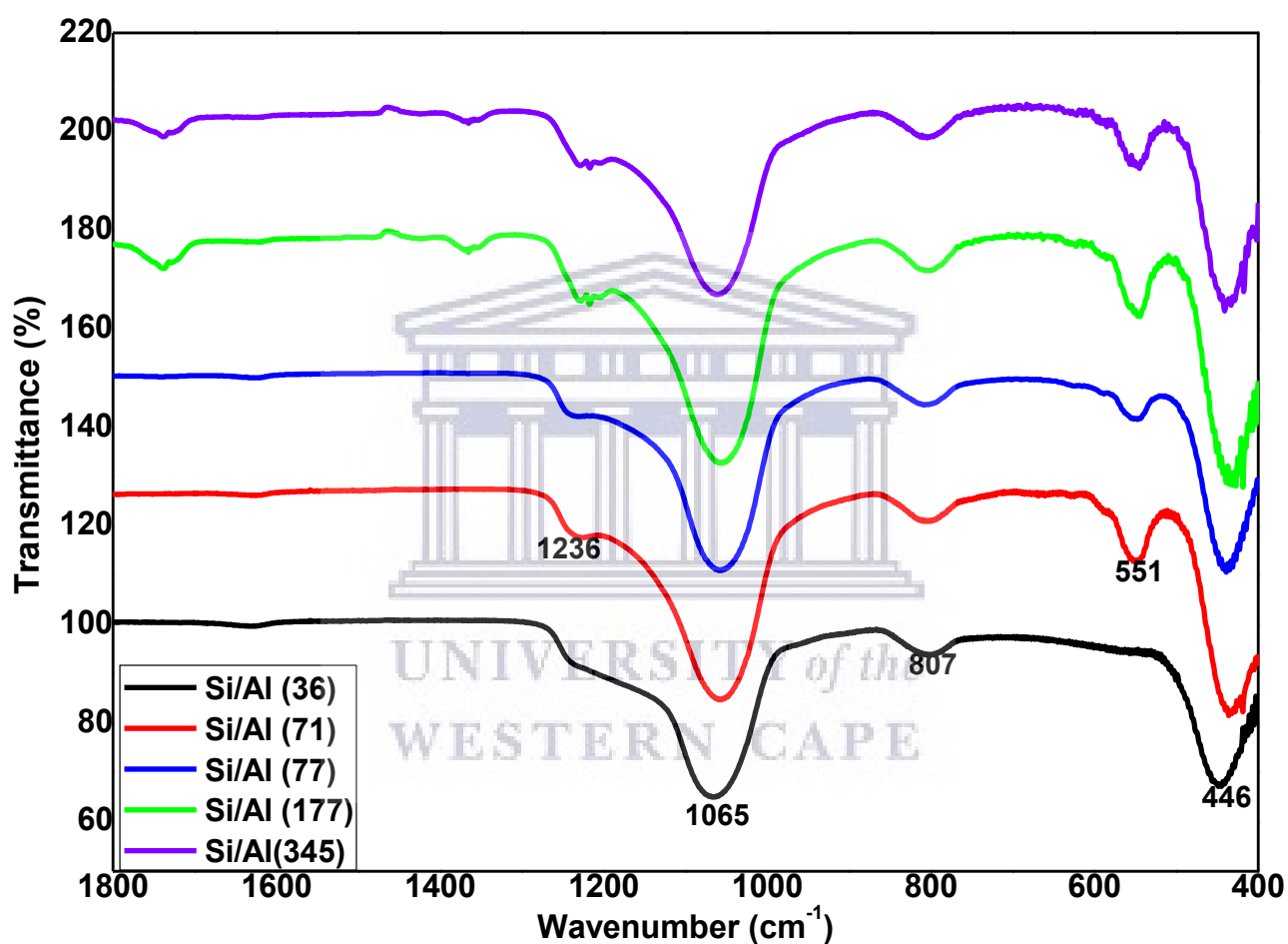


Figure 21: FTIR spectra of the prepared zeolite catalysts with variable Si/Al molar ratios

Figure 22 represents the infrared absorption spectra for the SA=36 prepared at different crystallization conditions as compared to the other zeolite materials. Also with the SA=36 prepared for 3 days at temperatures of $150\text{ }^{\circ}\text{C}$, there are no peaks observed at 551 cm^{-1} and 1236 cm^{-1} regions. This could be due to the large Al content present in the batch mixture, which resulted in slower crystallization kinetics, hence

hindering the formation of crystals at the given crystallization conditions. However, when the crystallization temperature was increased to 180 °C and time to 6 days, the peak at 551 cm⁻¹ region which is characteristic of the ZSM-5 crystalline structure is observed. This means that in a batch mixture with high Al content, higher crystallization temperature and time is needed to facilitate the nucleation and crystallization of ZSM-5 crystals.

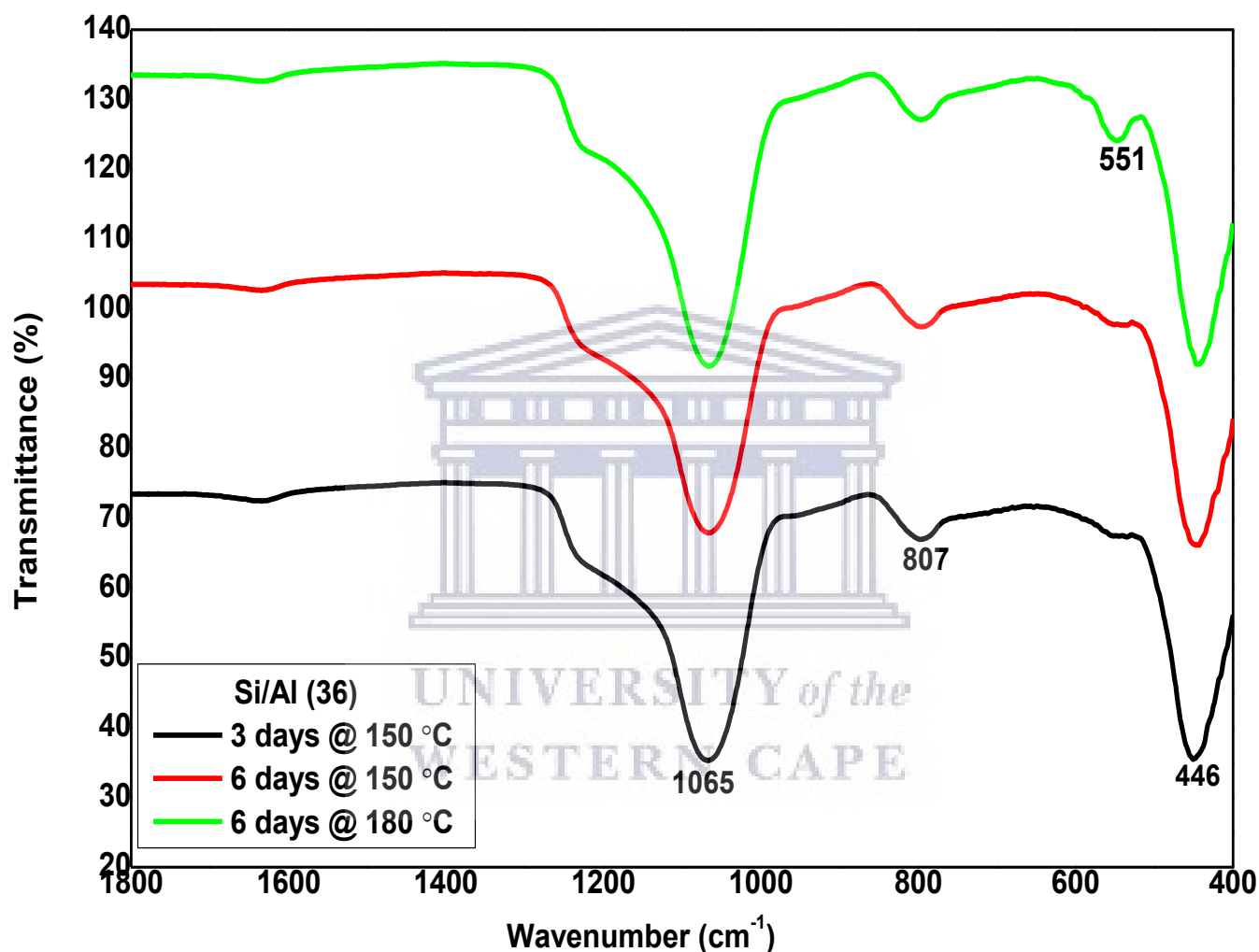


Figure 22: FTIR spectra of the SA=36 prepared at variable temperatures from 150-180 °C for 3-6 days

4.3 X-ray Diffraction [XRD]

The XRD analysis was done to determine the crystal structure, phase purity and the crystal size of the synthesized zeolite materials. Figure 23 below represents the XRD patterns of the wide and small angle [inset] of the prepared zeolite catalysts with variable Si/Al molar ratios in the range 36-345. These zeolite

materials were crystallized at 150 °C for 48 hrs. The XRD patterns were all taken within a 2θ degree range from 0-60° for the wide angle and 0-5° for the small angle.

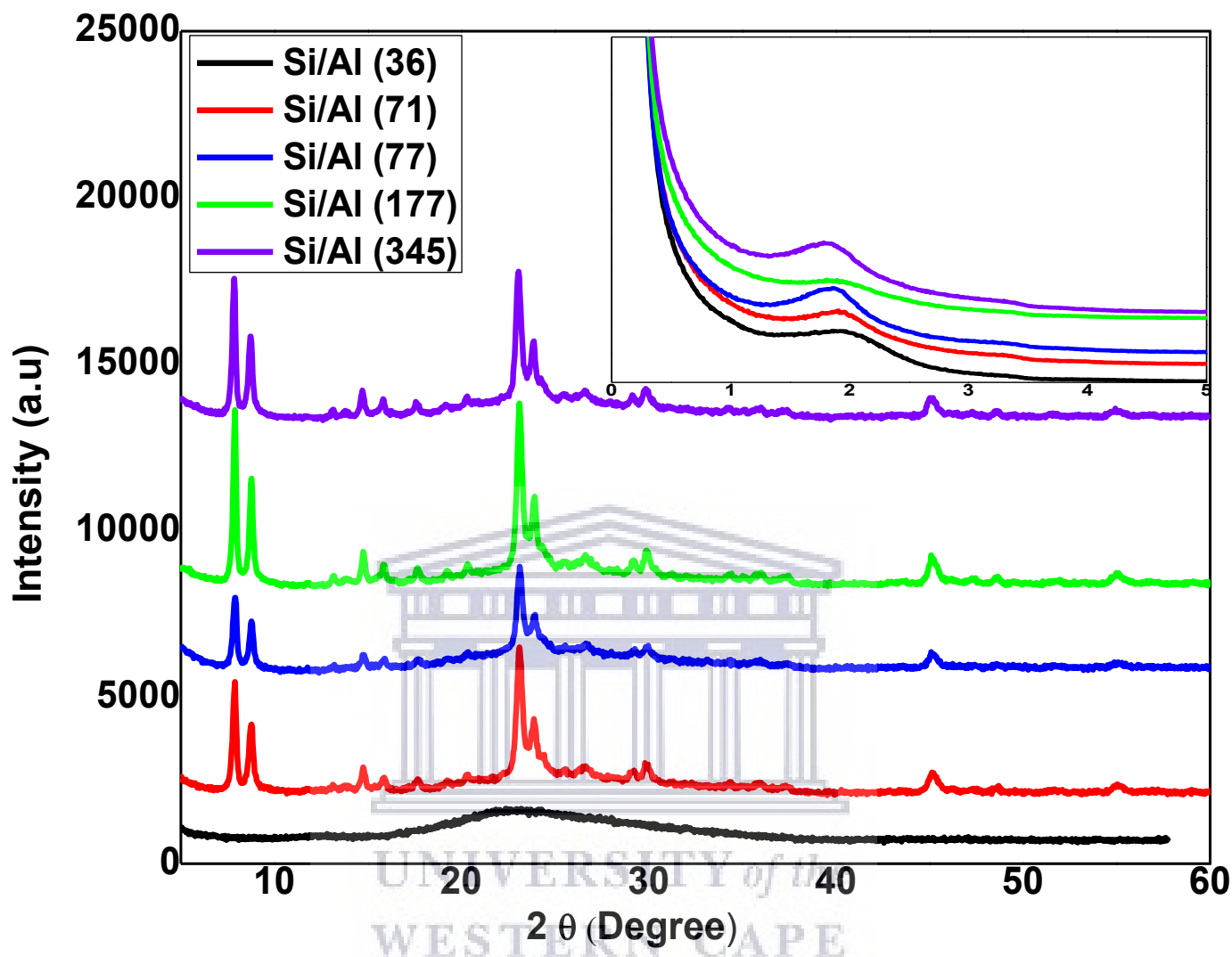


Figure 23: Wide and small angle [inset] XRD patterns of the synthesized hierarchical zeolite having variable Si/Al molar ratios in the range [36-345]

The sharp intense peaks observed in the XRD patterns of the zeolite samples with variable Si/Al ratios shown in Figure 23 indicate the nature of crystallinity of the prepared materials. The strong intensity peaks are observed at $\sim 7-9^\circ$ and $22-25^\circ$ for the wide angle and at $\sim 1.8-2^\circ$ for the small angle, except for the SA=36 which shows an amorphous structure with one broad peak observed at around 23° . These strong intense peaks indicate that the synthesized zeolite materials are crystalline and demonstrate a typical MFI topology zeolite framework with high purity. The intense peaks observed at 2θ values between $22-25^\circ$

indicate the degree of crystallinity of the hierarchical ZSM-5 type zeolite with a partially ordered mesoporous structure. The peaks observed at $\sim 1.8-2^\circ$ represent a certain degree of ordering of the mesoporous structure (5–7). The Si/Al ratio is found to have an impact on the peak intensities as the crystallinity of the materials differs with the different amounts of the Si and Al source used. The SA=177 has the greatest peak intensity followed by the SA=345. However, there is no precise correlation on the observed intensities as the SA=71 has a larger peak intensity as compared to the SA=77. There is no shift observed on the peak positions indicating that the structure of these zeolites was not affected by the variation of the Si/Al ratio and a crystalline ZSM-5 structure is obtained. However, this does not apply to the SA=36 since it does not show any peaks but only an amorphous structure. The amorphous broad structure found on the SA=36 is due to the large Al source loaded during the synthesis, hindering the formation of crystals.

The SA=36 was then further recrystallized at different crystallization conditions which involved higher temperatures of 150-180 °C and extended period of time from 3 to 6 days. The XRD patterns of SA=36 for wide and small angle [inset] are observed in Figure 24. It can be observed from the peak intensities that crystals start to form from this material as the crystallization temperature and time are increased. The SA=36 crystallized at a temperature of 180 °C for 6 days is more crystalline as compared to the one crystallized at 150 °C for 3 and 6 days. The SA=36 prepared at these conditions is then labelled as SA=36". Therefore, it can be concluded that the SA=36 in Figure 23 had an amorphous structure and the crystallization conditions used to prepare the other zeolite materials does not work for the preparation of the SA=36. The peak observed at around 1° in the small angle [inset] is probably due to the raised crystallization temperature and time. The characterization temperature and time could not be extended any further. According to Oswald's rule of successive phase transformation, impurities may start to form when the crystallization time is too long, especially at such high temperatures (8).

Table 8 represents the calculated relative % crystallinity for the prepared materials. Equation 4.1 below was used to perform the calculation for the % crystallinity for each ZSM-5 material. The calculation was done by adding up the characteristic peak intensities for each ZSM-5 material and then divided by the sum of the peak intensities of the standard or reference ZSM-5 material. In this case, a commercial zeolite with SA=80

was used as a standard or reference ZSM-5 material. This calculation is consistent with the observed peak intensities as the SA=177 has the highest calculated % crystallinity and SA=36" with the least. The crystallinity obtained for SA=36" is too low and not suitable for this study. Therefore, the intended zeolite was not successfully prepared and has an amorphous structure as compared to the other zeolites. This also relates with the FTIR results as to why the expected peaks that are characteristic of the ZSM-5 crystalline structure are not observed in SA=36. Hence, the SA=36" catalyst will not be discussed further in this study since it will not be used for catalytic testing.

$$\% \text{ Crystallinity} = \frac{\sum \text{intensities of the sample peaks}}{\sum \text{intensities of the reference peaks}} * 100 \dots \dots \dots [4.1]$$

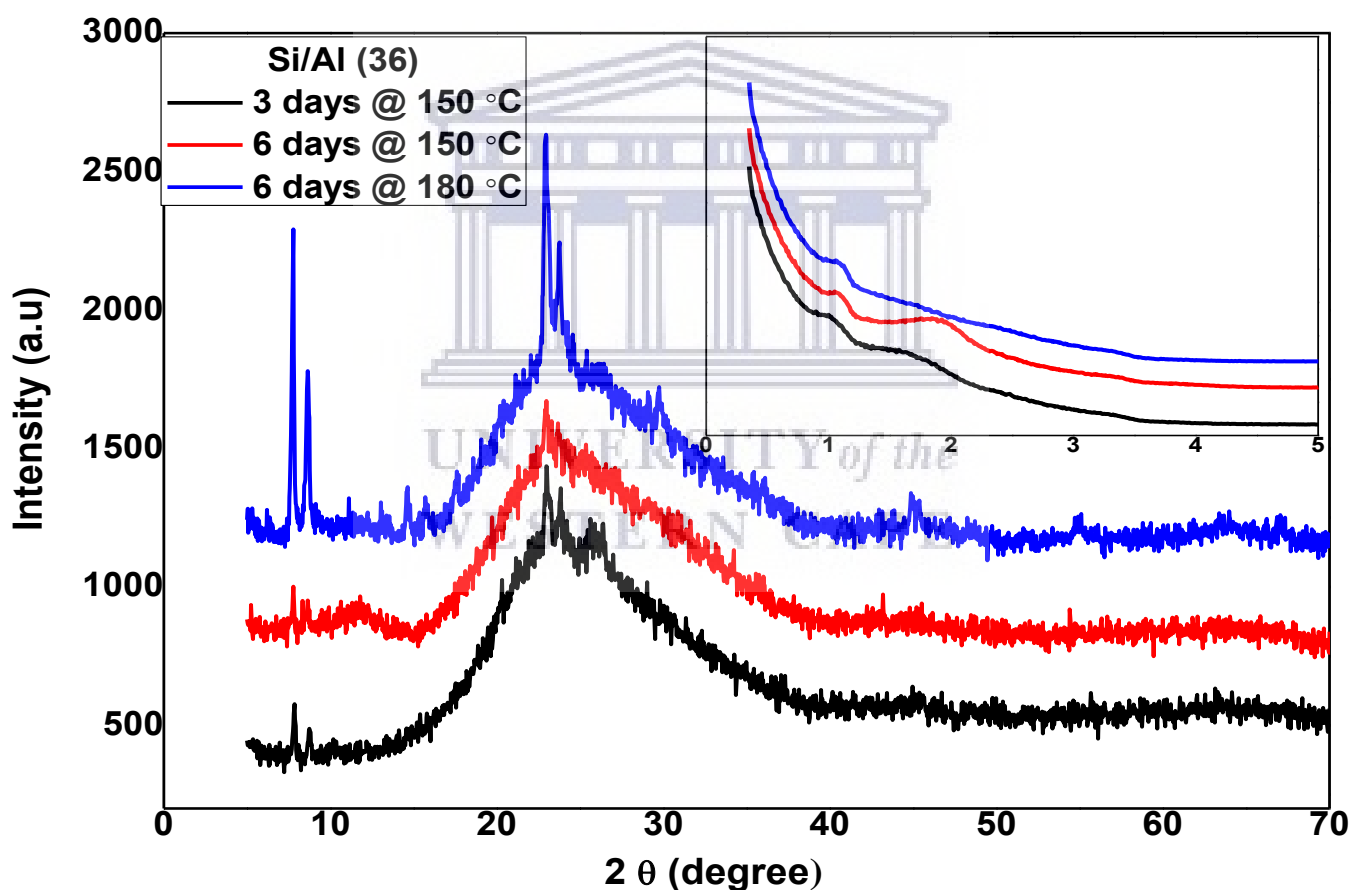


Figure 24: Wide and small angle [inset] XRD patterns of the SA=36" prepared for 3-6 days at temperatures of 150-180 °C.

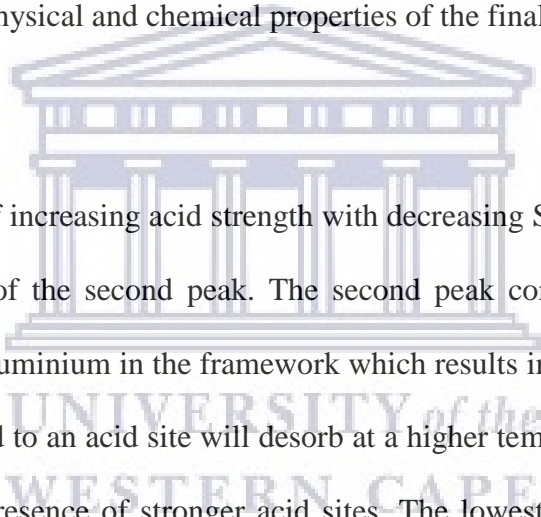
Table 8: Calculated peak intensities and their corresponding relative % crystallinity of the prepared zeolite samples.

Si/Al ratio	Sum of the peak intensities	% Crystallinity
36''	6543	34
71	14470	75
80 [Reference ZSM-5]	19364	100
77	10873	56
177	18774	97
345	15645	81

4.4 Ammonia-Temperature Programmed Desorption [NH₃-TPD]

NH₃-TPD analysis was performed in this study to evaluate the strength and amount of acid sites in the prepared HZSM-5 zeolites. Figure 25 below shows three desorption peaks that appear at temperature range of 195-205 °C for weak acid sites and 363-567 °C for strong acid sites. A third peak is observed at 598-882 °C. To the best of our knowledge, such observation of HZSM-5 zeolites showing three desorption peaks with strong acid sites at such high temperatures has not been reported before. Theoretically, strong acid sites appear at a temperature range of 300-500 °C and correspond to the strong Bronsted and Lewis acid sites that are of catalytic importance. However, further tests were conducted to investigate whether the prepared materials were thermally stable and the observed third peak was not due to thermal decomposition. The

relative integrated intensities for each peak are shown in Table 9 below. The total acidity calculated from the weak and strong sites of these prepared zeolite materials is found to decrease as the Si/Al increases. Looking at the total acidity for each ratio, it follows this trend; SA= 71 > 77 > 177 > 345. Theoretically, this type of trend is expected from the previously reported literatures. This may be caused by an increase in the aluminium content, which is largely responsible for the formation of acidic sites in zeolites. The XRF results confirmed that the aluminum content increased with a decrease in Si/Al ratio. Shiraz *et al* (9), reported on ZSM-5 catalysts with different Si/Al ratios from 10-50. They observed that the total acidity of these zeolites decreased as the Si/Al ratio increased. The SA=10 had a total acidity of 27.02 mmol NH₃/g cat and SA=50 had a total acidity of 19.93 mmol NH₃/g cat. They also believed that this strongly suggested the presence of aluminum in extra-framework positions. The results revealed that the molar ratio of Si/Al of the starting gel mixture plays a great role on the physical and chemical properties of the final products.



Another observable trend is that of increasing acid strength with decreasing Si/Al ratio. This can be observed by looking at the peak maxima of the second peak. The second peak corresponding to stronger sites is generally due to the presence of aluminium in the framework which results in the formation of Bronsted acid sites. NH₃ which is strongly bound to an acid site will desorb at a higher temperature therefore peak shifts to higher temperature indicate the presence of stronger acid sites. The lowest Si/Al ratio i.e. SA=71 has the highest peak maxima at 389 °C. As the ratio increases the temperature of the peak maxima decreases as SA=345 has the lowest peak maxima of 321 °C. SA=177 however, has a higher peak maxima than SA=77 which may be due to the larger amount of strong acid sites compared to SA=77. The trend of decreasing acid strength follows as such SA=71>177>77>345. This trend is important as it will be shown in the catalytic evaluations of these catalysts that their performances follow the same trend. The chemical property of acidity can be directly linked to the activity of the catalyst. In general it can be concluded that the effect of Si/Al ratio on acidity is that as Si/Al ratio increases both the strength and quantity of acid sites decrease.

Table 9: NH₃-TPD temperature and acid quantity of HZSM-5 zeolites with different Si/Al ratios

Ratio	Peak number	Temperature [°C]	Acid Quantity [μmol/g]	Total Acidity
71	1	205	517	629
	2	389	112	
77	1	197	220	261
	2	363	41	
177	1	195	178	255
	2	376	77	
345	1	197	38	92
	2	321	54	

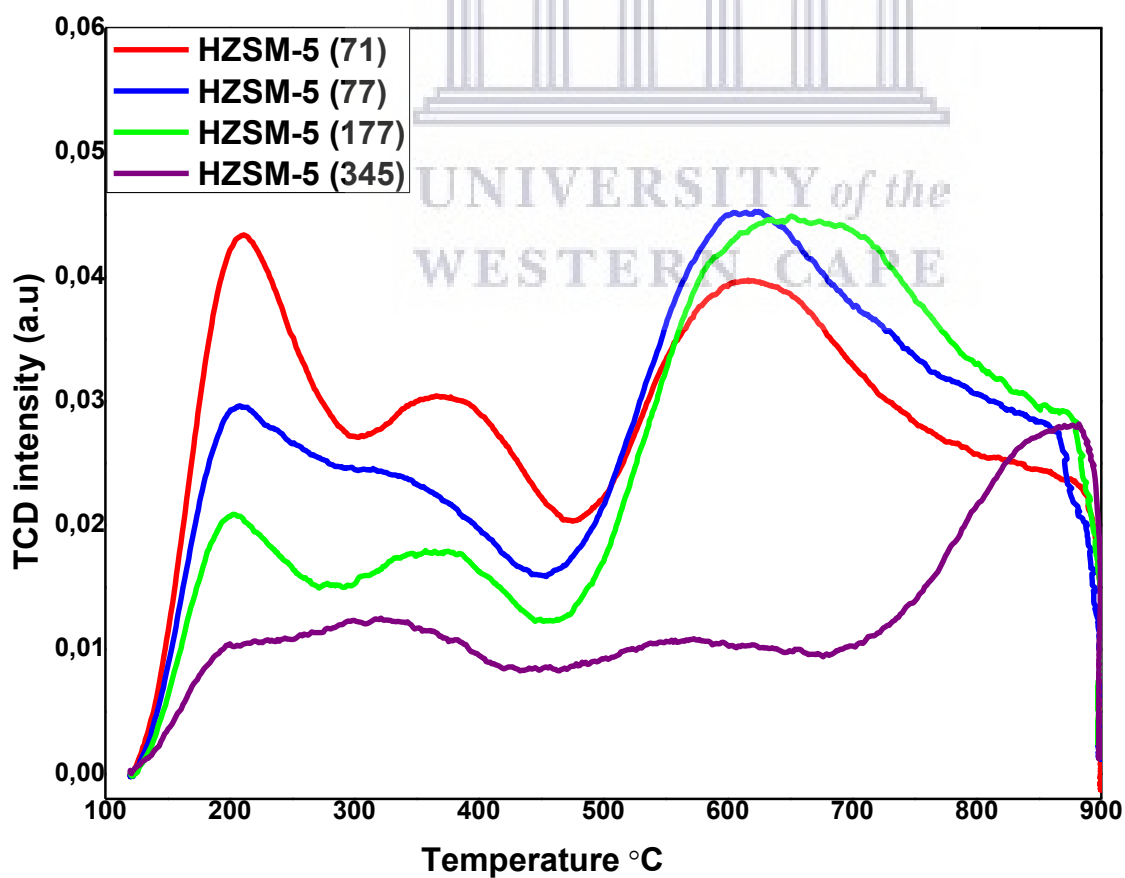


Figure 25: NH₃-TPD profiles of the synthesized HZSM-5 zeolites with different Si/Al ratios.

4.5 Thermogravimetric Analysis [TGA]

Thermogravimetric analysis [TGA] was performed in this study to determine the thermal stability and the fraction of the volatile components on the prepared zeolite catalysts. SA=77 was used for thermal treatment investigation since it has the highest intensity of the unknown third peak in the NH₃-TPD profiles. The response of the SA=77 to the thermal treatment is shown in Figure 26 below. TGA shows loss of weight in the temperature range of 40-120 °C. This is due to loss of moisture in the pores and on the surface of the material. The catalyst then becomes stable from the temperatures of 120-800 °C. This proves that the catalyst is thermal stable and the third peak found on the prepared catalysts is not due to thermal decomposition. The reason for the formation of high temperature 3rd peak in the TPD analysis is still unclear and further investigations are required.

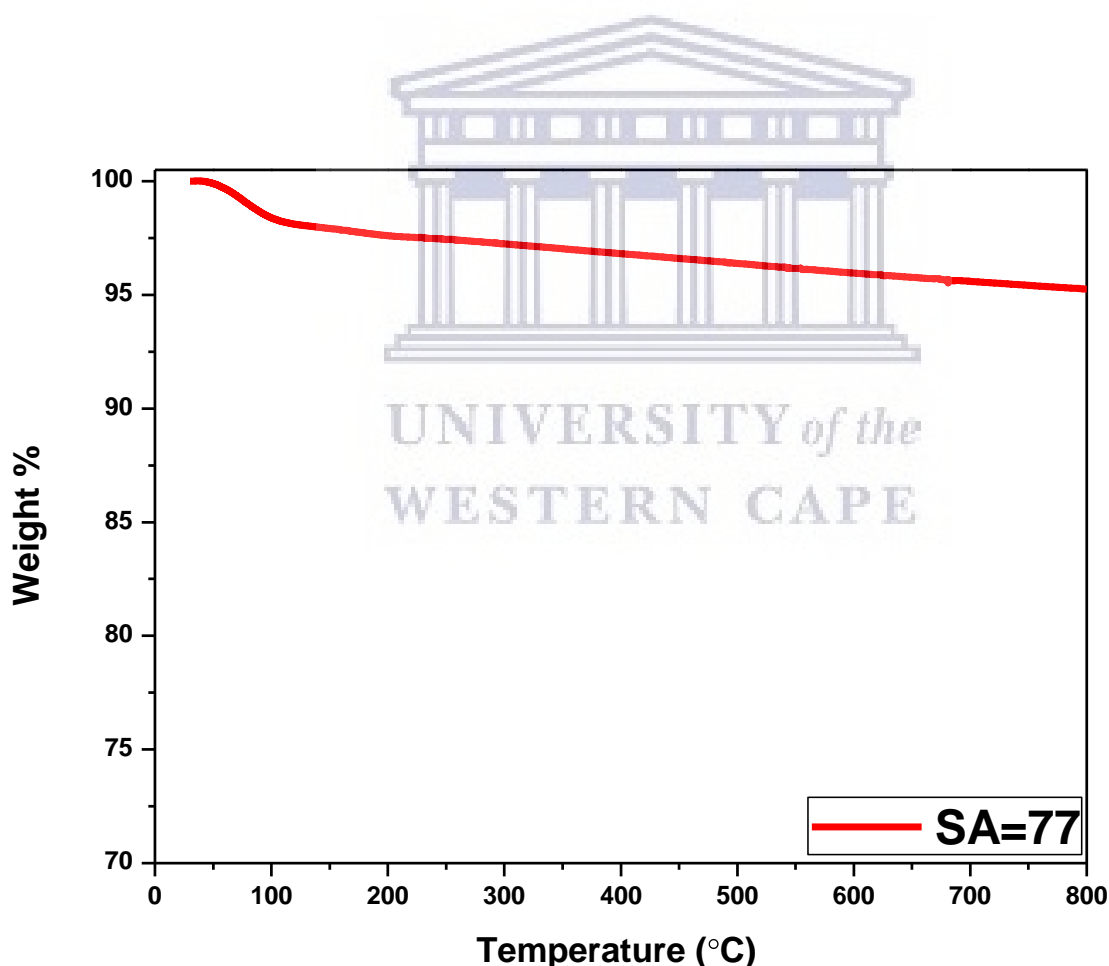


Figure 26: TGA profile showing the thermal behaviour of SA=77.

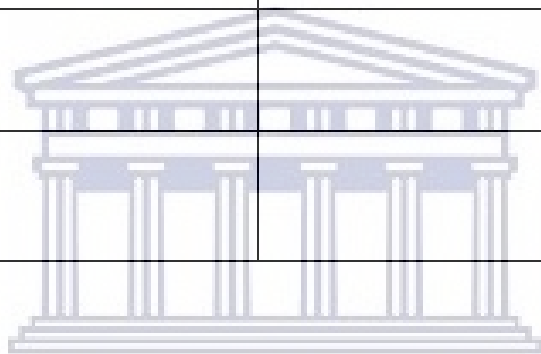
4.6 High Resolution Scanning Electron Microscopy [HRSEM]

HRSEM analysis was employed in the study to establish the surface morphology as well as the elemental composition of the prepared zeolite catalysts. Figure 27 displays the HRSEM micrographs of the synthesized hierarchical zeolites all taken at the same scale view of 200 nm which shows high resolution images. The prepared materials all reveal morphologies that are spherically shaped and uniformly aggregated together, forming large stacks of crystals with observable open spaces within the large crystals (6). A sponge-like morphology with worm-like holes is observed in all the synthesized materials. The type of morphology is similar to the one reported by Junjiang *et al* (5). This proves that some pores were successfully generated during the fabrication of these materials. The materials appear to have retained their structural morphology even with the variation in the Si/Al ratios with observed agglomerated crystals. The Si/Al ratio did not have any observable effect on morphology i.e. shape and size, as all catalysts possessed the same surface structure. “ImageJ” [a java based image processing program] was used to calculate the pore-sizes for these materials. The calculated average pore sizes are observed in Table 10. The pore sizes of the worm-like holes in sponge-like morphology of all samples fall in the macropore range, i.e. greater than 50 nm. This indicates macropores may be successfully generated on the outer structure of the zeolite crystals. The method used to synthesize the materials in this project was adopted from Junjiang *et al* (5). On their research work, they confirmed that they produced mesoporous and macroporous structures of Hp-ZSM by N₂ physisorption and Hg intrusion porosimetry analysis respectively, where the macropore diameter was estimated over the whole mercury intrusion pressure range using the Washburn equation. Furthermore, the worm-like holes observed in their SEM images were correlated to the presence of macropores. Therefore, the similar worm like structures observed in our materials [HRSEM] with openings greater than 50 nm may indicate that macropores were successfully generated in these materials. There is no clear observable trend on whether the pore sizes increase as the Si/Al ratios increase. The SA=77 is found to have the highest average pore size of 85 nm, followed by SA=345 with an average of 79 nm. The SA=177 has an average pore size of 68 nm. The SA=77 is found to have the lowest average pore size of 54 nm as compared to the other catalysts. The SA=71 and SA=345 shows good and clear pores looking like worm holes that are highlighted by the black arrows within the micrographs. These ratios also show high crystallinity from the calculated XRD relative %

crystallinity results. The pores for SA=77 and SA=177 are not clearly evident since the crystals are packed on top of each other, especially for SA=77. This could be due to its low calculated XRD relative % crystallinity.

Table 10: Calculated average macropore sizes for the prepared materials from SEM analysis.

Si/Al Ratio	Average pore size (nm)
71	85
77	54
177	68
345	79



UNIVERSITY *of the*
WESTERN CAPE

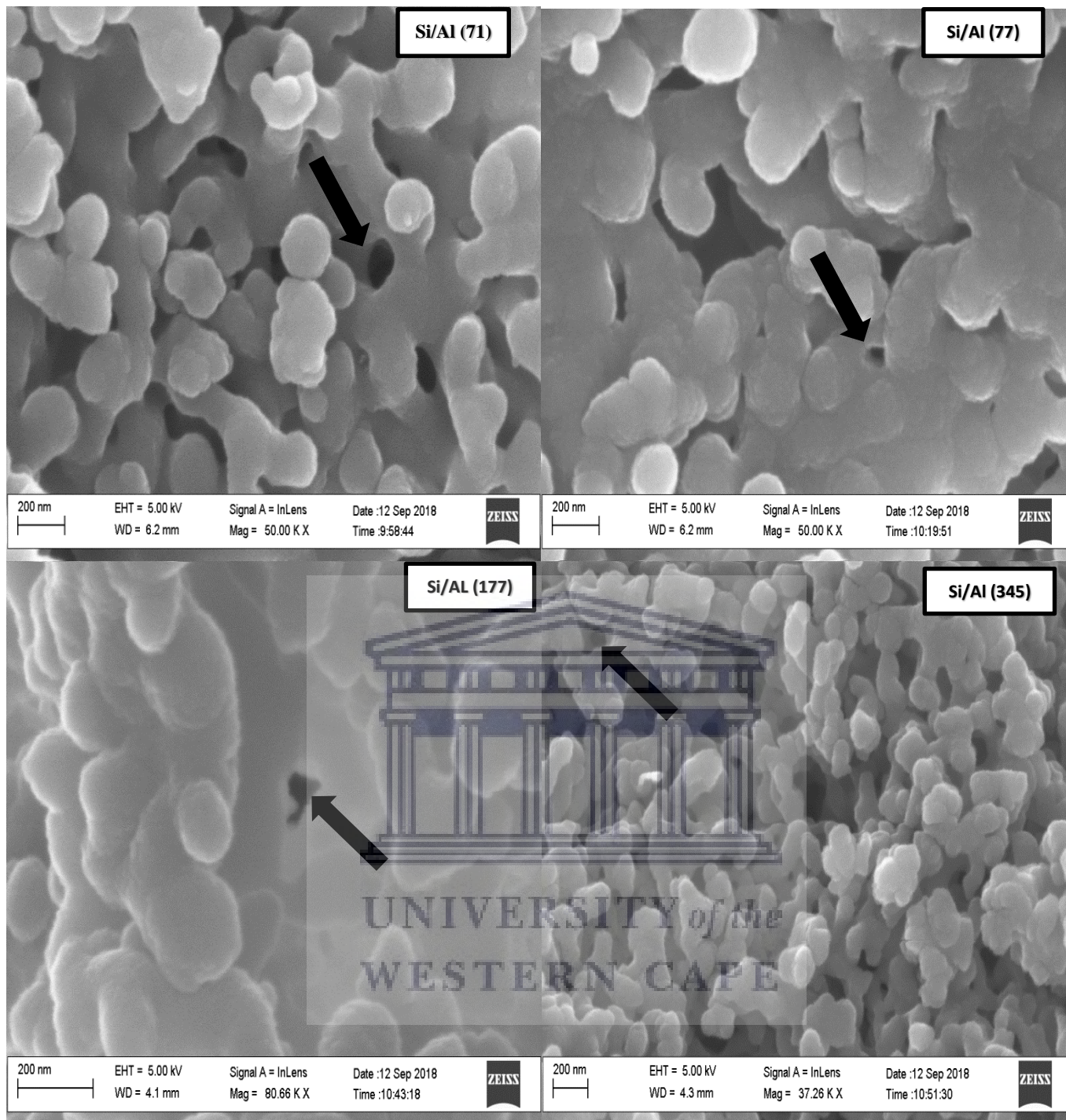


Figure 27: SEM micrographs of the hierarchical ZSM-5 with variable Si/Al ratios in the range [71-345] synthesized at 150 °C for 48 hr.

4.7 Nitrogen adsorption-desorption analysis

Brunauer Emmet and Teller [BET] was used in this study to determine the pore-size distribution as well as the pore volumes and surface area measurements of the synthesized catalysts.

Table 11: Textural properties of the prepared HZSM-5 zeolites with different Si/Al ratios

Sample	BET surface (m ² /g)	t-plot micro-pore (m ² /g)	t-plot external (m ² /g)	Micro-pore volume (cm ³ /g)	Total pore volume (cm ³ /g)
SA=71	618	103	515	0.066	0.542
SA=77	455	36	418	0.039	0.409
SA=177	533	50	483	0.040	0.416
SA=345	614	67	546	0.054	0.626

Table 11 represents the specific surface area [SSA] and the porosity of the prepared materials. The SA=71 is observed to have the highest SSA of 618 m²/g given by its micropore area of 103 m²/g and an external surface area of 515 m²/g. The high SSA found in the material is due to the development of mesopores with narrow pore size distribution. Moreover, a hierarchical structure with 3 pore ranges, i.e. micro, meso and macropores has been developed. The following trend has been observed; SA=71>345>177>77. SA=77 has the lowest SSA of 455 m²/g and micropore area of 36 m²/g compared to the other synthesized materials. This relates well with the XRD results as the SA=77 have got the lowest relative % crystallinity, indicating the material may have lower SSA due to a poorly formed crystal structure compared to the synthesized catalysts. Furthermore, SA=77 has got the smallest observed macropores from the HRSEM results. Therefore, the differences in surface areas are likely to be related to variations in crystallinity than Si/Al ratios. The SSA and the micropore areas are observed to increase again from the ratio of 177 to that of 345.

All the adsorption-desorption curves of the synthesized hierarchical ZSM-5 zeolites exhibit typical isotherms with behaviour of both Type I and Type IV. They also demonstrate a H1 hysteresis loop as displayed in Figure 28 below. This is proven by a notable uptake of N₂ at moderately high pressures, followed by a hysteresis loop that suggests an instantaneous occurrence of ordered mesoporosity as well as inherent micropores of ZSM-5 within the synthesized zeolites (5). There is also an evident capillary condensation that takes place at relative pressures [P/P₀] of approximately 0.4 to 1.0 which proves that these materials have a great amount of pores seen in the mesopore range of 2-50 nm.

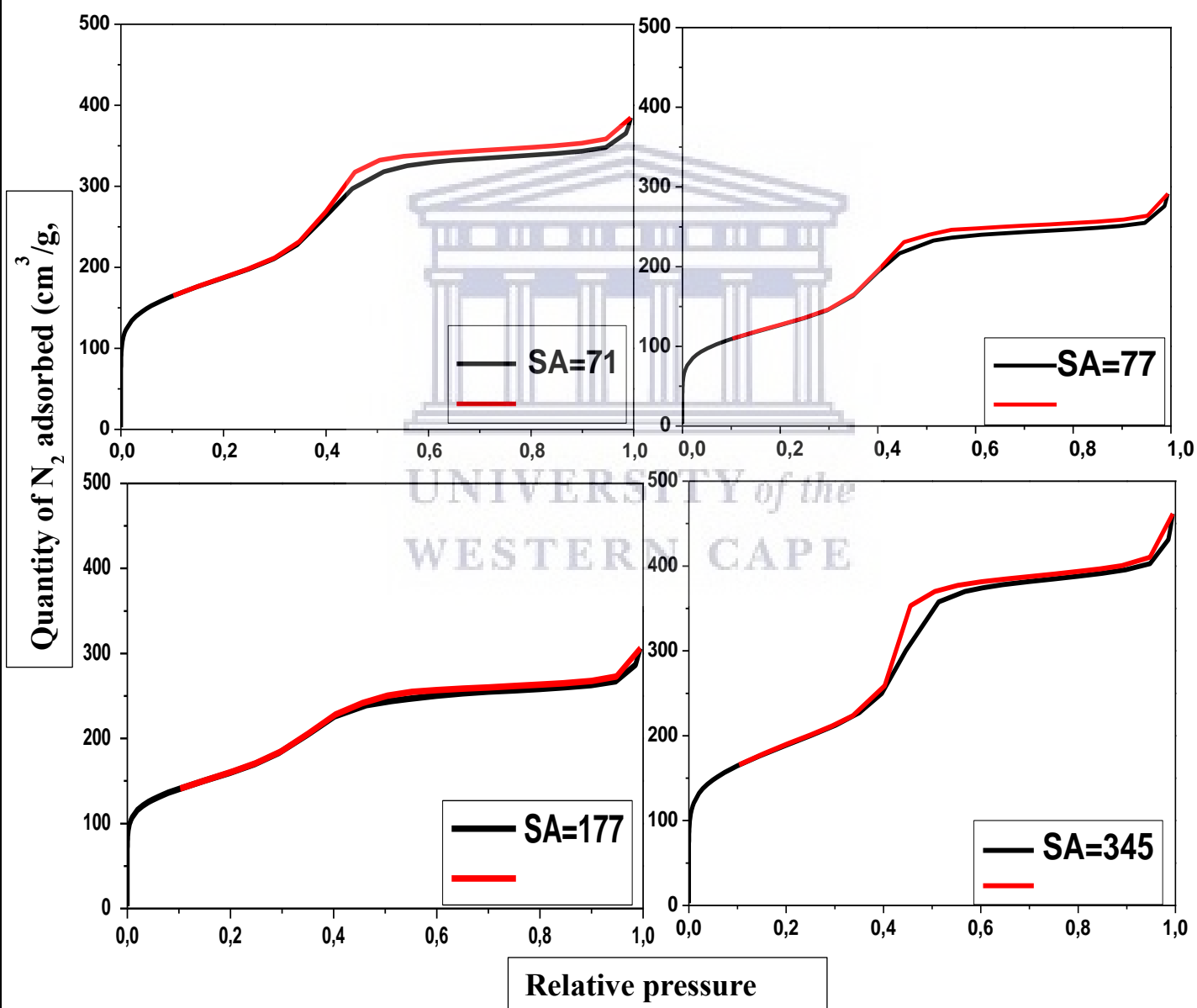


Figure 28: N₂ adsorption-desorption isotherms of the synthesized HZSM-5 materials.

The corresponding BJH pore-size distributions displayed in Figure 29 indicate that all the synthesized materials have highly ordered mesopores with a very narrow pore size distribution. The pore diameters range between 5-7 nm, which leads to a high SSA and pore volume. The SA=345 in the corresponding BJH pore-size distribution shows a second peak in the pore diameters of 6.5 to 7 nm. This could be due to its observed high total pore volume of 0.626 cm³/g and the highest uptake of N₂. There is no specific order that shows whether the nitrogen uptake increase with an increase in the Si/Al ratios of the synthesized materials, since the SA=345 has got the highest uptake of N₂, followed by SA=71, then SA=177 and the lowest intake is found at SA=77.

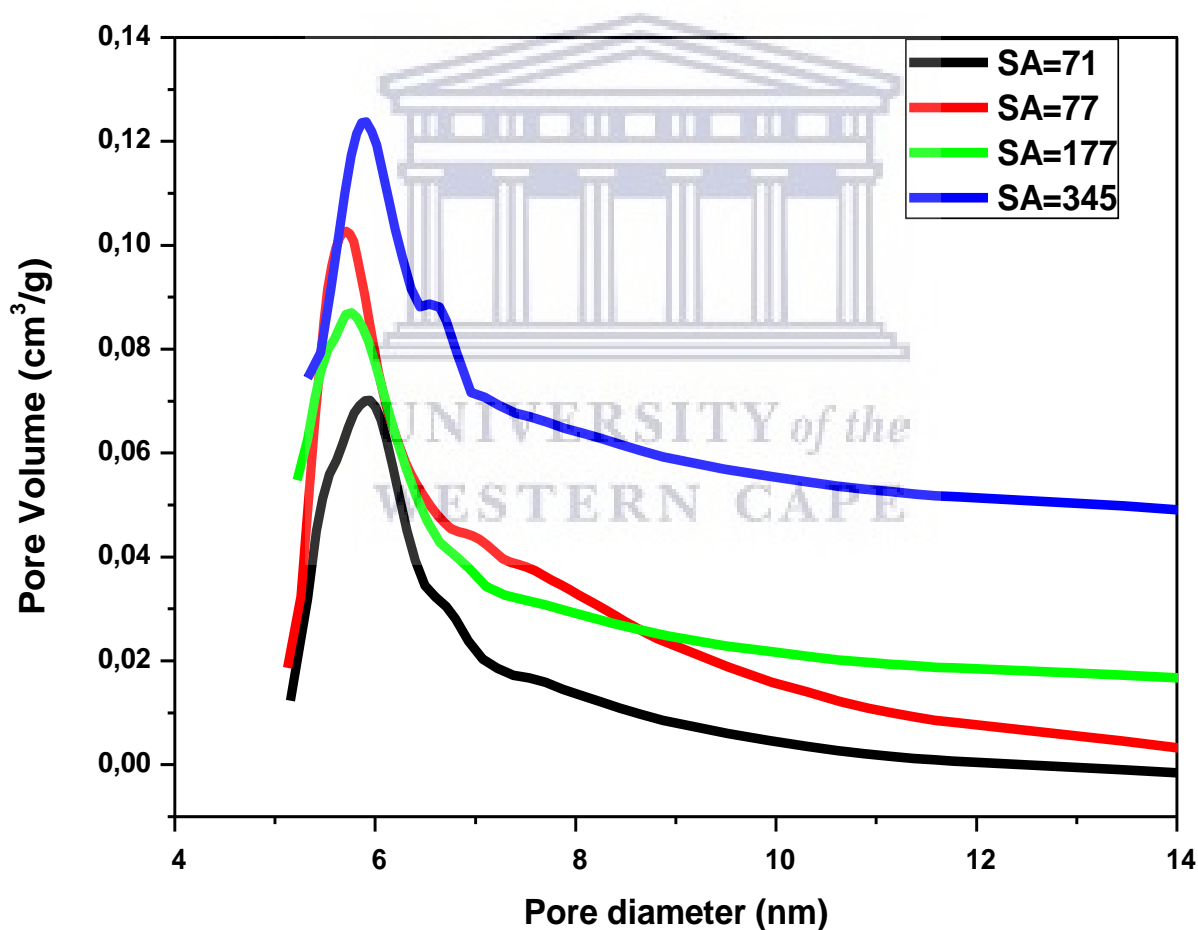


Figure 29: Corresponding BJH pore size distribution of the synthesized HZSM-5 materials.

4.8 Conclusion

In general, all the characterization techniques used in this study suggest that the prepared materials were synthesized successfully via steam-assisted hydrothermal approach. This was proven by the FTIR absorption peaks and XRD patterns that reflect the crystallinity of ZSM-5 zeolites and a degree of crystallinity of the hierarchical ZSM-5 type zeolite. The XRF results also show that the prepared materials have Si/Al ratios that are close to the expected ratios. According to the HRSEM results, the synthesized materials demonstrate large porosity in the mesoporous and macropore range and suggested the hierarchical material with 3 pore regimes was successfully synthesized. The SEM images confirm that macropores were generated, whereas the N₂ adsorption and desorption isotherms confirm mesopores and micropores. Furthermore, they show high crystallinity, surface areas as well as high total acidity. However, the SA=36 was not successfully prepared under the same synthesis approach used for all other materials. This was probably due to its large aluminum content present in the batch mixture, which resulted in slower crystallization kinetics, hence hindering the formation of crystals at given crystallization conditions. Even after altering the crystallization conditions by increasing the temperature and time, a high crystalline SA=36 was not successfully formed. Further work is needed in future to investigate if why the low SA=36 does not become crystalline under these working conditions. NH₃-TPD results show three desorption peaks that appear at a temperature range of 195-205 °C for weak acid sites and 363-567 °C for strong acid sites. A third peak is observed at 598-882 °C. To the best of our knowledge, such observation of HZSM-5 zeolites showing three desorption peaks with strong acid sites at such high temperatures has not been reported before. However, further tests were conducted by TGA analysis to investigate whether the prepared materials were thermally stable and that the observed third peak was not due to thermal decomposition. TGA results show loss of weight in the temperature range of 40-120 °C which is due to loss of moisture in the pores and on the surface of the material. The catalyst then becomes stable from the temperatures of 120-800 °C. This proves that the catalyst is thermally stable and the third peak found on the prepared catalysts is not due to thermal decomposition. The reason for the formation of high temperature 3rd peak in the TPD analysis is still unclear and further investigations are required. The prepared materials are expected to enhance the selectivity towards olefins, particularly ethylene and propylene due to their large pore sizes which leads to better diffusions.

4.9 References

1. Niu X.R, Li J, Zhang L, Lei Z.T, Zhao X.L, Yang C.H. ZSM-5 functionalized in situ with manganese ions for the catalytic oxidation of cyclohexane. *RSC Adv.* 2017;(7):50619–50625.
2. Narayanan S, Vijaya J.J, Sivasanker S, Ragupathi C, Sankaranarayanan T.M, Kennedy L.J. Hierarchical ZSM-5 catalytic performance evaluated in the selective oxidation of styrene to benzaldehyde using TBHP. *J Porous Mater.* 2016;(23):741–752.
3. Li Y, Sun H, Feng R, Wang Y, Subhan F, Yan Z, Subhan F, Yan Z, Zhang Z, Liu Z. Synthesis of ZSM-5 zeolite from diatomite for fluid catalytic cracking (FCC) application. *Appl Petro Res.* 2015;(5):347–353.
4. Schmidt F, Lohe M.R, Büchner B, Giordanino F, Bonino F, Kaskel S. Improved catalytic performance of hierarchical ZSM-5 synthesized by desilication with surfactants. *Micro Meso Mater.* 2013;(165):148–157.
5. Li H, Jin J, Wu W, Chen C, Li L, Li Y, Zhao W, Gu J, Chen G, Shi J-L. Synthesis of a hierarchically macro-/mesoporous zeolite based on a micro-emulsion mechanism. *J Mater Chem.* 2011;(21):193-195.
6. Gao Y, Zheng B, Wu G, Ma F, Liu C. Effect of the Si/Al ratio on the performance of hierarchical ZSM-5 zeolites for methanol aromatization. *RSC Adv.* 2016;(6):83581–83588.
7. Zhou J, Liu Z, Li L, Wang Y, Gao H, Yangdong W, Yang W, Xie Z, Tang Y. Hierarchical mesoporous ZSM-5 zeolite with increased external surface acid sites and high catalytic performance in o-xylene isomerization. *Chinese J Catal.* 2013;(34):1429–1433.
8. Farkaš A, Rožić M, Barbarić-Mikočević ž. A review on sustainable synthesis of zeolite from kaolinite resources via hydrothermal process. *J Hazard Mater.* 2005;(28):25–33.
9. Shirazi L, Jamshidi E, Ghasemi M.R. The effect of Si/Al ratio of ZSM-5 zeolite on its morphology, acidity and crystal size. *Cryst Res Technol.* 2008;(43):1300–1306.

CHAPTER 5: Catalytic Activity Investigations

Chapter Overview

This section deals with optimisation of the reaction conditions and the evaluation of the catalytic performances of the synthesized materials via catalytic cracking of hexane, dodecane and tyre derived oil [TDO]. The effects of reaction conditions such as temperature, WHSV and nitrogen diluent: feed ratio on the activity and selectivity were investigated. The main objective of this study is to do develop a catalytic system that favours the formation of olefins, particularly ethylene and propylene. The best optimum condition will be chosen based on their catalytic selectivity towards the formation of ethylene and propylene. The catalytic activity of the synthesized materials will then be tested at the optimised reaction conditions.

5.0 Optimisation studies

5.1 Effect of temperature on the catalytic cracking of hexane

The first study conducted was on the effect of temperature on catalytic activity. All the catalytic cracking reactions for optimization studies were performed using hexane as a model feed over a commercial ZSM-5 with SA=80 on a bench scale quartz-tube reactor. Figure 30 below shows hexane conversions over a period of 6 hours. The activity of the catalyst is determined from the amount of hexane converted and the selectivity is determined from the products formed on what has been converted. The activity of the catalyst is calculated from the amount of hexane that is converted. All the hexane that was present in the final product was assumed to be due to unconverted feed at the end of the reaction. As observed from Figure 30 below, conversion increases with an increase in temperature from 450-550 °C. The highest conversion of 98 % was found at high temperatures of 550 °C. This high conversion is expected to occur at high temperatures because C-C bonds can easily break at these temperatures as compared to lower temperatures. The conversion then slightly decreases with time until 87 % during the last hour [6th hour]. The second highest conversion of 84 % is obtained at 500 °C and the conversion decreases to about 69 %. The lowest conversion of 61 % is found at 450 °C and decreases slightly to 55 %. The decrease in conversion observed is with TOS.

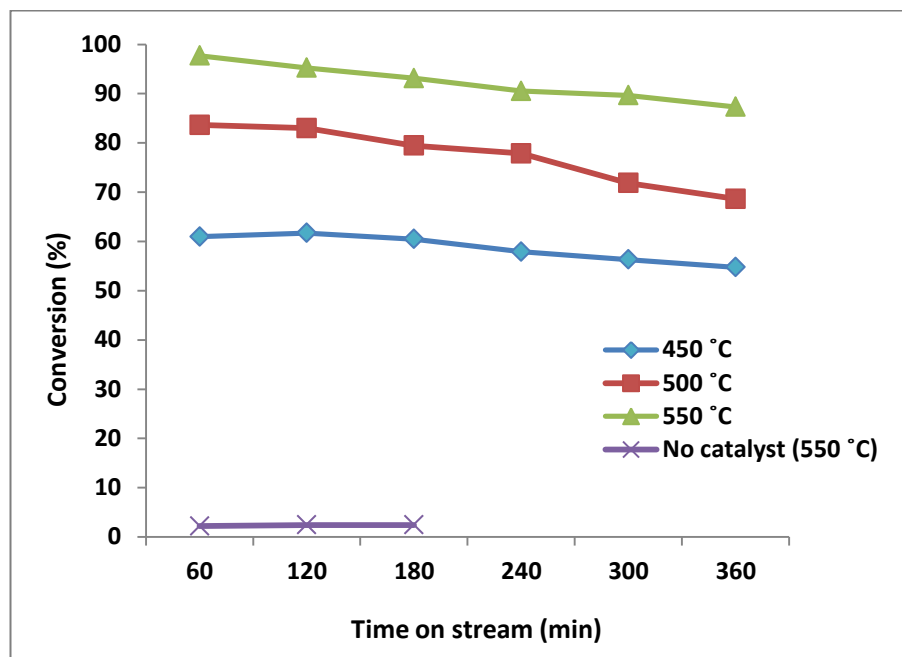


Figure 30: Catalytic conversions of hexane obtained when varying the temperature conditions. The reactions were carried out at different temperatures of 450, 500 and 550 °C. The following reaction conditions were used: Time on stream [TOS] = 6 hrs, N₂: Hexane dilution ratio = 1:1, feed flow rate = 0.1 ml/min, P = 1 atm, WHSV = 8 hr⁻¹, commercial ZSM-5 with SA = 80, catalyst mass = 0.5 g and also without a catalyst.

The highest decrease in conversion of 15 % is found to occur at 500 °C. The second highest decrease in conversion of 10 % occurs at 550 °C but still has the highest conversion. The smallest decrease in conversion of 6 % is found at 450 °C. This small decrease in conversion may be attributed to the lower activity of the catalyst which leads to fewer products from side reactions that cause deactivation of the catalyst. When the reaction is carried out under the same conditions at temperature of 550 °C but without the use of a catalyst, the conversion greatly drops to 3 % meaning that most of hexane [> 95%] does not convert into the desired products. This suggests that the high conversion obtained from other reactions is due to the use of a catalyst and not due to thermal cracking. The decrease in conversion that is observed when using these conditions could be due to wide range of products formed during the reaction such as paraffins, benzene, toluene, ethylbenzene and xylenes [BTEX] as observed in Figure 31 below. These products are known as coke precursors which lead to the formation of coke that ends up blocking the active sites on the catalyst. This may result in a drop in the activity of the catalyst. Similar results were observed by Konno *et al* (1) during

the catalytic cracking of n-hexane over nano-scale ZSM-5 zeolites with different Si/Al ratios [50, 150 and 300], without a catalyst and different temperatures [550, 600 and 650 °C]. They observed that the initial catalytic conversions increased with an increase in reaction temperatures. They concluded that the observed decrease in conversion was due to diffusion resistance of the produced light olefins, which lead to further reactions resulting in the production of aromatics and coke. A summary of their obtained results is displayed in table 12 below.

Table 12: Effect of temperature on catalytic cracking of n-hexane over nano-scale ZSM-5 catalysts with different Si/Al ratios and without the use of a catalyst (1)

Si/Al ratio	Temperature [°C]	Conversion [C-mol %]
50	550	72.3
150		58.5
300		17.5
No catalyst		1.2
50	600	93.1
150		81.8
300		38.2
No catalyst		4.8
50	650	99.4
150		95.7
300		66.7
No catalyst		20

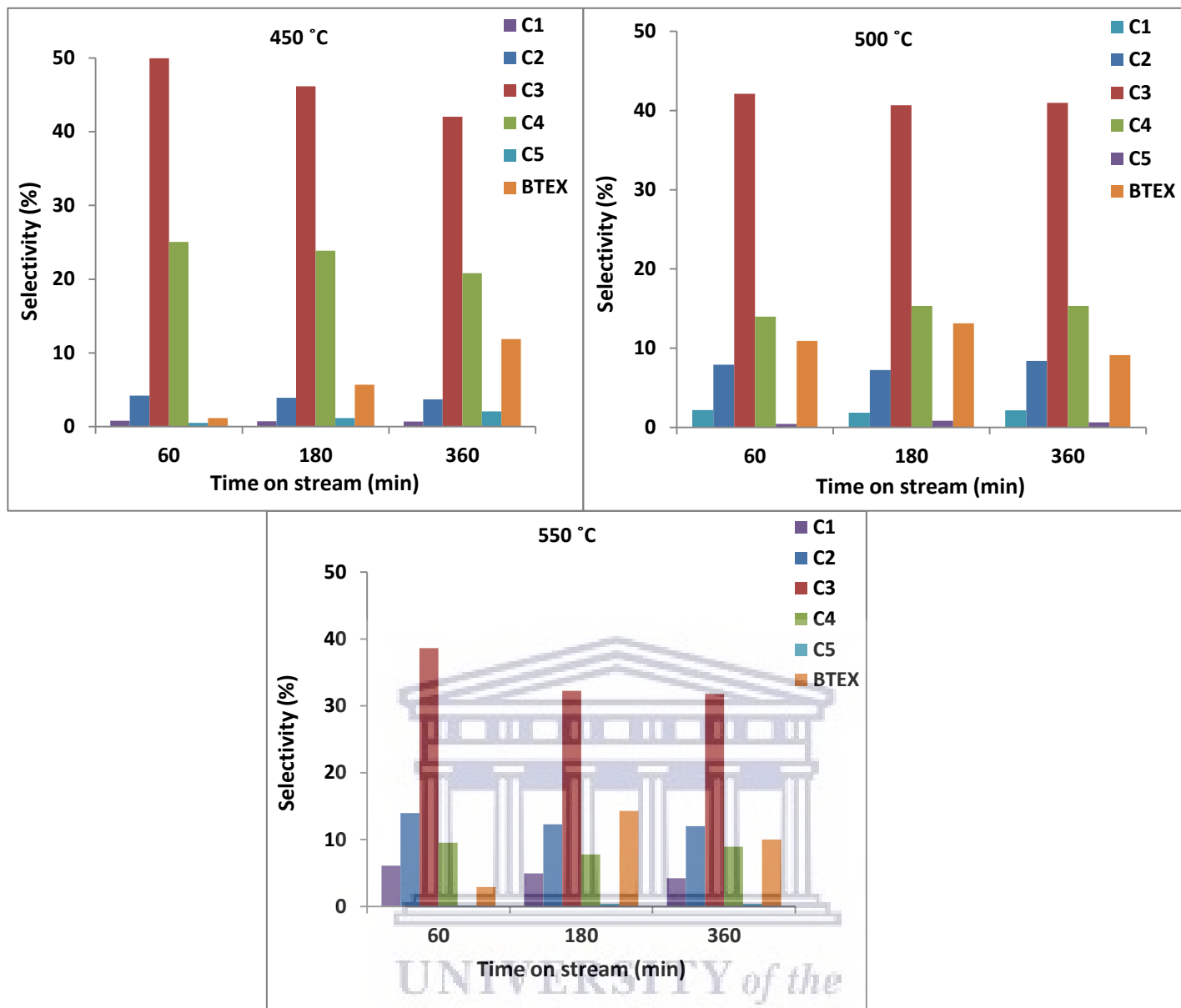


Figure 31: Selectivity towards paraffins and the BTEX products at different temperatures of 450, 500 and 550 °C formed during the 1st, 3rd and the 6th hour.

In the cracking of hexane, a wide product distribution is observed showing the formation of various products such as olefins, paraffins aromatics. This indicates that many other reactions occur besides cracking such as isomerization and hydrogen transfer etc. Figure 31 shows selectivity towards paraffins and BTEX products formed during the 1st, 3rd and the 6th hour of the reaction. The selectivity towards paraffins, especially for C₃ and C₄ is initially higher at temperatures of 450 °C and start to decrease with TOS. A further decrease in paraffins is observed as the temperature is increased from 500 °C to 550 °C. On the other hand, the BTEX products start to slightly increase as the temperature increases but with no much noticeable change at high temperatures. This indicates that there is aromatization taking place as the temperature is ramped up.

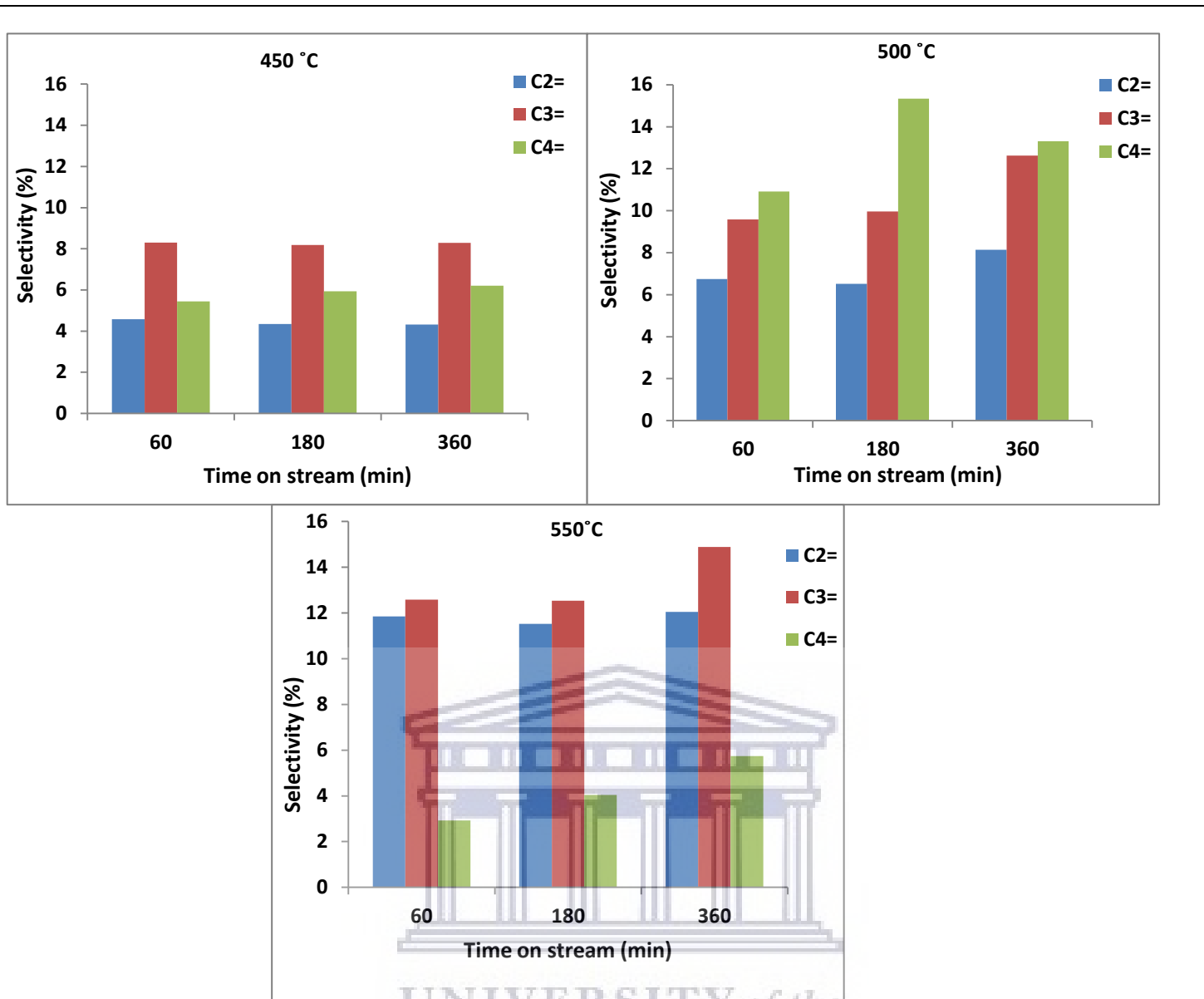


Figure 32: Selectivity to olefins [C2= to C4=] at different temperatures of 450, 500 and 550 °C during the 1st, 3rd and 6th hour.

Figure 32 shows the selectivity towards lower olefins i.e. ethylene, propylene and butenes respectively at different temperatures of 450, 500 and 550 °C during the 1st, 3rd and 6th hour TOS. When using 450 °C during the reaction, the selectivity towards propylene and butenes is higher, and the selectivity towards ethylene is lower. There is no change in the selectivity towards propylene as it is produced from 8 % during the 1st hour of the reaction until the 6th hour. Ethylene is found to be 5 % during the 1st hour to 4 % in the 6th hour. Butenes are found to be 5 % during the 1st hour to 6 % during the 6th hour respectively. At 500 °C, the selectivity is also high towards propylene and butenes and slightly lower for ethylene. In this case, the desired products of ethylene and propylene are found to be produced more when using high temperatures of

550 °C. At 550 °C, the selectivity towards propylene increases very slightly from 13 % during the 1st hour to 15 % during the 6th hour. There is no change in the selectivity towards ethylene as it is 12 % throughout the reaction. Butenes have been produced as small amounts and only show a slight increase from 3 % during the 1st hour to 6 % during the 6th hour. It can be observed that high temperatures favour more selectivity towards propylene. As the temperature increases, selectivity towards propylene also increases. This can be observed in Figure 32 where selectivity towards propylene increase with TOS as the temperature of the reaction increases from 450-550 °C. On the other hand, the selectivity towards paraffins is found to decrease with an increase in temperature as observed in Figure 32. This observation is due to fast dehydrogenation [e.g., paraffin to olefin] occurring at high temperatures, where produced olefins and BTEX products increase with a decrease in paraffins (1) as well as the higher cracking activity at higher temperatures, leading to a greater selectivity to olefins. Similar results were also observed by Konno *et al* (1) when they investigated the application of nano ZSM-5 with variable Si/Al ratios at different temperatures of 500, 600 and 650 °C. Light olefins and BTEX products increased with a decrease in paraffin selectivity. The total selectivity of light olefins and BTX products was 52.1 % at 500 °C, 60.4 % at 600 °C and 67.3 % at 650 °C. The total selectivity of paraffins was 43.3 % at 500 °C, 35 % at 600 °C and 26 % at 650 °C. They concluded that this observation was due to rapid dehydrogenation taking place at high temperatures. Other similar results were observed by Kubo *et al* (2) when they investigated the relationships between selectivities at a conversion of ca. 50 % and reaction temperatures of n-Heptane cracking over HZSM-5 with Si/Al = 31. They observed that there was an increase in ethylene and propylene selectivities at high reaction temperatures of 650 °C than at 450 °C. However, the propylene to ethylene ratio decreased from 3 at 450 °C to 1.4 at 650 °C. This was due to an increase in ethylene whereas at 450 °C, propylene increased in larger amounts. They also observed that the selectivities for propane and butanes decreased with higher reaction temperatures and the selectivities for methane and ethane increased, while those for BTX products did not have a noticeably change at higher temperatures. They deduced that the observed change in selectivity with reaction temperature may be due to greater dominance of monomolecular cracking over bimolecular cracking at higher temperatures.

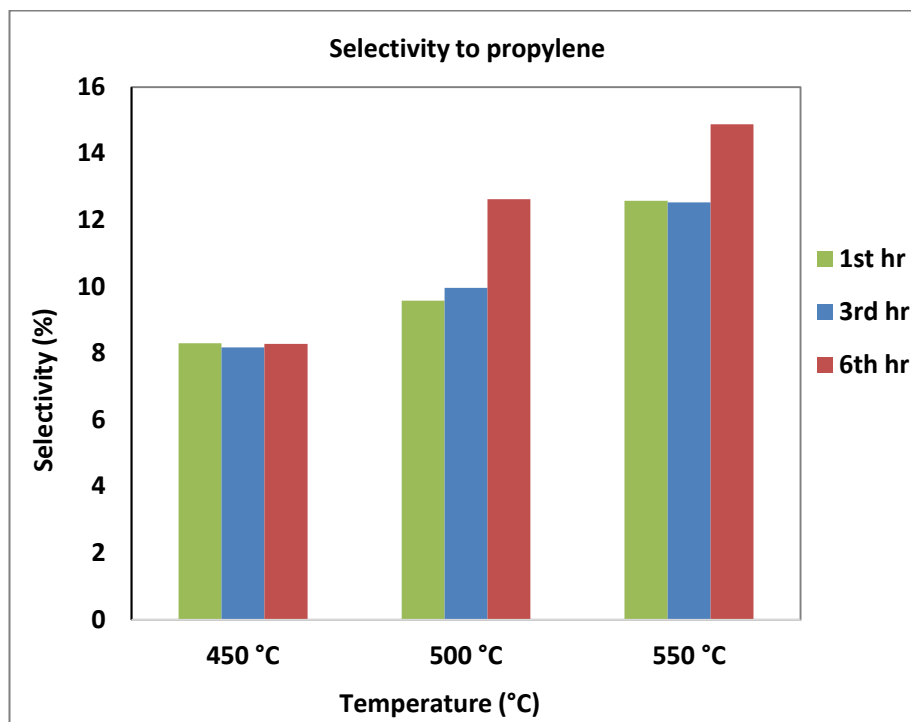


Figure 33: Selectivity towards propylene at different temperatures of 450-550 °C.

Figure 33 shows comparison in selectivity to propylene when using different temperatures. It can be observed that more propylene is produced when using high temperatures. The trend shows that as the temperature increases from 450-550 °C, there is more propylene produced from the 1st to the 6th hour. Therefore, 550 °C is found to be the suitable temperature for enhancing selectivity towards propylene.

5.2 The effect of catalyst loading on the catalytic cracking of hexane.

The effect of the catalyst loading was also studied and performed on a bench scale quartz-tube reactor using a commercial ZSM-5 with SA=80. The reactions were now carried at different catalyst loadings of 0.25g, 0.5g and 0.75g. The temperature of 550 °C has been used since it was found as the best temperature for enhancing selectivity to propylene. Figure 34 shows the hexane conversions over a period of 6 hours obtained when using these reaction conditions.

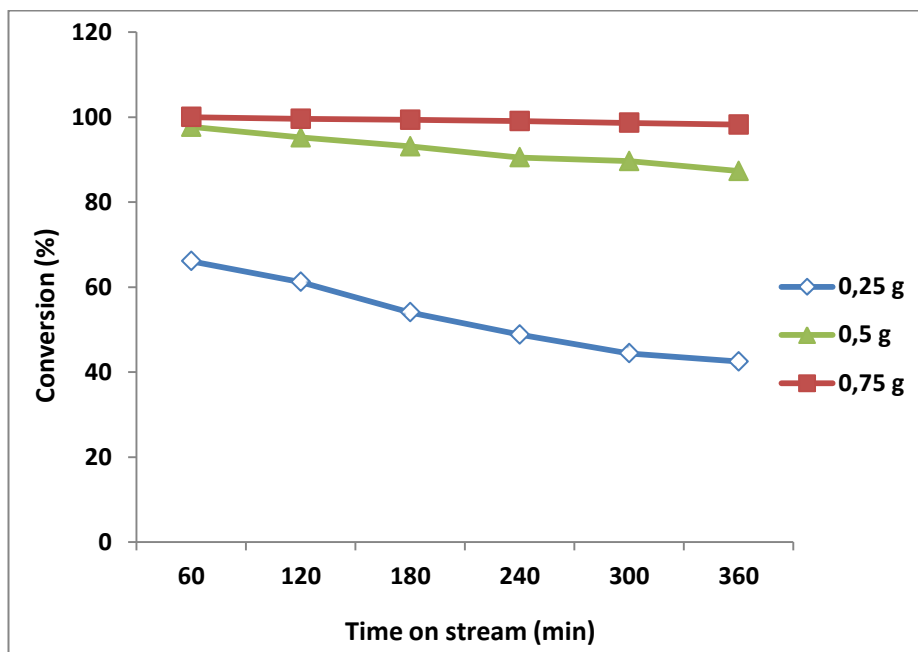


Figure 34: Catalytic conversions of hexane obtained when varying the catalyst loadings. The following reaction conditions were used: Time on stream [TOS] = 6 hrs, T=550 °C, commercial ZSM-5 with SA = 80, N₂: Hexane dilution ratio = 1:1, feed flow rate = 0.1 ml/min, P = 1 atm, WHSV = 15.82 hr⁻¹ when the catalyst mass = 0.25 g, WHSV = 8 hr⁻¹ when the catalyst mass = 0.5 g and a WHSV = 5.27 hr⁻¹ when the catalyst mass = 0.75 g.

As observed from Figure 34, an increase in catalyst loading results in an increase in conversion. The catalyst with a loading of 0.75 g is found to have the highest initial conversion of 100% and the conversion slightly decreases to 98 % during the last hour of the reaction. The decrease in conversion is very small and only drops by approximately 2 % showing that the catalyst is more stable with a high catalyst loading. The catalyst loading of 0.5 g is found to have the second highest initial conversion of 98 % and the conversion decreases to 87 % during the last hour of the reaction. This results in the second smallest decrease in conversion of 11 % with TOS. This is due to the fact that there are more accessible acid sites available with a higher catalyst loading that are able to perform many reactions such as cracking, aromatization, isomerization and hydrogen transfer, converting the feed [hexane] and resulting in a wide product distribution. The catalyst loading of 0.25 g is found to have the lowest initial conversion of 66 % and the conversion decreases to 42 % during the last hour. This is the largest decrease in conversion of approximately 24 % as compared to the catalyst loading of 0.5 g and 0.75 g. The decrease in conversion that

is observed when using a small catalyst loading may be due to less active acid sites available for further cracking reactions to occur and shorter residence time of the feed on the catalyst. Similar results were observed by Xian *et al* (3) when they investigated the effect of catalyst loading during the catalytic cracking of n-dodecane over HZSM-5 zeolite under supercritical conditions. They used different masses of 0.375, 0.75, 1 and 1.5 g of the HZSM-5 catalyst. They observed that the initial conversions decreased as the catalyst loadings decreased and this was due to a decrease in residence time, while the catalyst deactivation was not considerably affected by the catalyst loading. The largest catalyst loading of 1.5 g had a high initial conversion of ~52 %, whereas the smallest catalyst loading of 0.375 g had a low initial conversion of 25 % respectively.

Figure 35 shows the selectivity towards olefins [$C_2=$ to $C_4=$] for different catalyst loadings of 0.25, 0.5 and 0.75 g respectively. As much as the catalyst loading of 0.75 g looks stable with a higher conversion, it was found to be less selective towards the desired products [olefins]. As observed from Figure 35, the selectivity towards ethylene products for the catalyst loading of 0.25 g remains 13 % during the 1st hour to the 6th hour of the reaction. There is also no change for the catalyst loading of 0.5 g. The selectivity towards ethylene remains 12 % throughout the reaction. The catalyst loading of 0.75 g only produces ethylene from 12 % during the 1st hour to 11 % during the 6th hour. The catalyst loading of 0.25 g is more selective to the desired product of propylene than any other olefin product being produced. It is observed that propylene is produced from 18 % to 20 % when using a catalyst loading of 0.25 g. When using the catalyst loading of 0.5 g, the selectivity towards propylene is produced from 13 % during the 1st hour to 15 % during the 6th hour. For loading of 0.75 g, the selectivity to propylene remains 11 % throughout the reaction and this is almost less than half of what is being produced when using a catalyst loading of 0.25 g.

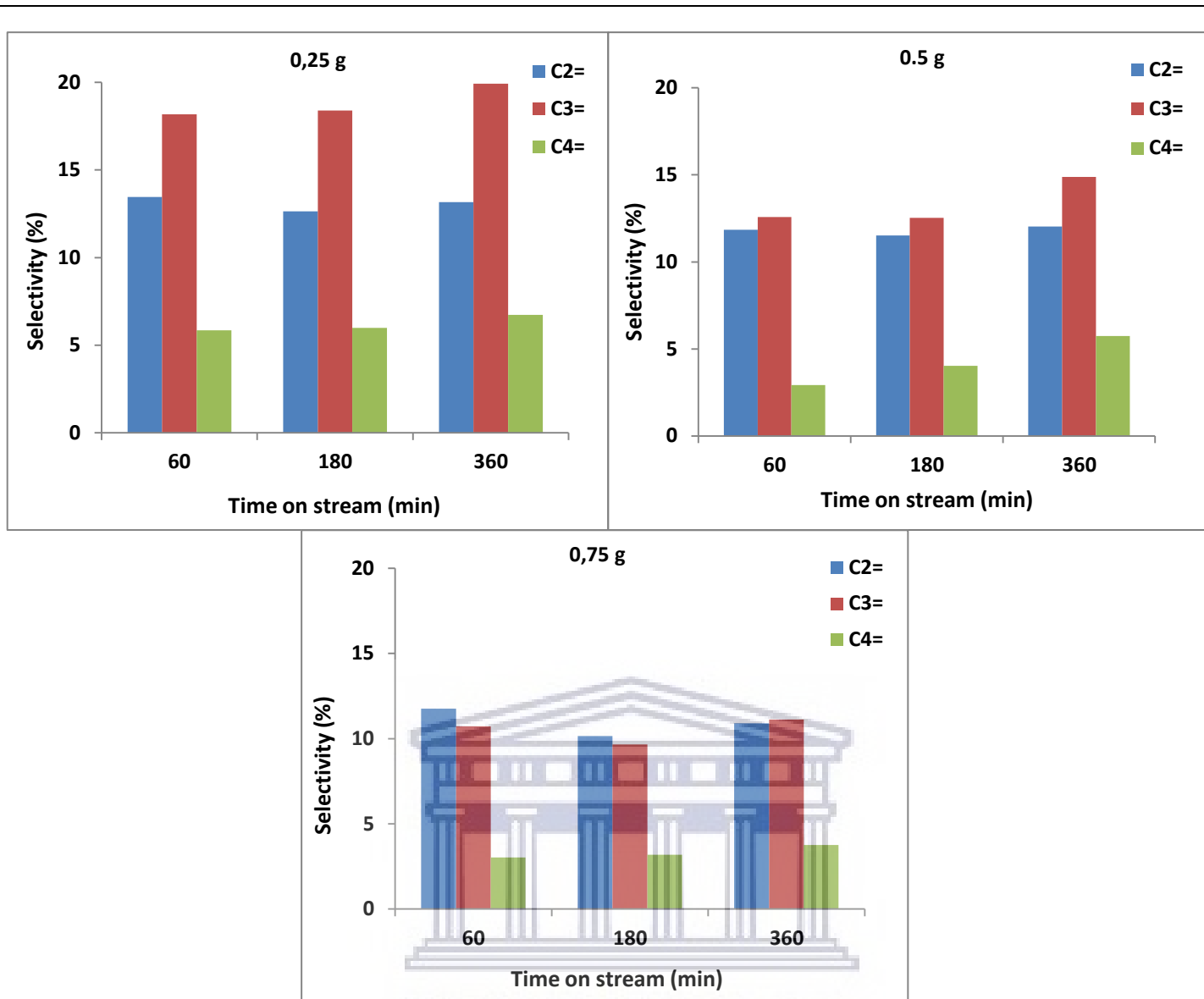


Figure 35: Selectivity to olefins [C2= to C4=] for different catalyst loadings of 0.25, 0.5 and 0.75 g.

There is not much change observed in the selectivity towards butenes as they seem to remain almost the same with TOS. When using the catalyst loading of 0.25 g, butenes are produced from 6 % during the 1st hour to only 7 % during the 6th hour. For the catalyst loading of 0.5 g, butenes are produced from 3 % and slightly increase to 6 % .When using 0.75 g of the catalyst butenes are only produced from 3 % during the 1st hour to 4 % during the 3rd hour. The high selectivity obtained when using a much less catalyst loading is due to its high WHSV. At a high WHSV, the feed will spend less time on the catalyst and mostly form the targeted products i.e. olefins which diffuse out of the catalyst before undergoing secondary reactions. However, at a low WHSV as the catalyst loading is increased, the feed spends more time on the catalyst and

the produced olefins which are highly reactive have more time to undergo secondary reactions, leading to many other products such as paraffins and BTEX products.

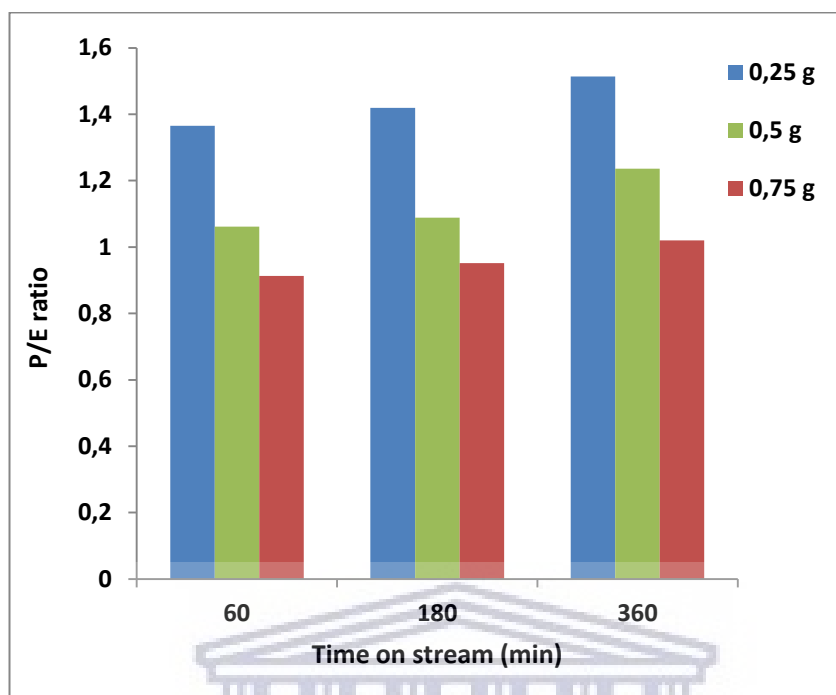


Figure 36: Propylene/Ethylene ratios for different catalyst loadings of 0.25, 0.5 and 0.75g.

Figure 36 shows propylene to ethylene ratios for different catalyst loadings of 0.25, 0.5 and 0.75 g during the 1st, 3rd and 6th hour. As expected, the lowest catalyst loading of 0.25 g demonstrates higher propylene to ethylene ratios as compared to when using the catalyst loading is 0.5 g and 0.75 g. This is due to a higher selectivity towards propylene with TOS at higher WHSV's. The P/E ratios obtained are greater than 1 for catalyst loadings less than 0.75 g, which are acceptable to meet the demands for propylene on an industrial level. Consequently, it can be concluded that the catalyst loading of 0.25 g is the best for enhancing the selectivity towards olefins.

5.3 The effect of N₂: Hexane dilution ratios

The effect of different N₂: Hexane dilution ratios were also studied during the catalytic cracking of hexane so as to find the best nitrogen to feed dilution ratios for testing the prepared catalysts. The N₂: Hexane dilution ratio of 0:1 means that there is no nitrogen used during the reaction. This was done to test whether

diluting the feed with nitrogen will have an effect on the catalytic test results, in particular the selectivity to olefins. Figure 37 below shows the obtained catalytic conversions that were taken over a period of 6 hours when using a catalyst loading of 0.25 g.

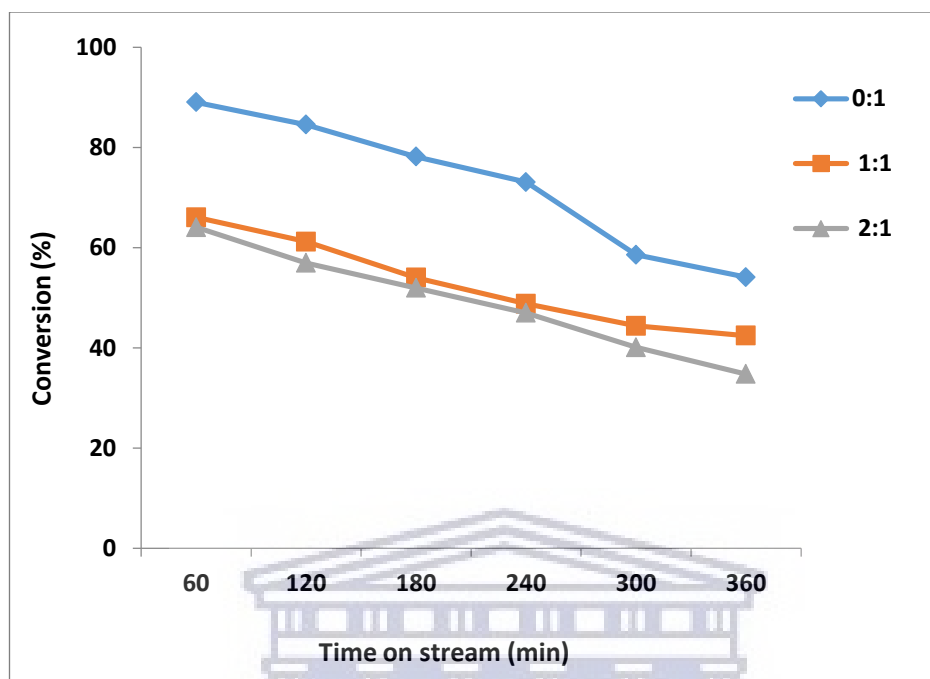


Figure 37: Catalytic conversions of hexane obtained when varying the N_2 : Hexane dilution ratios. The reactions were carried using different nitrogen to feed ratios [N_2 : Hexane] under the following conditions: Time on stream [TOS] = 6 hours, N_2 : Hexane dilution ratios = [0:1, 1:1 and 2:1], feed flow rate = 0.1 ml/min, $T = 550\text{ }^\circ\text{C}$, Catalyst mass = 0.25 g, $P = 1\text{ atm}$ and a $WHSV = 15.82\text{ hr}^{-1}$.

As observed from Figure 37, the N_2 : Hexane ratio of 0:1 has got the highest starting conversion as compared to the other ratios. This is expected as there is no nitrogen involved in the reaction. Hence, there is no dilution of the feed which allows more feed molecules to interact with active sites. The conversion for this reaction starts at 89 % and decreases to 54 %. When nitrogen is introduced in the reaction, the conversion starts to decrease. It can be observed from the ratio of 1:1 that the conversion starts from 66 % and further continues to drop to 43 %. This may be due to the feed having a shorter contact time with the catalyst since it is carried by nitrogen. This is done to dilute hexane and to help prevent any side reactions that may occur when the feed spends a long period of time in contact with the catalyst. When using a dilution ratio of 2:1, a further drop in conversion is observed from 64 % to 35 %. As much as the ratio of 0:1 has got the

highest starting conversion, it also has got the largest decrease in conversion of 35 % over the period of 6 hours as compared to the other ratios followed by the ratio of 2:1 with a decrease of 29 %. The ratio of 1:1 has got the lowest decrease of 23 %. This means the ratio of 0:1 and 2:1 deactivates at a faster rate than that of 1:1.

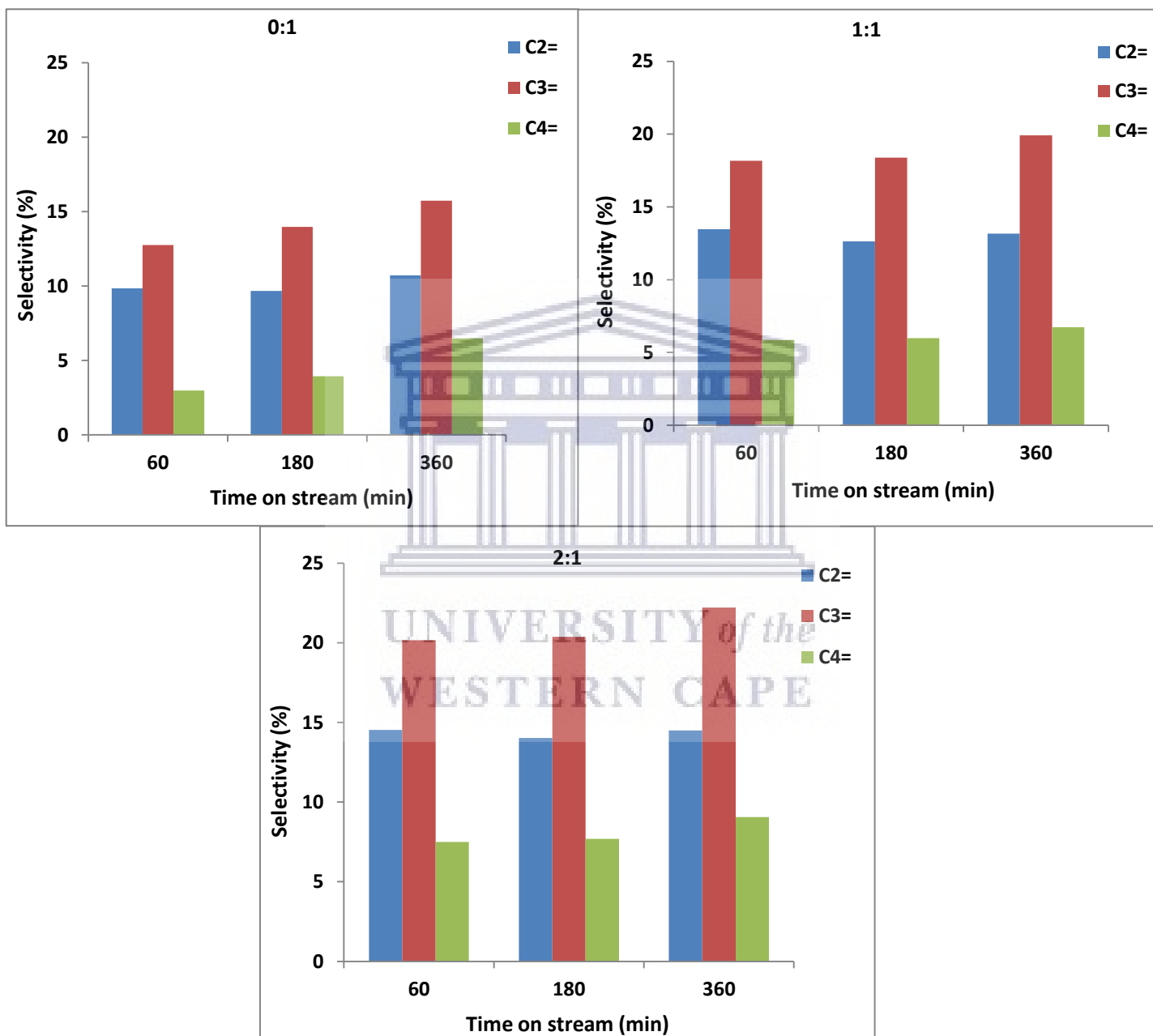


Figure 38: Selectivity to olefins [C2= - C4=] when varying the N₂: Hexane dilution ratios over a period of 6 hours.

Figure 38 shows the selectivity towards olefins when varying the nitrogen to hexane dilution ratios. The dilution ratio of 0:1 shows the lowest selectivity towards olefins. A very slight increase in selectivity towards ethylene is observed from 10 % during the first hour to 11 % during the 6th hour. The selectivity towards propylene also slightly increases from 13 % during the 1st hour to 16 % during the 6th hour. A slight increase is observed in selectivity towards butenes from 3 % to 6 %. However, there is a significant increase in selectivity towards olefins when introducing nitrogen during the reactions. This can be observed from both reactions with the ratios of 1:1 and 2:1. It is evident that the use of nitrogen has an effect in boosting the selectivity towards olefins. Looking at the dilution ratio of 1:1 and 2:1, the selectivity towards all the produced olefins have increased as compared to the ratio of 0:1. For 1:1, selectivity towards ethylene remains at 14 % during the 1st hour to the 6th hour of the reaction. The selectivity towards propylene slightly increases from 18 % to 20 % and butenes are produced slightly from 6 % to 7 %. The reaction ratio of 2:1 shows the highest increase in the olefin products as compared to all the other ratios. However, this increase is almost the same as to the ratio of 1:1 since there is no much difference in the dilution ratios. The selectivity towards ethylene is the same as it is observed to be 14.5 % during the 1st hour and the 6th hour of the reaction. The selectivity towards propylene slightly increases from 20 % to 22 % with TOS and the butenes from 8 % to 9 %.

Figure 39 below shows propylene to ethylene ratios obtained from different N₂: Hexane dilution ratios. All the calculated P/E ratios increase with an increase in the N₂: Hexane dilution ratios and are found to be increasing from the 1st to the 6th hour of each reaction. This shows that for each reaction, propylene is the most produced olefin which is a desired product. The ratio of 2:1 shows the highest P/E ratio as expected since it has the highest propylene produced, followed by the ratio of 1:1 and lastly, that of 0:1. The ratio of 0:1 has the highest starting conversion, but this conversion has the largest decrease of 35 % as compared to the other ratios. Furthermore, it is observed to have the lowest selectivity towards olefins and the highest selectivity towards paraffins and BTEX products. The ratio of 1:1 has a starting conversion of 66 % with the lowest decrease of 23 %. The dilution ratio of 2:1 has got the highest selectivity towards olefins as compared to the other ratios. As much as the ratio of 2:1 is more selective towards olefins, there is only a very slight difference in the produced amounts when comparing it to the ratio of 1:1. The ratio of 2:1 also has the

second largest decrease in conversion of 29 %. It is most advisable to work with the catalyst that is more stable and more selective to the ideal product. Furthermore, industrially it would be best to work with a lower dilution ratio to save costs. Hence, the dilution ratio of 1:1 is found as the condition which best balances activity, selectivity and stability.

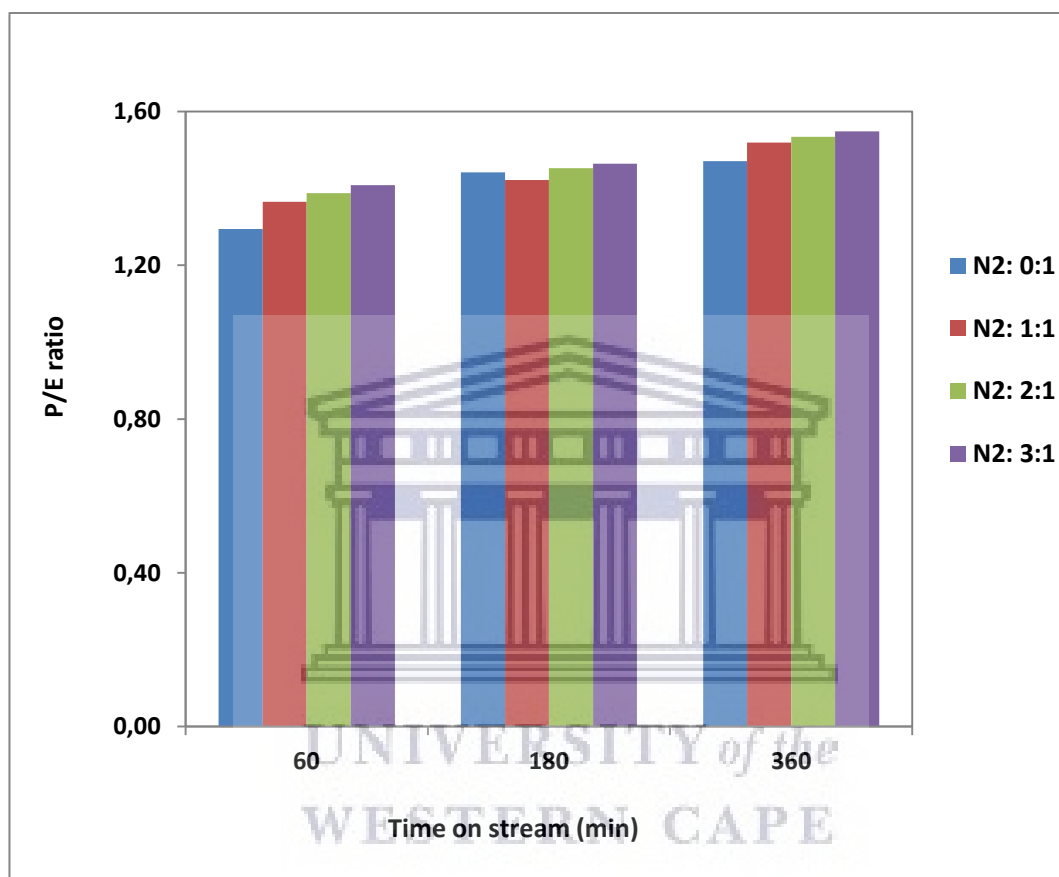


Figure 39: P/E ratios for different N₂: Hexane dilution ratios.

5.4 Catalytic cracking of hexane over hierarchical ZSM-5 catalysts with different Si/Al ratios.

Catalytic cracking of hexane was studied over the prepared hierarchical ZSM-5 catalysts with different Si/Al ratios using the designated optimum conditions. Figure 40 below shows the conversions of the prepared HZSM-5 catalysts over a period of 6 hours obtained when using these reaction conditions.

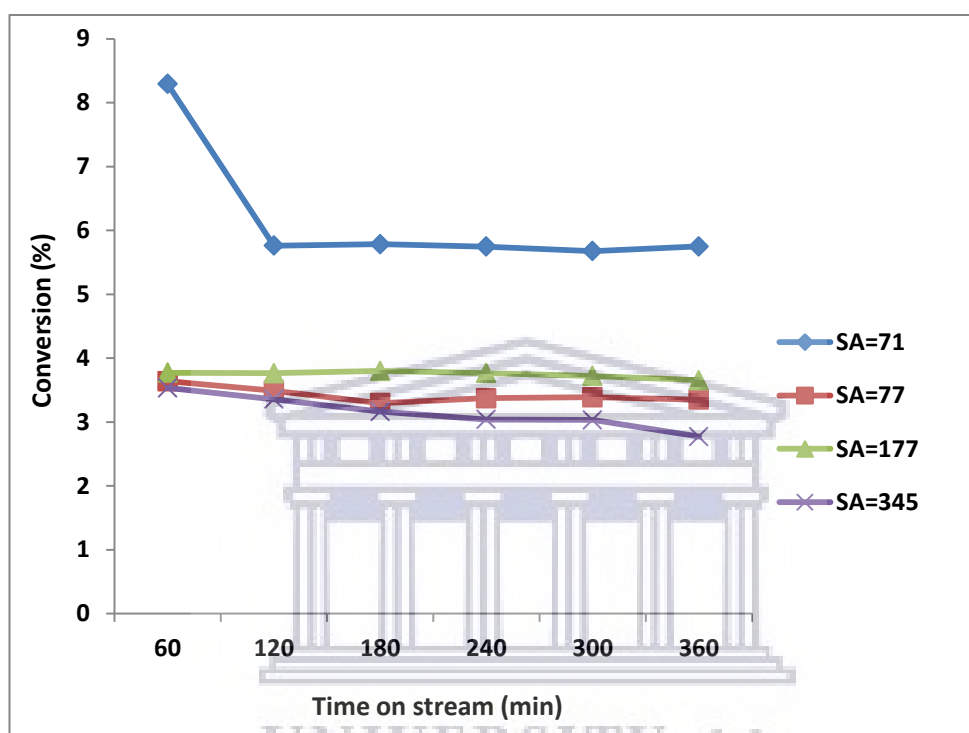


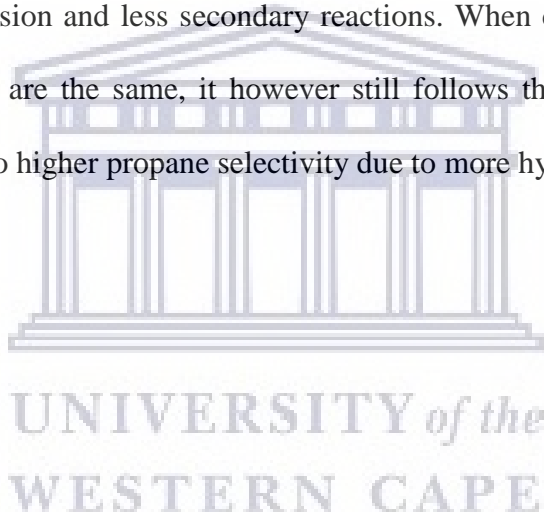
Figure 40: Catalytic conversions of hexane obtained from using HZSM-5 catalysts. All the catalytic cracking reactions were performed on a bench scale quartz-tube reactor using hexane as a model feed. The reactions were carried under these conditions: $T = 550\text{ }^{\circ}\text{C}$, Time on stream [TOS] = 6 hours, N_2 : Hexane dilution ratio = 1:1, feed flow rate = 0.1 ml/min, $P = \text{atm}$, $\text{WHSV} = 15.82\text{ hr}^{-1}$ and a catalyst mass = 0.25 g.

As observed from Figure 40, the obtained conversions appear in very low amounts. The catalyst with the SA=71 has got the initial highest conversion of 8.3 % during the 1st hour which decreases to 5.7 % during the 2nd hour and then it was stable as the reaction proceeds to the 6th hour. The observed initial decrease in conversion may be that the catalyst was still reaching its steady state. The initial conversions are lower for the catalysts with SA=77, SA=177 and SA=345. However, all these catalysts are stable as the conversion remains the same throughout the reaction. The lowest conversion is found on the catalyst with the SA=345,

with an initial conversion of 3.5 % which slightly decreases to 2.8 % during the 6th hour. The highest conversion is found on the catalyst with the lowest Si/Al ratio, while the lowest conversion is found on the catalyst with a high Si/Al ratio. From the studies of the materials physicochemical properties, it is shown that the effect of Si/Al ratio mainly affected the zeolite materials acidic properties. The Si/Al ratio had an effect on both the acid site quantity as well as the site strength. The general observed trend is that catalytic activity is inversely proportional to Si/Al ratio. From the NH₃-TPD results, the SA=71 has the highest total acidity and the SA=345 has the lowest acidity, hence the observed trend in conversion. However, a closer look shows a correlation between the activity, i.e. conversion and acid strength of the strong acid sites. In the NH₃-TPD desorption at temperatures above 300 °C are generally ascribed to strong Bronsted acid sites formed from the aluminium atoms within the framework of the crystal structure. The trend observed from the NH₃-TPD results in terms of acid strength of the strong acid sites showed a decrease in the order SA=71>177>77>345. The same trend is observed in the catalytic activity of the materials as noticed in Figure 40. Therefore, it can be said that the catalytic activity is mainly due to the acid strength of the strong Bronsted sites rather than the total acidity or acid site quantity. The activity for these synthesized catalysts is found to be stable at these conversions even though they are very low as compared to the commercial catalyst with SA=80. Even though the commercial catalyst has a Si/Al molar ratio that is close to SA=71 and SA=77 which should be similar in terms of acidity, it still has smaller pores that are only in the microporous range. Therefore, the observed low conversions found when using the prepared catalysts may be due to large pores that were generated during the fabrication of these HZSM-5 catalysts. This may have allowed the hexane feed to pass through the catalyst pores with much less interaction with the active sites. This is further investigated by carrying out testing reactions with larger molecules and is discussed in the sections below.

Figure 41 shows the selectivity towards paraffins and BTEX products produced when using the HZSM-5 catalysts with different Si/Al ratios. A wide distribution of paraffins and BTEX products is observed with the use of these prepared catalysts. This indicates that there are side reactions such as aromatization, isomerization, dehydrogenation and hydrogenation occurring during these reactions. The SA=71 is more selective to paraffins, especially the C₂ and C₃ products with less BTEX products produced with TOS.

However, there are more C₃ products produced than C₂ paraffins with this catalyst. This is probably related to its stronger acidity that lead to a slightly higher conversion as compared to the other catalysts. As the Si/Al increases, there are more BTEX products produced as well as more C₂ than the C₃ paraffins. This is caused by the low acidity as well as lower conversions as the Si/Al ratio increases. The product distribution as a function of conversion indicate that hydrogen, methane, ethane, ethylene, propylene and butenes are primary products. On the other hand, propane and butane are secondary products and are produced by hydrogen transfer reactions of the corresponding olefins (2). Thus at high conversions such as those observed when using the commercial catalyst, the propane amount is high due to secondary hydrogen transfer. In the case of the prepared catalysts, propane is produced in less amounts than when using the commercial catalyst. This is likely due to larger pores which leads to less interaction with the small hexane molecule, resulting in less conversion and less secondary reactions. When comparing only the synthesized materials in which the properties are the same, it however still follows that the catalyst i.e. SA=71 with stronger and higher acidity leads to higher propane selectivity due to more hydrogen transfer reactions.



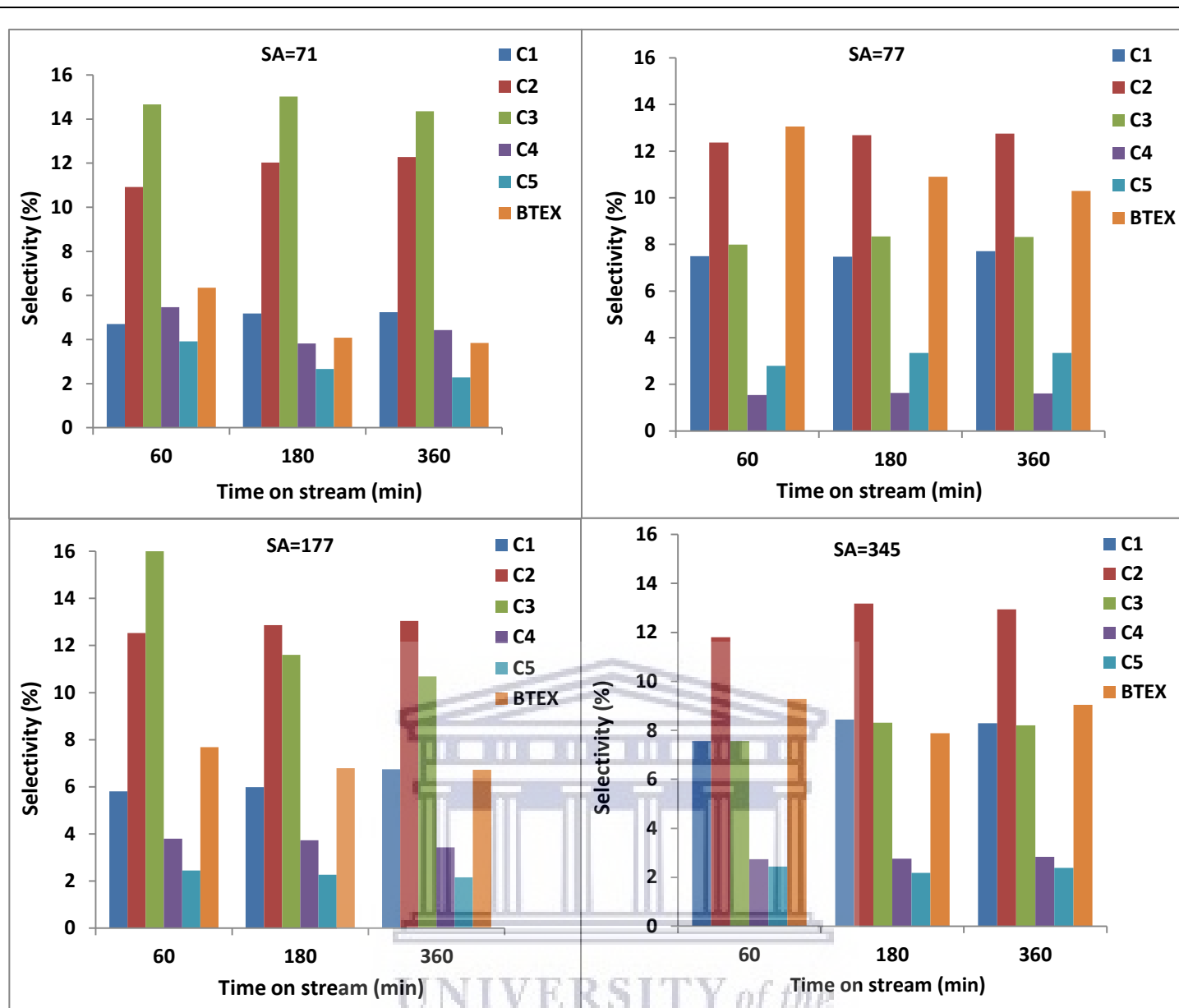


Figure 41: Selectivity towards paraffins and BTEX products for HZSM-5 catalysts.

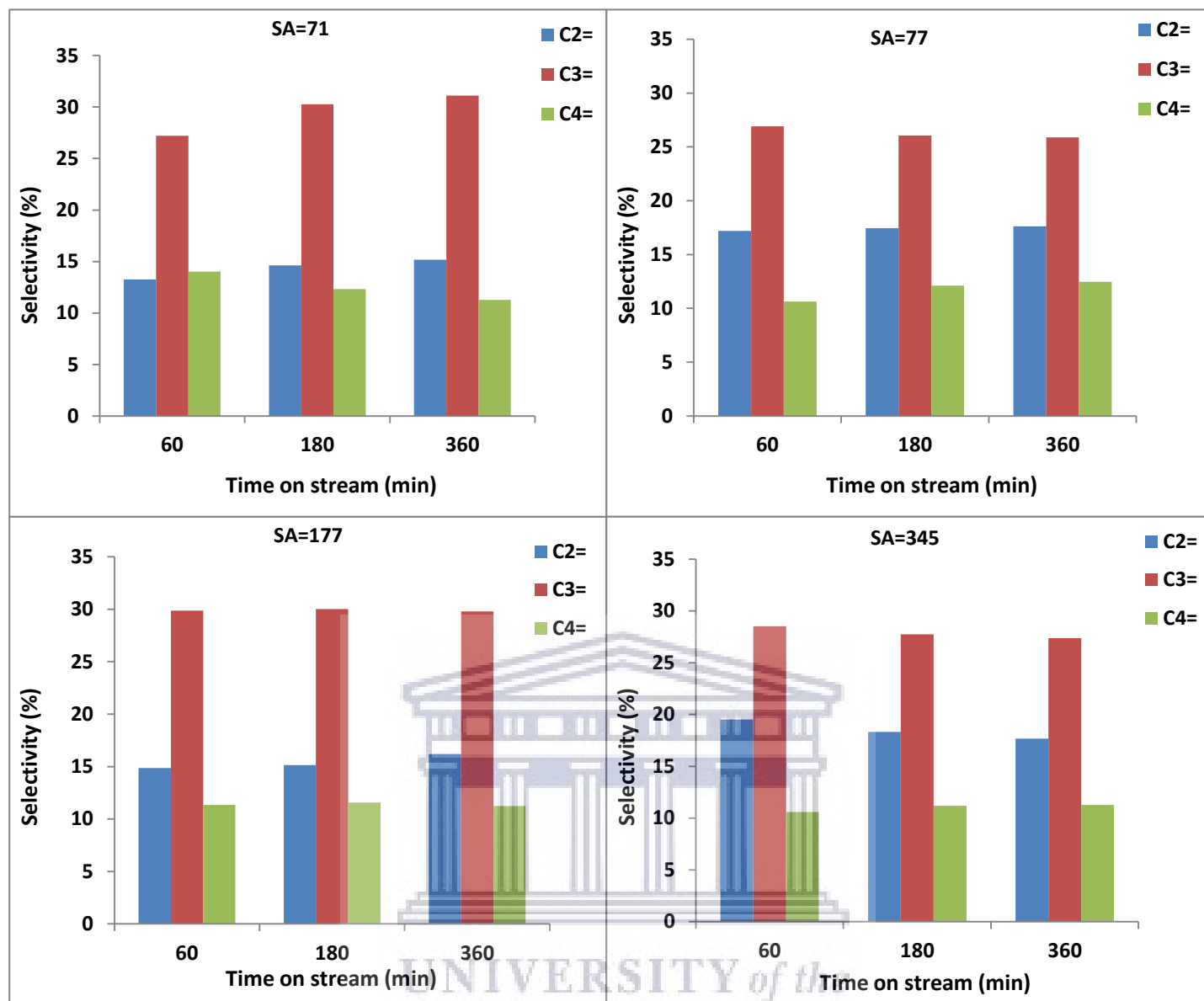


Figure 42: Selectivity to olefins [C₂= - C₄=] products for HZSM-5 catalysts.

Figure 42 shows the selectivity towards olefins [C₂= - C₄=] products produced when using the prepared hierarchical zeolites during the catalytic cracking reactions. It is truly interesting to see that even though these prepared catalysts reveal very low conversions, there is a slight increase towards olefins as compared to when using the commercial ZSM-5 with SA=80. The slight increase in olefins is due to the bigger pores in the prepared HZSM-5 catalysts. The large pores allow better diffusion through the catalyst, resulting in small hexane molecule to easily pass through and react very slightly. This results in low conversions where better selectivities to olefins are obtained. It is observed from Figure 42 that the lowest SA=71 has the highest selectivity towards propylene which increases with TOS as compared to the other ratios. This high

selectivity is associated with the slight drop in conversion as well as the strong acid sites this catalyst has, as observed from the NH₃-TPD results. The selectivity towards propylene is found to be slightly lower as the Si/Al ratio increases and follows the trend observed for the conversions as well as acid strength of the strong Bronsted sites i.e. SA=71>177>77>345. This indicates that the selectivity to propylene is dependent on the conversion which is in turn dependent on the strength and amount of acid sites available. It is also observed that the selectivity towards ethylene slightly increase with TOS as the Si/Al ratio increases. This may also be due to the decrease in strong acid sites as the Si/Al ratio increases. Therefore, it is evident is evident that the variations in the Si/Al ratio affect the acidity of the materials which results in differences in catalytic performance in terms of activity, selectivity and stability.

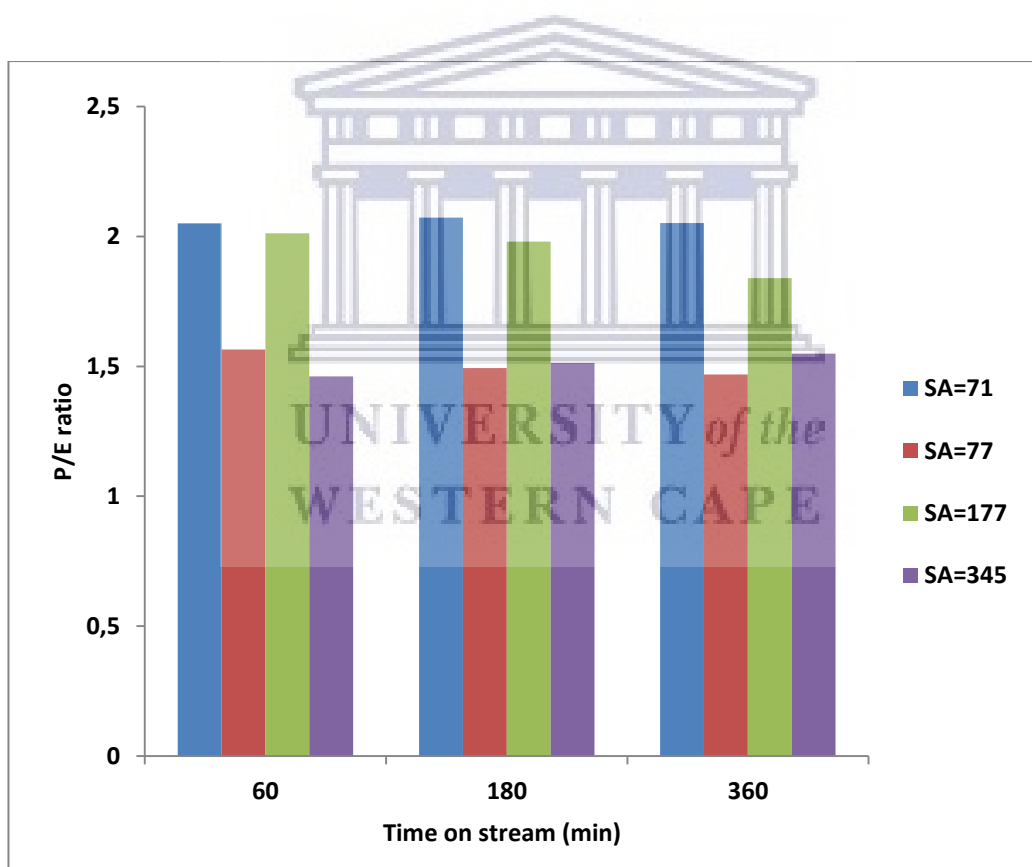


Figure 43: P/E ratios for the prepared HZSM-5 catalysts with different SA ratios.

Figure 43 displays the propylene to ethylene ratios for the prepared HZSM-5 catalysts with different Si/Al ratios during the 1st, 3rd and the 6th hour of the reaction. All the catalysts display high propylene to ethylene ratios [P/E > 1]. The P/E ratios remain the same with TOS for all the catalysts. However, the P/E ratios of

the catalysts slightly differ as the catalysts with stronger Bronsted acid sites [SA=71] have slightly higher ratios than the ones with higher Si/Al ratio [SA=345] and lower strength acid sites. The P/E ratios also decrease in the same order as conversion and selectivity to olefins i.e. SA=71>177>77>345. The catalyst with SA=71 has got the highest P/E ratio of 2.1 as compared to the other catalysts. This is due to its high acidity and higher conversion, leading to a high selectivity towards propylene and low selectivity to ethylene. Therefore, it can be concluded that the SA=71 is found to be the best catalyst for enhancing the selectivity towards olefins when using hexane as a feed since it more stable and demonstrates an increase in selectivity towards light olefins with TOS.

5.5 Catalytic cracking of dodecane

Catalytic cracking of dodecane was studied and performed on a bench scale quartz-tube reactor using the prepared HZSM-5 catalyst with SA=71 and a commercial ZSM-5 catalyst with SA=80. This study was conducted to investigate the catalyst performance and the effect of the pore sizes on catalytic conversions and product distribution when using a longer chain hydrocarbon such as dodecane. The effect of the pore size is determined by comparing the synthesized ZSM-5 catalyst with additional mesopores and macropores to a commercial ZSM-5 catalyst. The HZSM-5 catalyst with SA=71 was chosen since it is found to be the best for enhancing the selectivity towards olefins than the other prepared HZSM-5 catalysts. Figure 44 below shows the catalytic conversions of dodecane when using the prepared zeolite with SA=71 and a commercial zeolite with SA=80.

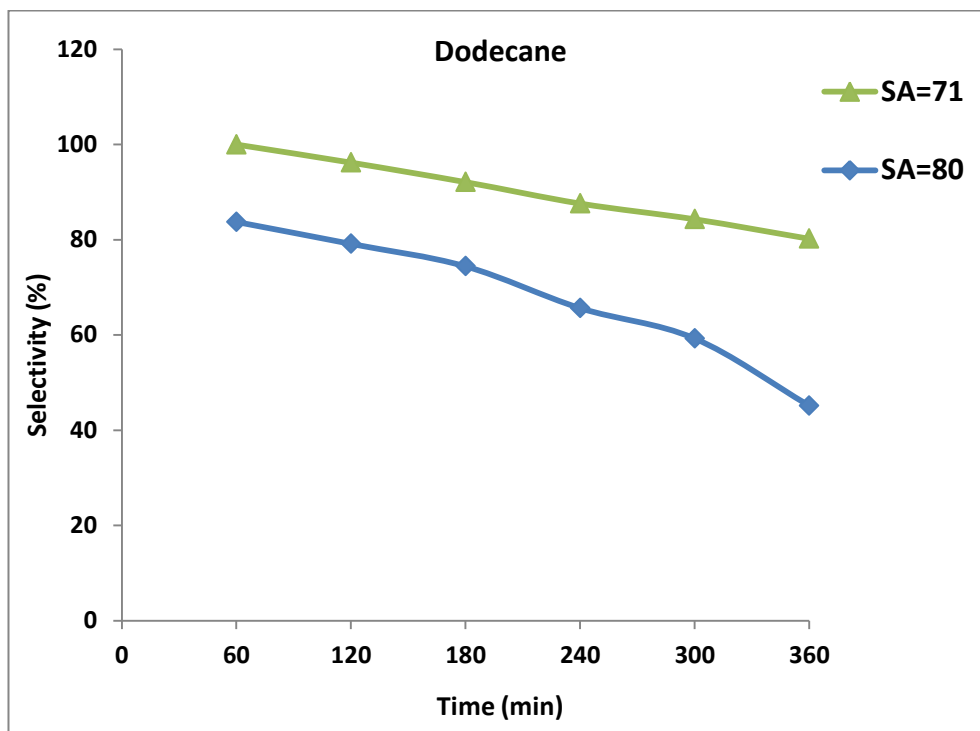


Figure 44: Catalytic conversions of dodecane obtained when using the synthesized zeolite with SA=71 and a commercial zeolite with SA=80. The catalytic cracking reactions were performed on a bench scale quartz-tube reactor using dodecane as a model feed. The reactions were carried under the following conditions: T = 550 °C, Time on stream [TOS] = 6 hours, N₂: Hexane dilution ratio = 1:1, feed flow rate = 0.1 ml/min, P = 1 atm, WHSV = 15.82 hr⁻¹ and a catalyst mass = 0.25 g.

As observed from Figure 44, the catalyst with SA=71 has got the highest initial conversion of 100 % during the 1st hour, which then slightly decreases to 80 % as the reaction proceeds to the 6th hour. When using the commercial catalyst, the initial conversion is found to decrease from 84 % during the 1st hour, to 45 % during the 6th hour. This is a large drop of 39 % in conversion when comparing it to the SA=71. Both catalysts have a similar Si/Al ratio which is related to acidity. The high initial conversions observed when using these catalysts could be due to their strong acidity. However, the higher initial conversion of 100 % observed when using the SA=71 is possibly due to acid sites being more accessible compared to the commercial zeolite catalyst with microporous structure. The SA=71 catalyst also has better catalyst stability as it showed a lower decrease in conversion with TOS. This may be due to better diffusion of a large hydrocarbon molecule through the catalyst with mesopores as compared to the one with micropores, which may hinder diffusion and lead to the greater formation of secondary products such as aromatics that act as

coke precursors and ultimately result in a decrease in activity. The effect of porosity on activity is also clearly highlighted. In the catalyst in which mesopores system is introduced, the activity of the catalyst is shown to dramatically increase when using the larger dodecane i.e. initial conversion = 100 % compared to the smaller hexane molecule with ~ 8 % initial conversion. A longer chain will be more interactive with the acid sites, leading to higher conversions as compared to when using hexane which is a shorter chain. Therefore, pore size can be considered to have a significant impact on catalytic activity. Furthermore, these results indicate that mesoporous ZSM-5 catalyst may be better suited to the cracking of larger hydrocarbon chains.

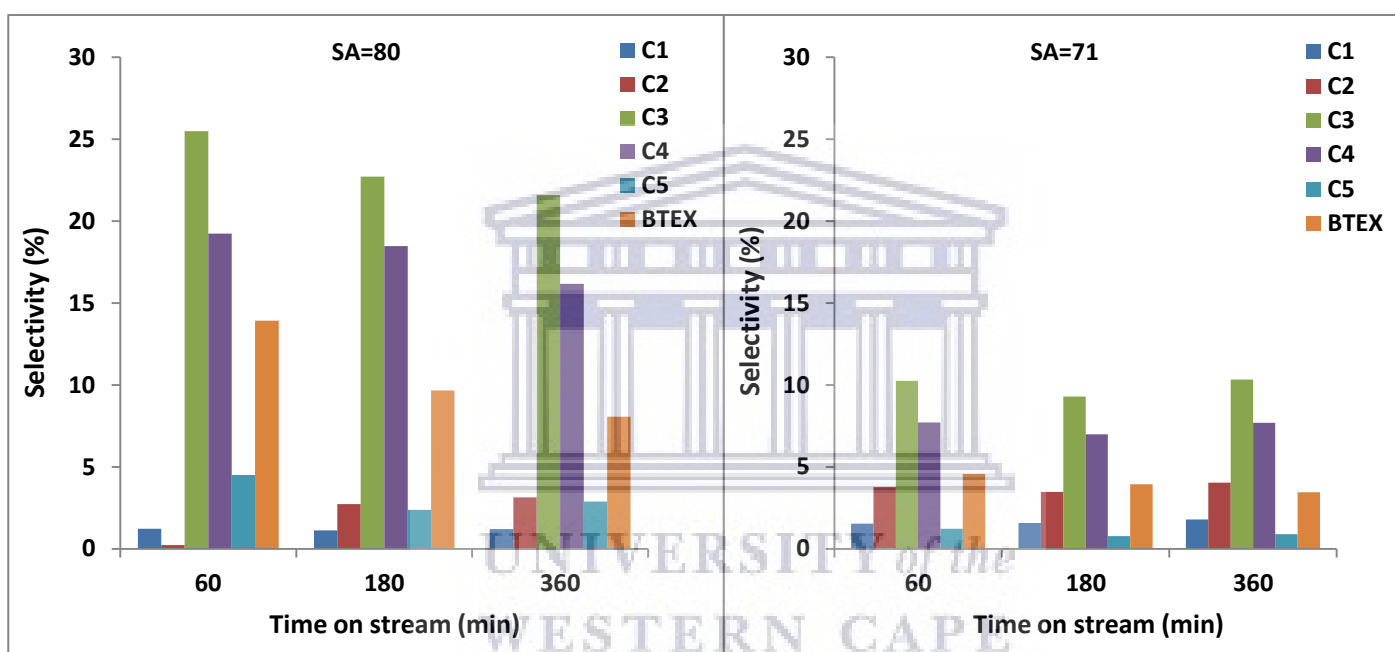


Figure 45: Selectivity towards paraffins and BTEX products formed when using the commercial catalyst with SA=80 and the prepared catalyst with SA=71.

Figure 45 shows selectivity towards paraffins formed during the 1st, 3rd and 6th hour of the reaction. It can be clearly observed that there are more paraffins and BTEX products formed with the SA=80 than the SA=71. This means that there are many other reactions taking place when making use of a commercial catalyst than that of the SA=71. These reactions are due to the micropores in the commercial catalyst, leading to slower diffusions of the large dodecane molecule. The molecule become restricted and stays longer in the pores of the catalyst, which results in secondary reactions after cracking such as isomerization, aromatization, dehydrogenation and hydrogenation occurring during these reactions. Moreover, dodecane is a bulkier

hydrocarbon and may not quickly pass through the pores of the catalyst as it would with a shorter hydrocarbon like hexane, especially in the microporous commercial catalyst. There is no much change observed in the produced paraffins and BTEX products formed with the SA=71 during the 1st to the 6th hour, as the product distribution seems to be the same. This may be due to the high conversion being maintained throughout the reaction, which continues to give high selectivity to olefins. However, there is an observed decrease in selectivity towards the paraffins and BTEX products over the SA=80 from the 1st hour to the 6th hour of the reaction as the conversion also drops. This observation is expected from a microporous zeolite, as there will be more side reactions taking place at higher conversions leading to a high yield of the unwanted products such as paraffins and the BTEX products. These unwanted products normally lead to coke formation which blocks acid sites and prevent secondary reactions, causing a decrease in conversion with TOS. The presence of coke will be determined in future work to confirm the observed results.

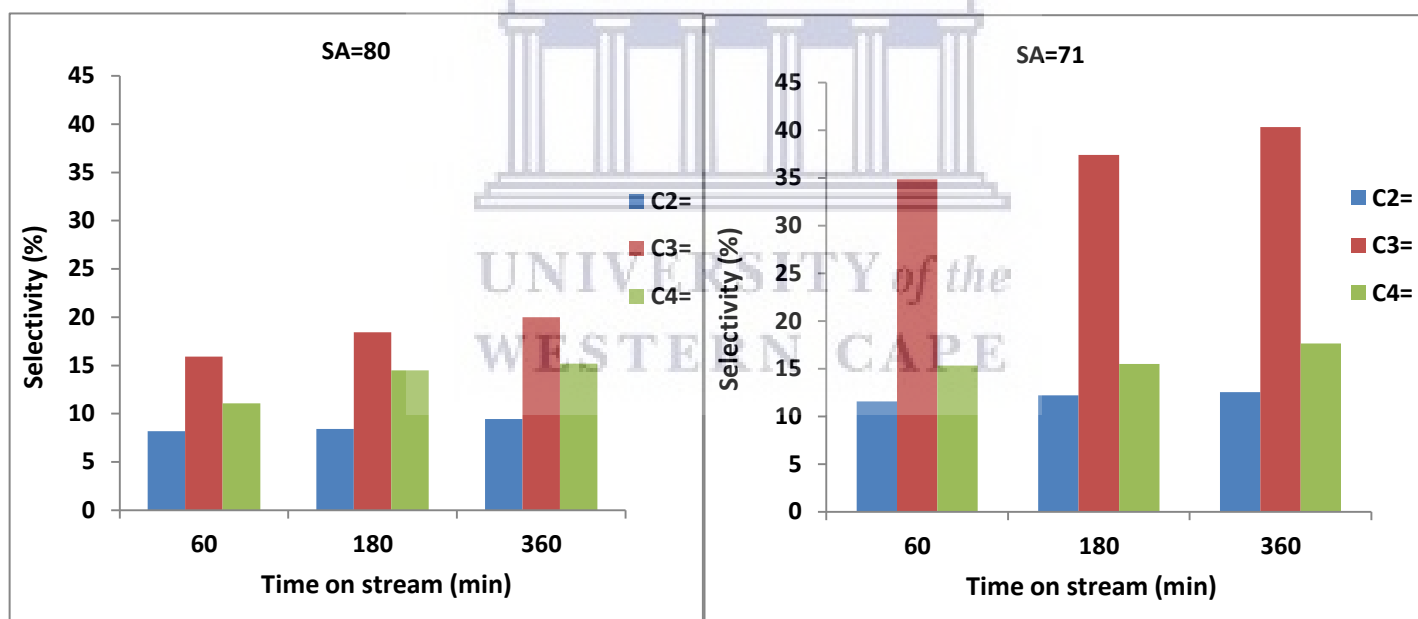


Figure 46: Selectivity towards olefins [C₂= to C₄=] products formed when using the commercial catalyst with SA=80 and the prepared catalyst with SA=71.

Figure 46 shows selectivity towards olefins [C₂= to C₄=] produced over a period of 6 hours when using a commercial catalyst with SA=80 and the synthesized catalyst with SA=71. The SA=71 shows the highest selectivity towards olefins from the 1st to the 6th hour of the reaction as compared to the commercial catalyst with SA=80. Furthermore, the SA=71 has higher P/E ratios of ~3 than the commercial catalyst with P/E

ratios of ~ 2 . As observed from Figure 46, ethylene is slightly produced from 8 % during the 1st hour to 9 % during the 6th hour of the reaction over the commercial catalyst. Propylene also increases from 16 % to 20 % and butenes increase from 11 % to 15 %. However, when using the synthesized catalyst with SA=71, the selectivity towards olefins is produced more than double of what is produced over a commercial catalyst. The selectivity towards ethylene increases very slightly from 12 % to 13 % during the 6th hour. The selectivity towards propylene increases from 35 % to 40 % and the selectivity towards butenes increases slightly from 15 % to 18 %. The observed increase in olefins over the SA=71 is due to its bigger pores as compared to the SA=80 with only micropores. The feed is able to easily access the catalyst acidic sites that are responsible for the formation of light olefins. Moreover, it is also able to quickly diffuse out of the catalyst without undergoing secondary reactions that may reduce olefin selectivity as compared to when using the SA=80.

Diao *et al* (4) observed similar results during catalytic cracking of n-dodecane [500 °C, 4 MPa] using hierarchical HZSM-5 zeolites membranes with tunable mesoporosity. The hierarchical zeolite with the largest mesopores exhibited superior catalytic performances. This zeolite showed the highest average activity of 28.62 % and an above 13 % improvement with a lowest deactivation as compared to the microporous catalyst with only 15.39 % average activity. The initial conversion for the microporous catalyst was 19.26 % and sharply dropped to 12.17% with TOS. These catalysts had similar acidic properties but the hierarchical ZSM-5 had larger mesopore size which lead to enhanced diffusivity of n-dodecane and cracking products. Moreover, the hierarchical ZSM-5 with the largest pores produced more olefins with less paraffins and BTX products than the microporous catalyst. They concluded that this was due to high diffusivity of the membrane which limited a secondary reaction and thus improved the stability of the catalyst.

5.6 Catalytic Cracking of Tyre Derived Oil [TDO]

Catalytic cracking of Tyre Derived Oil [TDO] was studied and performed on a bench scale quartz-tube reactor using the prepared HZSM-5 catalyst with SA=71 and a commercial ZSM-5 catalyst with SA=80. This type of feed was used to investigate whether the use of the prepared hierarchical ZSM-5 catalyst with larger pores would be better for catalytic cracking of bulky molecules than light naphtha for which hexane was used as a model feed. In this study, the product distribution when using the two different catalysts was investigated. Figure 47 below shows the selectivity towards paraffins and BTEX products formed when using a commercial catalyst with SA=80 and the prepared catalyst with SA=71.

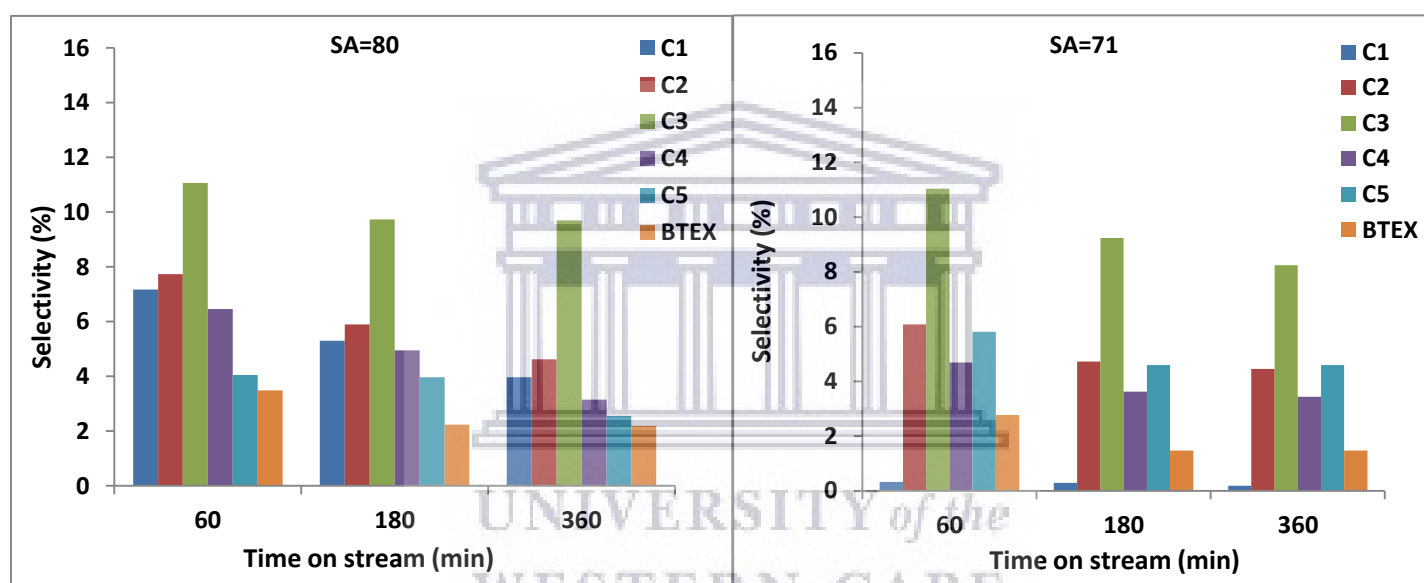


Figure 47: Selectivity towards paraffins and BTEX products formed when using a commercial catalyst with SA=80 and the prepared catalyst with SA=71. The catalytic cracking reactions were performed on a bench scale quartz-tube reactor using TDO as a model feed. The reactions were carried under the following conditions: T = 550 °C, Time on stream [TOS] = 6 hours, N₂: TDO dilution ratio = 1:1, feed flow rate = 0.1 ml/min, P = 1 atm, WHSV = 15.82 hr⁻¹ and a catalyst mass = 0.25 g.

As observed from Figure 47, there is a wide distribution in the selectivity towards paraffins as well as BTEX products when using both catalysts. This indicates that there are competing reactions such as aromatization, isomerization, dehydrogenation and hydrogenation taking place. This is expected since TDO is a bulky

feedstock and may lead to limited diffusion and transfer of reactants and products molecules within the pores of the catalyst. However, the SA=71 has got bigger pores which could possibly lead to better accessibility to active sites as well as improved diffusion of reactants and products compared to the microporous commercial catalyst. This results to less formation of unwanted products. This is also evident on the selectivity towards methane which is produced in very small amounts throughout the reaction, but in higher amounts when using the commercial catalyst.

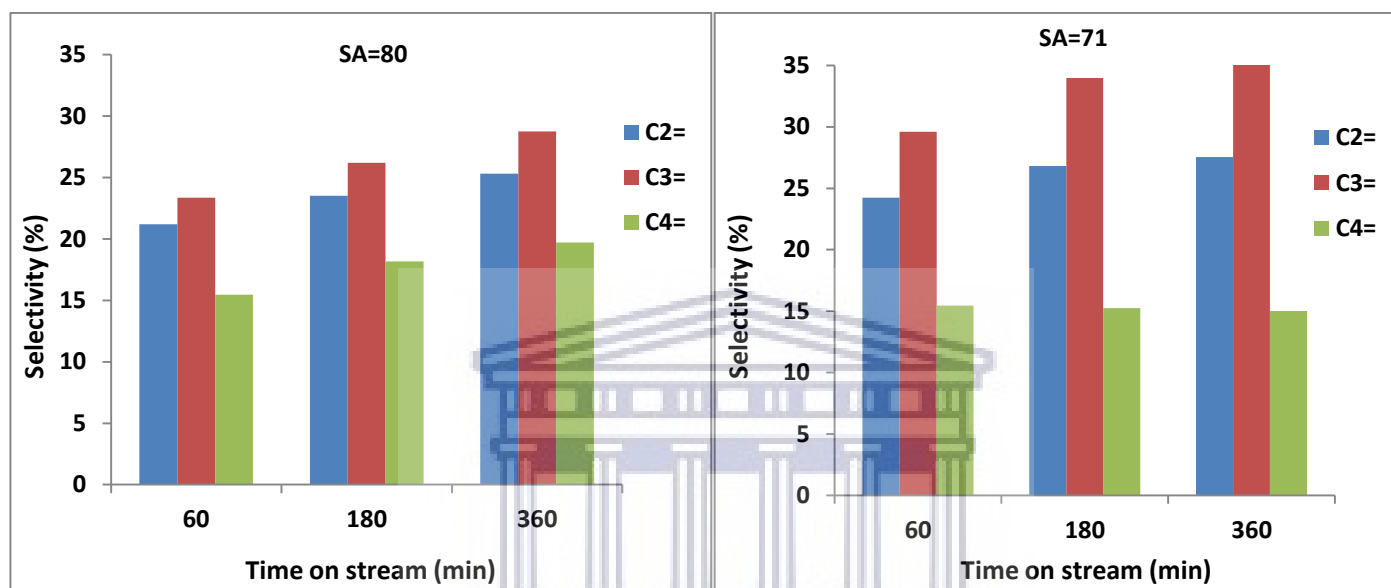


Figure 48: Selectivity towards olefins [C₂= to C₄=] products formed when using the commercial catalyst with SA=80 and the prepared catalyst with SA=71.

Figure 48 shows selectivity towards olefins [C₂= to C₄=] produced over a period of 6 hours when using a commercial catalyst with SA=80 and the synthesized catalyst with SA=71. The SA=71 shows the highest selectivity towards olefins from the 1st to the 6th hour of the reaction as compared to the commercial catalyst with SA=80. Furthermore, the SA=71 shows higher P/E ratios of ~ 1.3 than the commercial catalyst with P/E ratios of ~1.1. As observed from Figure 48, the selectivity towards ethylene increases from 21 % during the 1st hour of the reaction to 25 % during the 6th hour when using the commercial catalyst. Selectivity towards propylene increases from 23 % to 29 % and the selectivity towards butenes increase from 15 % to 20 %. When using the synthesized catalyst, selectivity towards ethylene increases from 24 % to 28 %. The selectivity to propylene increases from 30 % to 35 % and selectivity towards butenes is found to be 15 %

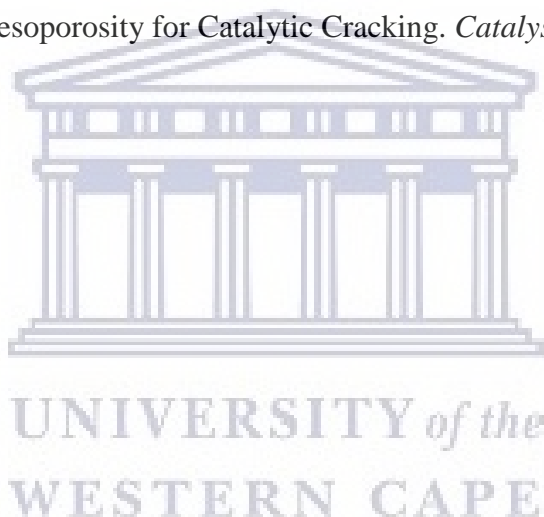
throughout the reaction. The improved selectivity towards ethylene and propylene when using the synthesized catalyst is due to its bigger pores which cause much less interactions with the feed and be able to quickly diffuse out of the catalyst without undergoing many unwanted side reactions.

5.7 Conclusion

The bigger pore sizes and the acidity of the prepared hierarchical ZSM-5 zeolites with different Si/Al ratios played a significant role during the catalytic cracking of hexane, dodecane and tyre derived oil at high temperatures of 550 °C. This allowed the reactants and product molecules to easily diffuse in and out of the pores of the catalyst and improve interaction with the active acid sites of the catalyst. This leads to higher catalytic conversions and greater yields towards olefins, particularly ethylene and propylene than when using a commercial catalyst. Very low catalytic conversions were observed when using a smaller hexane molecule during the catalytic cracking with these HZSM-5 zeolite materials. This suggests that the hexane feed was passing through the catalyst pores with very less interactions with the active sites. However, when using one of the prepared HZSM-5 catalyst [SA=71] with hierarchical pore structure and higher acidity for the catalytic cracking of dodecane and tyre derived oil, the catalytic conversions as well as the selectivity towards olefins was improved. This suggests that there was better diffusion through the catalyst pores and the feed molecules were able to have much better interaction with the active sites of the catalyst. Furthermore, the P/E ratios were observed to be higher during the catalytic cracking of both dodecane and tyre derived oil over the prepared hierarchical ZSM-5 catalyst as compared to when using a commercial catalyst. This suggests that the prepared catalyst is most effective on cracking of longer chains as well as bulky molecules, and would be a more suitable catalyst for cracking oils such as those used as feedstocks in the FCC process. The catalyst also demonstrates high yields of greater than 60 % for ethylene + propylene during the catalytic cracking of dodecane. Therefore, the synthesis of hierarchical ZSM-5 with micro, meso and macropore structure, as well as good amount and strength of acid sites may be a worthy candidate as a cracking catalyst which meets the industry demands of high selectivity to light olefins and improved propylene to ethylene ratio.

5.8 References

1. Konno H, Tago T, Nakasaka Y, Ohnaka R, Nishimura JI, Masuda T. Effectiveness of nano-scale ZSM-5 zeolite and its deactivation mechanism on catalytic cracking of representative hydrocarbons of naphtha. *Microporous Mesoporous Mater.* 2013;(175):25–33.
2. Kubo K, Iida H, Namba S, Igarashi A. Selective formation of light olefins by catalytic cracking of naphtha components over ZSM-5 zeolite catalysts. *J Japan Pet Inst.* 2018;(61):10–19.
3. Xian X, Liu G, Zhang X, Wang L, Mi Z. Catalytic cracking of n-dodecane over HZSM-5 zeolite under supercritical conditions : Experiments and kinetics. *Chem Eng Sci.* 2010;(65):5588–5604.
4. Diao Z, Cheng L, Hou X, Rong D, Lu Y, Yue W, Sun D. Fabrication of the Hierarchical HZSM-5 Membrane with Tunable Mesoporosity for Catalytic Cracking. *Catalysts.* 2019;(5):1-13.



CHAPTER 6: Conclusions and Recommendations

Chapter Overview

This chapter provides a summary of the main findings of this thesis by underlining an overview of the activities and contributions of the results from a scientific and industrial point of view. Recommendations for future work are also outlined.

6.0 Summary and Conclusions

The aim of this project was to synthesise hierarchical macro/mesoporous ZSM-5 zeolite crystals with variable Si/Al ratios and test them as catalytic cracking catalysts. ZSM-5 zeolites have been used worldwide for the production of light olefins, particularly ethylene and propylene which are greatly used for their importance as feedstocks for producing useful materials. The literature review revealed that hierarchical zeolites in the macro and/or mesoporous range play a major role in the production of light olefins due to their larger pore sizes. In general, hierarchical zeolites should allow easy access of large reactant molecules to catalytically active sites. In previous studies, the use of hierarchical zeolites demonstrated high catalytic activities, enhanced selectivities towards olefins, low deactivation rates, high thermal/hydrothermal stability and longer catalyst life than the parent microporous ZSM-5 catalyst. Hence, the use of hierarchical zeolite catalysts during the catalytic cracking process has been recommended as one of the best methods for enhancing the production of light olefins.

During this study, the fabrication of the hierarchical ZSM-5 zeolites with different Si/Al ratios in the range of 30-300 was performed via steam-assisted hydrothermal synthetic approach making use of stoichiometric quantities of sodium aluminate as an aluminum source, tetraethyl orthosilicate as a silica source, tetrabutylammonium hydroxide and hexadecyltrimethylammonium bromide. A process known as crystallization was then performed at high temperatures of 150 °C using a plastic Teflon flask placed inside a large stainless steel autoclave. Lastly, the zeolite was ion exchanged and calcined at 550 °C for 3 hours to convert to the H-form.

The synthesized materials were then characterized fully to study their physical and chemical properties. XRF spectroscopy method was employed in the study to determine the Al₂O₃ and the SiO₂ contents of the prepared ZSM-5 materials and XRF analysis showed that the calculated actual ratios were close to the batch ratios, except for the material with a batch ratio of 30 which did not completely crystallize. FTIR spectrometry was used to evaluate the functional groups present in the synthesized materials and to confirm the structure of ZSM-5 zeolite. The found intensity of the transmittance bands confirmed that the material reflects the crystallinity of ZSM-5 zeolites and is assigned to the five-membered rings of MFI zeolites. XRD analysis which was employed in the study to determine the crystal structure and phases present further confirmed that the prepared materials have a degree of crystallinity of the hierarchical ZSM-5 type with a partially ordered mesoporous structure. However, the SA=36 did not reflect the structure of a high crystalline ZSM-5 material. This was probably due to the large Al content present in the batch mixture which resulted in slower crystallization kinetics, hence hindering the formation of crystals at the given crystallization conditions. Therefore, the Si/Al ratio in particular the aluminium content is shown to have an effect on the formation of the ZSM-5 zeolite. The strength and amount of acid sites in the prepared materials was analysed by NH₃-TPD. Surprisingly, the NH₃-TPD profiles showed three desorption peaks. To our best knowledge, such observation of HZSM-5 zeolites showing three desorption peaks has not been reported before. The total acidity calculated from the weak and strong acid sites of the prepared materials was found to decrease as the Si/Al increases in the following trend; SA=71>77 >177>345. Furthermore, the materials showed an increase in desorption temperature of the peak corresponding to strong acid sites as the Si/Al ratio decreased. This followed in the order SA= SA=71>177 >77>345. TGA analysis was performed to determine the thermal stability and the fraction of the volatile components on the SA=77 since it had the highest intensity of the unknown third peak in the NH₃-TPD profiles. The material showed a little loss of moisture in the pores and on the surface, proving that it was thermally stable and the third peak found on the prepared catalysts was not due to thermal decomposition. However, the observation of this peak still warrants further investigation.

The synthesized materials were also characterized microscopically using HRSEM to establish the surface morphology and the elemental composition of the prepared materials. The HRSEM micrographs revealed

morphologies that are spherically shaped and uniformly aggregated together, forming stack of crystals with observable open spaces within the large crystals. A sponge like morphology with worm-like holes in the macropore range [>50 nm] were also observed, proving that some macropores were successfully generated during the fabrication of these materials. The pore-size distribution as well as the pore volumes and surface area measurements of the prepared materials were also investigated by BET analysis. The SA=71 showed the highest SSA of $618 \text{ m}^2/\text{g}$ given by its micropore area of $103 \text{ m}^2/\text{g}$ and an external surface area of $515 \text{ m}^2/\text{g}$. The high surface area in the material was due to the development of mesopores with narrow pore size distribution. Moreover, a hierarchical structure with 3 pore ranges, i.e. micro, meso and macropores was proven to be developed. The corresponding BJH pore-size distributions also show that all the synthesized materials have highly ordered mesopores with a very narrow pore size distribution. The pore diameters range between 5-7 nm, which leads to a high SSA and pore volume.

The catalytic performance of the prepared materials was tested via catalytic cracking of hexane, dodecane and tyre derived oil. At first, the effects of reaction conditions such as temperature, nitrogen diluent to feed ratio and WHSV on the catalyst activity and selectivity were investigated. All the catalytic cracking reactions for optimization studies were performed using hexane as a model feed over a commercial ZSM-5 with SA=80 on a bench scale quartz-tube reactor. Firstly, it was confirmed that at the highest temperature of $550 \text{ }^\circ\text{C}$, the cracking was catalytic and not thermal. Then the effect of temperature showed that as the temperature increased from $450 \text{ }^\circ\text{C}$ to $550 \text{ }^\circ\text{C}$, an increase in catalytic conversion was also observed. The increase in conversion observed with increase in temperature is expected and was attributed to more energy in the system to reach the activation energy to break C-C bonds, resulting in higher conversion of the reactant to cracked products. The selectivity towards paraffins was found to be higher at $450 \text{ }^\circ\text{C}$ and decreased with TOS as the temperatures increased to $550 \text{ }^\circ\text{C}$. On the other hand, the BTEX products as well as the olefin products, ethylene and propylene in particular started to increase with TOS as the temperature increased. This observation was attributed to the higher cracking activity at higher temperatures, leading to a great selectivity to olefins. The highest temperature of $550 \text{ }^\circ\text{C}$ was shown to be the best for enhancing selectivity to olefins.

The second study was conducted on the effect of catalyst loading at the optimum temperature of 550 °C. The catalytic conversions increased with an increase in catalyst mass used, resulting in 0.25 g to have the lowest conversion and 0.75 g with the highest conversion. However, the selectivity towards olefins and P/E ratios decreased with an increase in the catalyst loading with TOS. The high selectivity obtained when using a much less catalyst loading is due to its high WHSV. Consequently, the catalyst loading of 0.25 g was found to be the best for enhancing the selectivity towards olefins.

The third study was conducted on the effect of nitrogen: hexane dilution ratios to find the best nitrogen to feed dilution ratios for balancing activity while maintaining a high selectivity to olefins. The catalytic conversions were found to decrease as the nitrogen to feed dilution ratio increased. This observation may be due to the feed having a shorter contact time with the catalyst since it is carried by nitrogen when the dilution ratio is higher. However, the catalysts were shown to be more stable at the nitrogen to feed ratios with the 1:1, resulting in the least catalyst deactivation. The selectivity towards olefins was found to increase with an increase in dilution ratios. The dilution ratio of 2:1 shows the highest selectivity towards olefins but was only fractionally higher than at the ratio of 1:1. It is evident that the use of nitrogen has an effect in boosting the selectivity towards olefins. However, it is most advisable to work with the catalyst that is more stable and more selective to the ideal product. Furthermore, industrially it would be best to work with a lower dilution ratio to save costs. Hence, the dilution ratio of 1:1 was found as the condition which best balances activity, selectivity and stability.

Catalytic cracking of hexane was studied over the prepared hierarchical ZSM-5 catalysts with different Si/Al ratios using the designated optimum conditions. The obtained conversions appeared in very low amounts. The catalyst with SA=71 had the initial highest conversion of 8.3 % which generally decreased as the Si/Al ratio increased, with SA=345 having the lowest conversion of 3.5 %. However, all these catalysts were found to be stable as the conversion remained the same throughout the reaction. The observed conversions were attributed to the acidity of the catalysts, in particular the strength of the strong Bronsted acid sites. From the NH₃-TPD results, the SA=71 had the highest total acidity and the SA=345 had the lowest acidity, while the strength of the acid sites in the catalyst followed the order SA=71>177>77>345. This resulted in the

catalytic activity of the catalysts following the exact same order. Therefore, it can be said that the catalytic activity is mainly due to the acid strength of the strong Bronsted sites rather than the total acidity or acid site quantity. The observed low conversions found when using the prepared catalysts may be due to large pores that were generated during the fabrication of these HZSM-5 catalysts as compared to when using the commercial catalyst with only micropores. This may have allowed the hexane feed to pass through the catalyst pores with very less interaction with the active sites.

The SA=71 was found to be more selective to paraffins, especially the C₂ and C₃ products with less BTEX products produced with TOS. There were more C₃ products produced than C₂ paraffins with this catalyst due to secondary hydrogen transfer reactions. This was probably related to its high acidity that led to a slightly higher conversion as compared to the other catalysts. Even though these prepared catalysts revealed very low conversions, there was a slight increase towards olefins as compared to when using the commercial ZSM-5 with SA=80. The slight increase in olefins was due to the bigger pores in the prepared HZSM-5 catalysts. The large pores allowed better diffusion through the catalyst, making hexane to easily pass through and react very slightly, resulting to low conversions where better selectivities to olefins are obtained. SA=71 had the highest selectivity towards propylene which increased with TOS as compared to the other ratios. This high selectivity is associated with the best conversion when using the SA=71 compared to other ratios. The selectivity towards propylene was found to be slightly lower as the Si/Al ratio increased and follows the trend observed for the conversions as well as acid strength of the strong Bronsted sites i.e. SA=71>177>77>345. This indicates that the selectivity to propylene is dependent on the conversion which is in turn dependent on the strength and amount of acid sites available. All the catalysts displayed high propylene to ethylene ratios [P/E > 1] with the best achieved for SA=71 of P/E ratio of 2.1. It is evident that variations in the Si/Al ratio affect the acidity of the materials which results in differences in the catalytic performance in terms of activity, selectivity and stability. Therefore, it was concluded that the SA=71 was the best catalyst for enhancing the selectivity towards olefins when using hexane as a feed since it was more stable and demonstrated an increase in selectivity towards light olefins with TOS. SA=71 was then further investigated by carrying out testing reactions with larger molecules.

Catalytic cracking of dodecane was studied and performed on a bench scale quartz-tube reactor using the prepared HZSM-5 catalyst with SA=71 and a commercial ZSM-5 catalyst with SA=80 to investigate their effect of pore sizes. The mesoporous SA=71 ZSM-5 catalyst showed a massive improvement in activity when cracking the larger dodecane compared to hexane. An initial conversion of 100 % was observed when using the catalyst with SA=71. The commercial catalyst which had an initial conversion of 84 % than the mesoporous catalyst also enhanced the stability of the catalyst. The comparison highlighted the effectiveness of introducing a hierarchical system which enhanced activity and stability. The improved results were attributed to better accessibility to active sites for the larger dodecane chain as well as better diffusion through the catalyst.

The SA=71 shows the highest selectivity towards olefins as compared to the commercial catalyst with SA=80. Furthermore, the SA=71 had a higher P/E ratios of ~3 as compared to the commercial catalyst with P/E ratios of ~2. The observed increase in olefins over the SA=71 was due to its bigger pores as compared to the commercial catalyst with only micropores. The feed was able to easily access the catalyst acid sites that are responsible for the formation of light olefins and diffuse out without undergoing secondary reactions.

Catalytic cracking of Tyre Derived Oil [TDO] containing a mixture of large hydrocarbons was also studied at the established reaction conditions. Both catalysts showed a wide product distribution. This indicated that there were competing reactions such as aromatization, isomerization, dehydrogenation and hydrogenation taking place. The SA=71 had the highest selectivity towards olefins as compared to the commercial catalyst. Furthermore, the SA=71 showed higher P/E ratios of ~1.3 than the commercial catalyst with P/E ratios of ~1.1. This provided further evidence of the improved catalytic properties of hierarchical ZSM-5 system.

The bigger pore sizes and the acidity of the prepared hierarchical ZSM-5 zeolites with different Si/Al ratios played a significant role during the catalytic cracking of hexane, dodecane and tyre derived oil at high temperatures of 550 °C. This allowed the reactants and product molecules to easily diffuse in and out of the pores of the catalyst and also interact with the active acid sites of the catalyst. This resulted to higher catalytic conversions and greater yields towards olefins, particularly ethylene and propylene as compared to when using a commercial catalyst. Therefore, the objectives of the study were achieved as the prepared

HZSM-5 catalysts demonstrated improved selectivity towards olefins. This also showed that the hierarchical ZSM-5 synthesized with narrow mesopore size distribution was more effective in the cracking of large hydrocarbons which meets industry demands of high olefin selectivity and high P/E ratio and may be suitable as FCC cracking catalyst.

6.1 Recommendations and Future Work

The preparation of the hierarchical ZSM-5 zeolites with different Si/Al ratios via steam-assisted hydrothermal synthesis was successful. However, the synthesis of SA=30 needs further investigation as to why it was not crystalline and could not demonstrate the structure of a ZSM-5 zeolite with the used method.

The NH₃-TPD profiles of the prepared materials demonstrate three desorption peaks. A third peak is observed at 598 – 882 °C. To the best of our knowledge, such observation of HZSM-5 zeolites showing three desorption peaks with strong acid sites at such high temperatures has not been reported before. Therefore, further investigations on the characterization of NH₃-TPD results would be necessary to find out the reason for the observed peak at such high temperatures.

The catalytic conversions are observed to be very low during the catalytic cracking of hexane with the prepared mesoporous ZSM-5 catalysts. One other possible way that has been mostly reviewed on literature on how to improve the catalyst conversion and selectivity towards light olefins is to dope the HZSM-5 zeolite catalysts with metals.

When using one of the prepared HZSM-5 catalyst [SA=71] with the largest pore sizes and higher acidity for the catalytic cracking of dodecane and tyre derived oil, the catalytic conversions as well as the selectivity towards olefins was improved. This suggests that the prepared catalysts would be more effective on cracking longer chains as well as bulky molecules. They would also be more suitable catalysts for cracking oils such as those used as feedstocks in the FCC process.